

**Analysis of forest-climate interactions,
applying the regional climate model REMO**

**Az erdő – klíma kölcsönhatás elemzése
a REMO regionális klímamodell segítségével**

DOKTORI (PhD) ÉRTEKEZÉS

Gálos Borbála

okl. környezetmérnök-tanár

Témavezetők:

Prof. Dr. Mátyás Csaba

Prof. Dr. Jacob, Daniela

Sopron
2010

**Analysis of forest-climate interactions,
applying the regional climate model REMO**

**Az erdő – klíma kölcsönhatás elemzése
a REMO regionális klímamodell segítségével**

értekezés doktori (PhD) fokozat elnyerése érdekében készült
a Nyugat-magyarországi Egyetem Kitaibel Pál Környezettudományi Doktori Iskolája
Biokörnyezet-tudomány programja keretében.

Írta:

Gálos Borbála

Témavezetők: Prof. Dr. Mátyás Csaba

Elfogadásra javaslom (igen / nem)

(aláírás)

Prof. Dr. Jacob, Daniela

Elfogadásra javaslom (igen / nem)

(aláírás)

A jelölt a doktori szigorlaton % -ot ért el,

Sopron, 2009. október 2.

a Szigorlati Bizottság elnöke

Az értekezést bírálóként elfogadásra javaslom (igen /nem)

Első bíráló: Prof. Dr. Mika János igen /nem

(aláírás)

Második bíráló: Dr. Gribovszki Zoltán igen /nem

(aláírás)

(Esetleg harmadik bíráló (Dr.) igen /nem

(aláírás)

A jelölt az értekezés nyilvános vitáján.....% - ot ért el

Sopron,

.....

a Bírálóbizottság elnöke

A doktori (PhD) oklevél minősítése.....

.....

Az EDT elnöke

Contents

Abstract	6
Kivonat	6
1. Introduction	8
1.1 Background and objectives	8
1.2 Structure of the dissertation.....	9
2. Climate change and forest-climate interactions	10
2.1 Climate change in Europe and in Hungary	10
2.1.1 Regional scale climate tendencies for Europe.....	10
2.1.2 Projected climate change for Hungary	12
2.2 Droughts and their effects on the forest ecosystems in Hungary.....	14
2.2.1 Definition and characteristics of droughts, drought indices.....	14
2.2.2 Drought vulnerability of the xeric forest limit	17
2.3 Feedback of forests on climate.....	20
2.3.1 Climatic role of forest ecosystems	20
2.3.2 Interception and its hydrologic role	23
2.3.3 Climatic effects of land cover change	27
2.4 Models as research tools for studying climate change.....	30
2.4.1 General aspects of climate modelling	30
2.4.2 Regional climate modelling	31
2.4.3 Land surface models.....	34
2.5 Discussion and research needs	36
3. Objectives and research questions	38
4. Data and methods	39
4.1 Simulation of climate change and forest-climate interactions applying the regional climate model REMO in Hungary	39
4.1.1 The regional climate model REMO	39
4.1.2 Simulation of climate change and drought trends in Hungary.....	45
4.1.3 Simulation of feedback of forest cover change on the regional climate and the climate change altering effect of afforestation in Hungary.....	48
4.2 Measuring and modelling interception on local scale.....	55
4.2.1 The Hidegvíz-Valley forest hydrological research area.....	55
4.2.2 The hydrologic model BROOK90	56
4.2.3 Application of BROOK90 for interception in the Hidegvíz-Valley	59
5. Results	62
5.1 Climate change and drought frequency.....	62
5.1.1 Validation of the regional climate model REMO for temperature, precipitation and droughts	62
5.1.2 Projected temperature and precipitation tendencies for the 21st century.....	64
5.1.3 Probability and severity of droughts in the 21st century.....	68
5.1.4 Spatial differences in the drought trends.....	70
5.1.5 Summary	72

5.2 Feedback of forest cover change on the regional climate	73
5.2.1 Climatic effects of maximal afforestation and deforestation	73
5.2.2 Effect of maximal afforestation in the region characterised by the largest possible forest cover increase.....	75
5.2.3 Interaction of the main climatic forcings of afforestation during the summer months	81
5.2.4 Climatic role of the potential afforestation survey	83
5.2.5 Summary	84
5.3 Climate change altering effect of afforestation	85
5.3.1 Magnitude of the feedback of maximal afforestation on precipitation compared to the climate change signal	86
5.3.2 Effect of maximal afforestation on the probability and severity of droughts	87
5.3.3 Influence of the extent of the present forest cover on the projected climate change.....	88
5.3.4 Comparison of the feedbacks of maximal afforestation on precipitation under moderate and enhanced climate change	89
5.3.5 Magnitude of the effects of deforestation compared to the climate change signal	90
5.3.6 Summary	91
5.4 Measuring and modelling of interception on local scale.....	92
5.4.1 Adaptation and validation of the hydrologic model BROOK90 for interception in the Hidegvíz-Valley	92
5.4.2 Sensitivity of the simulated interception to the precipitation intensity	93
5.4.3 Summary	94
6. Discussion and Conclusions.....	95
7. Outlook.....	98
8. Theses of the dissertation.....	100
Acknowledgements.....	101
References	102
Annex.....	114

Abstract

Forest-climate interactions have been investigated for Hungary in the 21st century, applying the regional climate model REMO. The projected tendency of temperature and precipitation means and the probability and severity of droughts have been analysed for summer, based on the results of IPCC-SRES¹ emission scenario simulations (B1, A1B, A2). For the assessment of the biogeophysical feedbacks of forest cover change on the regional climate, REMO was driven by three different land cover change scenarios. At the end of the 21st century (2071-2100), effects of maximal afforestation (forests over all vegetated area) and deforestation (forests replaced by grasslands) have been investigated for Hungary. For 2021-2025, the climatic influence of the potential afforestation survey has been studied.

Based on the simulation results, under enhanced climate change (2051-2100), the probability and severity of droughts can be significantly higher, the consecutive dry periods may last longer than in the second half of the 20th century. The simulated increase of the probability of extreme dry summers is largest in the southwest part of Hungary.

For the 21st century, maximal afforestation weakens the projected climate change signal by increasing evapotranspiration and precipitation and decreasing surface temperature over the whole country, for the whole summer period. This climate change weakening effect differs among regions. It is simulated to be the largest in the northeastern area (here, 50% of the projected precipitation decrease can be relieved), whereas the smallest in the southwestern part of the country. The potential afforestation has a very slight feedback on the regional climate compared to the maximal afforestation scenario.

How experiences from local-scale measurements and modelling of interception can contribute to a more detailed representation of forest-related hydrological processes in the regional climate model needs further investigations.

Kivonat

A disszertáció aszályos nyarak valószínűségének és szélsőségességének várható alakulását, valamint az erdőterület-változás lehetséges klímamódosító hatását elemzi, a REMO regionális klímamodell segítségével. A 21. századi éghajlati viszonyok becsléséhez különböző IPCC-SRES¹ kibocsátási forgatókönyveken (B1, A1B, A2) alapuló modellfuttatások eredményeit hasonlítja össze. A magyarországi erdők klimatikus értékét három felszínborítás-változási forgatókönyvre számszerűsíti. A 2071-2100-as időszakra vizsgálja, hogy a feltételezett maximális erdőtelepítéssel (minden növényzettel borított felszín erdő), valamint a hazai erdőterületek gyepvel történő helyettesítésével milyen irányban és mértékben befolyásolhatók az előrejelített hőmérséklet- és csapadéktendenciák. A 2021-2025-ös periódusra a rossz adottságú és gyenge minőségű szántók helyére tervezett erdők regionális léptékű éghajlati hatásait elemzi.

A modellszimulációk eredményei alapján 21. század második felében mindhárom kibocsátási forgatókönyv esetén szignifikánsan megnőhet a száraz nyarak gyakorisága, szélsőségessége, akár minden második nyár aszályos lehet. Az összefüggő száraz periódusok hosszabbá válhatnak, mint a 20. század második felében. A melegedő-szárazodó tendencia az ország délnyugati részén a legnagyobb.

¹ Intergovernmental Panel on Climate Change - Special Report on Emissions Scenarios

Az erdőterület változás, amennyiben nagy kiterjedésű, összefüggő területeket érint, hatással van a regionális klímára. A 21. század végén maximális erdőtelepítéssel az erőteljes szárazodó tendencia az ország egész területén jelentősen enyhíthető. Az erdőterületek növekedésével a nyári hónapban az evapotranspiráció és a csapadékmennyiség növekszik, a felszínhőmérséklet csökken, melynek nagysága régióként eltérő. A REMO regionális klímamodell eredményei alapján a legnagyobb hatás az ország északkeleti részén várható, ahol maximális erdőtelepítéssel a klímaváltozással járó csapadékmennyiség-csökkenés fele kiegyenlíthető. A délnyugati országrészben a legkisebb az erdősítés csapadéknövelő hatása. A gazdaságtalan szántók helyén potenciálisan megvalósítható, országos átlagban 7%-os erdőterület növekedésnek nincs jelentős hatása a regionális éghajlati viszonyokra.

Az intercepció lokális szintű mérése és modellezése során szerzett tapasztalatok alkalmazhatóságának lehetősége a regionális klímamodell hidrológiai folyamatainak pontosabb leírásában további vizsgálatokat igényel.

1. Introduction

1.1 Background and objectives

Natural vegetation is a dynamic component of the climate system. Not only the distribution of vegetation is determined and limited by temperature and precipitation conditions, but also vegetation has an effect on the biogeophysical properties of the land surface, which plays a key role in determination of weather and climate.

Changes of the land cover due to climatic conditions and human influence feed back to the atmosphere, lead to the enhancement or reduction of the original climate change signal. Forests, due to their larger leaf area and roughness length, lower albedo and deeper roots compared to other vegetated surfaces, affect the exchange of water, energy and momentum with the atmosphere. These processes are very complex and their variability is large both in time and space. Several papers have addressed the warming effect of boreal forests and the cooling and moistening effect of tropical forests. Most uncertain is the climatic effect of temperate forests, they can cool or warm the surface air temperature depending on the characteristic of the studied region. On local scale, the forest-related socio-economic and ecosystem services are well known. But recent studies have shown that the regional scale effects can differ from both the local and global scale tendencies.

Hungary has a special ecologic position on the border zone of closed forests and forest steppe (lower forest limit), which is especially vulnerable. The increase of drought frequency can lead to decrease of the forest cover across this region. This phenomenon is not typical in humid areas of the world.

In the last century, afforestation is started to increase and it is planned to continue also in the near future. Climatic effects of the possible reduction or the proposed increase of forest cover in Hungary for longer future time periods are still unknown. Information about the forest-climate interaction is essential not only for the sustainment of the ecological services of forest and for the assessment of their climate protecting effects, but also for the development of adaptation strategies in the next decades.

Therefore this study investigates the biogeophysical feedbacks of forest cover change

- on the regional climate,
- in the temperate zone, in a relative small region (Hungary),
- for the future (21st century).

To study forest-climate interactions for long time periods and to get information about climate change and tendency of climatic extremes, regional climate modelling is essential due to the relatively coarse resolution of recent general circulation models. For the simulation of the climatic feedbacks of forest cover change, forest-related processes of the investigated region have to be represented realistically in the climate model. This study is focusing on interception. To understand the processes of interception in a forest ecosystem more in detail, local scale measurements and modelling are essential. The aim is to point out the basic meteorological and stand characteristics connected to interception, which should be included also in a regional climate model for more detailed and appropriate representation of the effect of forests on the water and energy balance on fine horizontal resolution.

To analyse future climatic conditions and forest-climate interactions during summer month (May, June, July, August) in Hungary, research questions of the dissertation are ordered into four groups:

- Climate change and drought trends
- Feedback of forest cover change on the regional climate
- Climate change altering effect of afforestation
- Measuring and modelling of interception on local scale

1.2 Structure of the dissertation

The dissertation is organised as follows:

After the introduction (*Chapter 1*), an overview on the recent climate change studies is given in *Chapter 2*, with special focus on Europe and Hungary. This chapter also addresses the effects of droughts on the forest ecosystems and the basic properties of forests, through which they affect climate, with special attention on the role of interception in the hydrologic cycle. It is followed by an overview on the climatic feedback of land-use change for different scales and regions and the theoretical background of regional climate modelling. Afterwards, based on the recent researches introduced in *Chapter 2*, the relevance of this work is explained.

The research questions are described in *Chapter 3*. Regarding the aim of the present study, a more detailed introduction is given for the models, data and methods applied (*Chapter 4*). In *Chapter 5* results of the regional and local scale simulations are presented and summarised. Results are discussed, conclusions are drawn and the possibilities for the practical application are stressed in *Chapter 6*. Finally, suggestions are given for the improvement of the methods and further research needs are pointed out (*Chapter 7*). In *Chapter 8*, theses of the dissertation are presented.

2. Climate change and forest-climate interactions

2.1 Climate change in Europe and in Hungary

Global climate simulations show the increase of the global average air temperature, widespread changes of precipitation, the melting of glaciers and ice caps and the rise of the mean sea level for the 21st century (IPCC 2007). The climate projections are results of climate model simulations driven by predefined greenhouse gas emission scenarios (IPCC 2001), which are introduced in detail in *Annex I*. The difference between the simulated climatic conditions for the future and for the present time period is the ***climate change signal***. The climate change signal on regional scale is different from the global means. Numerous international research projects and scientific papers address climate change and its impacts on different spatial and temporal scales and sectors. *Sect. 2.1.1* gives an overview of the future tendencies of temperature and precipitation means and extremes for Europe, while *Sect 2.1.2* focuses on the expected changes in Hungary. In both sections, temporal and spatial distributions and differences are also discussed.

2.1.1 Regional scale climate tendencies for Europe

Temperature and precipitation means. There are several recent EU-projects² carried out in the last decade, to predict climate change and its impacts in Europe for the 21st century. For the period 2021-2050 all regional climate models predict a quite robust (i.e. above the noise generated by the internal model variability and consistent across multiple climate models) surface warming in Central and Eastern Europe. The annual precipitation shows an increase in the Northeast and decrease in the Southwest regions. Around a neutral zone (Hungary, Rumania) precipitation changes are quite small.

At the end of the 21st century, a warming is expected in all seasons over Europe, which is stronger than in the first half of the 21st century. All models agree that the largest warming for summer is projected to occur in the Mediterranean region, Southern France and over the Iberian Peninsula. Less warming is projected over Scandinavia. For winter the maximum warming occurs in Eastern Europe (*Giorgi et al. 2004, Christensen and Christensen 2007*).

For precipitation, the largest increase is predicted in winter, whereas the decrease is the strongest in summer. Changes in the intermediate seasons (spring and autumn) are less pronounced. Results of the regional model simulations show a north-south gradient of annual precipitation changes over Europe, with positive changes in the north (especially in winter) and negative changes in the south (especially over the Mediterranean area in summer). The line of zero change moves with the seasons. This transition zone can be characterised by the largest spread between models (*Christensen and Christensen 2007*).

Spatial distribution of the projected temperature and precipitation changes in summer refers to a marked shift towards a warmer and drier climate for Southern and Central Europe (*Vidale et al. 2007*).

² <http://ensembles-eu.metoffice.com/>, <http://prudence.dmi.dk/>, <http://www.clavier-eu.org>, <http://www.cecilia-eu.org>

Temperature and precipitation extremes. On the example of the temperatures the three basic cases of the changes of climatic means and extremes due to climate change are the following (IPCC 2001):

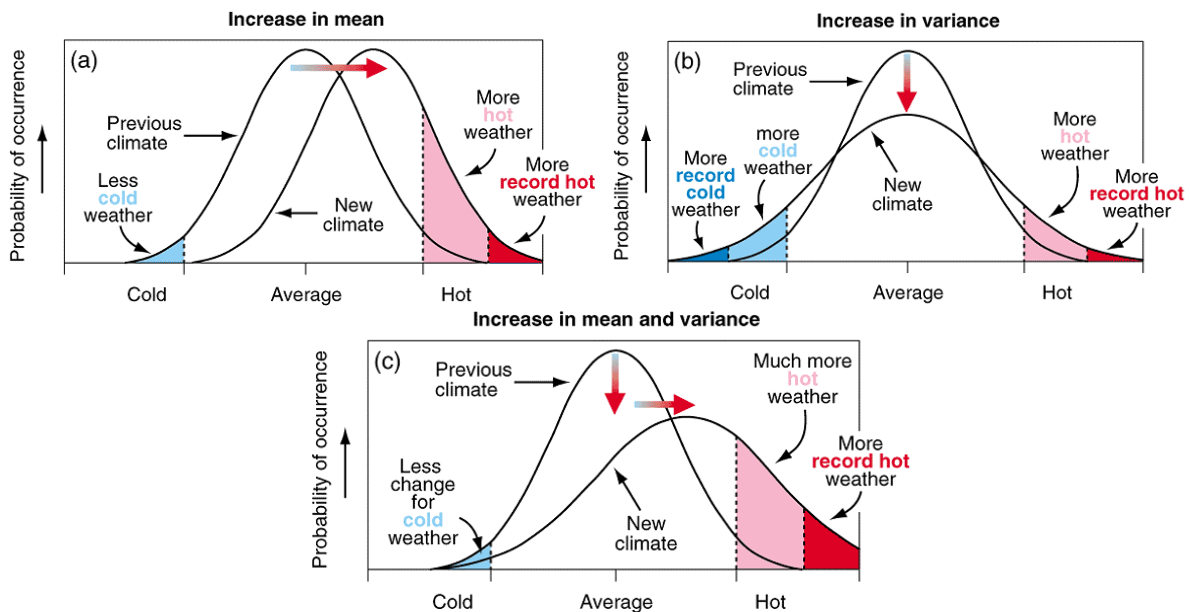


Figure 1. Schematic illustration of the effect on extreme temperatures when (a) the mean temperature increases, (b) the variance increases, and (c) when both the mean and variance increase for a normal distribution of temperature (IPCC 2001, WG I, Fig. 2.32)

- Increase in the mean temperature (*figure 1a*): warming occurs without changes in the temperature variability. The range between the hottest and coldest temperatures i.e. the shape of the probability density function remains the same, which refer to more hot and less cold extremes.
- Increase in the variance of temperature (*figure 1b*): the mean temperature remains the same but its variability increases, which leads to more cold and more hot extremes.
- Increase in the mean and variance of temperature (*figure 1c*): warming occurs together with increased probability of hot extremes and stagnant or decreased probability of cold extremes. The distribution function is wider and flatter and is shifted in the direction of higher temperatures.

Recent results from enhanced greenhouse-gas scenarios over Europe suggest that during the summer season the third case (*figure 1c*) might be valid. It means that not only the climatic means are changing, but there is also an increase in the inter-annual variability of the future temperature and precipitation values, which leads to higher probability of extremes compared to the present-day conditions (Schär et al 2004, Giorgi et al. 2004, Seneviratne et al. 2006, Kjellström et al. 2007, Vidale et al. 2007). In the frame of the STARDEX project³, numerous indices were defined to analyse the tendency of temperature and precipitation extremes for Europe. The STARDEX scenarios indicate increases/decreases in the frequency and intensity of hot/cold extremes, together with more spatially and seasonally variable changes in the occurrence of rainfall extremes. The increase in summer temperature variability projected for Central and Eastern Europe is influenced by both the soil-moisture–temperature feedback and the atmospheric circulation (Seneviratne et al. 2006).

³ http://www.cru.uea.ac.uk/projects/stardex/reports/STARDEX_FINAL_REPORT.pdf

The considerable enhancement of inter-annual variability of the European summer climate as well as the changes of the hydrological cycle are often associated with higher risks of heat waves and extension of the length of dry spells. For 2071-2100 frequency, intensity and duration of heat waves are expected to increase over Europe. Especially the Mediterranean region might be affected by earlier and longer droughts (Beniston et al. 2007). In contrast, for parts of Scandinavia a reduction in length of summer droughts is projected. The intensification of the regional hydrological cycle can lead to shorter return times of heavy precipitation events (e.g. Christensen and Christensen 2003, Pal et al. 2004, Semmler and Jacob 2004). For summer, the number of days with intense precipitation is very likely to increase in the north-eastern European regions, which can result in severe flood episodes despite of the reduction the summer mean precipitation in the main part of the continent (Christensen and Christensen 2003, Beniston et al. 2007). The Central-Mediterranean and Central-Western Europe seem to be especially vulnerable to increases in both summer drought and flood (Pal et al. 2004).

2.1.2 Projected climate change for Hungary

Temperature and precipitation means. Based on the results of the CLAVIER project⁴, the projected increase of annual mean temperature in Hungary can be approximately 1.4°C for the period of 2021-2050 relative to 1961-1990 (Szépszó and Horányi 2008). For the precipitation, the country is situated around a neutral zone surrounded by increasing precipitation in the Northeast and decreasing precipitation in the Southwest. So the predicted changes of the annual precipitation are quite weak in this region. The spatial distribution of precipitation change shows that the reduction of the summer precipitation sum is the largest in the southern part of the country (Szépszó and Horányi 2008).

For the end of the 21st century, all participating regional climate models of the PRUDENCE project⁵ show a quite robust surface warming (Christensen 2005, Mika 2007). The largest temperature increase is expected in summer (4.5-5.1°C; figure 2), whereas the smallest warming is predicted for spring, compared to 1961-1990 (Bartholy et al. 2007). Climate change signal for temperature is largest in the southern and eastern areas. On daily time scale, both maximum and minimum temperatures can be higher. In summer the projected increase of daily maximum temperatures is larger than the warming of the daily minimums, which refers to larger daily temperature amplitudes (Bartholy et al. 2007).

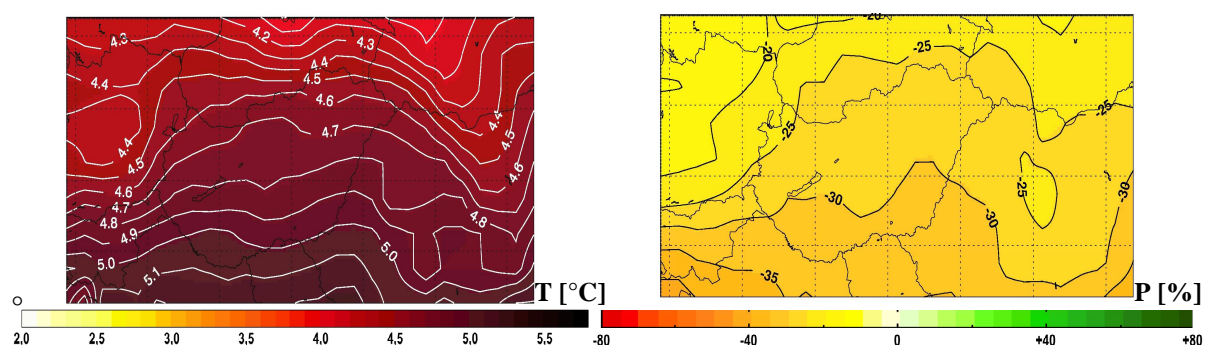


Figure 2. Changes of the summer temperature mean (*T*; left) and precipitation sum (*P*; right) 2071-2100 vs. 1961-1990, A2 IPCC-SRES emission scenario (Annex I; Bartholy et al. 2007)

⁴ <http://www.clavier-eu.org>

⁵ <http://prudence.dmi.dk>

The annual precipitation sum is not expected to change significantly, whereas its distribution is affected by climate change. Summer was the wettest season in the 20th century but it becomes the driest in case of A2 scenario (*Annex I*) and the driest winter tends to be the wettest (based on the results of the CLAVIER project, this tendency is also typical for the near future). In summer, the projected precipitation decrease is 24-33% for the A2 (*figure 2*) and 10-20% for the B2 scenario (*Annex I*). In winter, the expected precipitation increase is 23-37% (A2) and 20-27% (B2). A slight precipitation increase in spring and a decrease in autumn are also expected (*Bartholy et al. 2007*). Depending on the season, magnitude of the climate change signals differ among regions. In northwest-Hungary drying of summers is the smallest while winter precipitation increase is the largest.

Temperature and precipitation extremes. For the 20th century several climate extreme indices have been analysed and compared for Hungary based on the guidelines suggested by the joint WMO-CCI/CLIVAR Working Group on climate change detection (*Bartholy and Pongrácz 2007*). Similarly to the global and continental trends (*Klein Tank and Können 2003*), for Central/Eastern Europe, strong increasing tendencies have been detected in case of the annual numbers of hot days, summer days, warm days, warm nights, and the heat wave duration index in the second half of the 20th century. Furthermore, intensity and frequency of extreme precipitation have increased, while the total precipitation amount has decreased (*Bartholy and Pongrácz 2007*).

For 2021-2050, all simulation results of the CLAVIER project agree on increasing numbers of tropical nights and decreasing numbers of frost days. The projected changes of the maximum number of consecutive dry days show a relatively clear annual cycle with decreasing maximum lengths of dry periods for winter and increasing maximum lengths of dry periods for spring, summer, and partly also for autumn.

For 2071-2100, this tendency is projected to continue under enhanced greenhouse gas concentrations. The frequencies of warm extremes (i.e. heat waves, hot periods, hot days) are expected to increase and the probability of cold extremes (i.e. frost days, cold days) is projected to decrease compared to 1961-1990. The number of days with precipitation could slightly decrease in Hungary, whereas days with heavy precipitation are expected to occur more often (*Szépszó 2008*).

For summer, the strong warming and drying can lead to the increased probability of severe droughts (*Mika 1988, 2007, Bartholy et al. 2007*). The larger amount of precipitation in March and April can result in high water level in the main rivers (*Radvánszky and Jacob 2009*). In the frame of the EU project CLAVIER, possible ecological and economical impacts of climate change have been evaluated more in detail. The clear impacts of climate change on water management, extreme events, natural ecosystems, human health and infrastructure underline the importance of the analyses of regional scale climate projections for the affected regions and sectors.

2.2 Droughts and their effects on the forest ecosystems in Hungary

2.2.1 Definition and characteristics of droughts, drought indices

Droughts are very complex natural disasters, many parameters are responsible for their occurrence (e.g. atmospheric circulation, precipitation, temperature, humidity, soil moisture). Contrary to other extreme meteorological events (flood, tornado, hurricane, hailstorm, frost), droughts are the most slowly developing ones, have the longest duration and the affected area is the largest. Beginning, end, probability and intensity of droughts are the least predictable among the atmospheric hazards (Pálfai 1994, Bussay et al. 1999, Jankó Szép et al. 2005, Dunkel 2009).

There is no general definition for droughts, it varies depending on the climate, soil and vegetation conditions of the region. Commonly used definitions are meteorological, agricultural, hydrological and socio-economic (Wilhite and Glantz 1985, Bussay et al. 1999). All these approaches seem to agree that droughts are caused by the precipitation deficit during a long time period. Figure 3 summarises the sequence of the most important processes related to droughts.

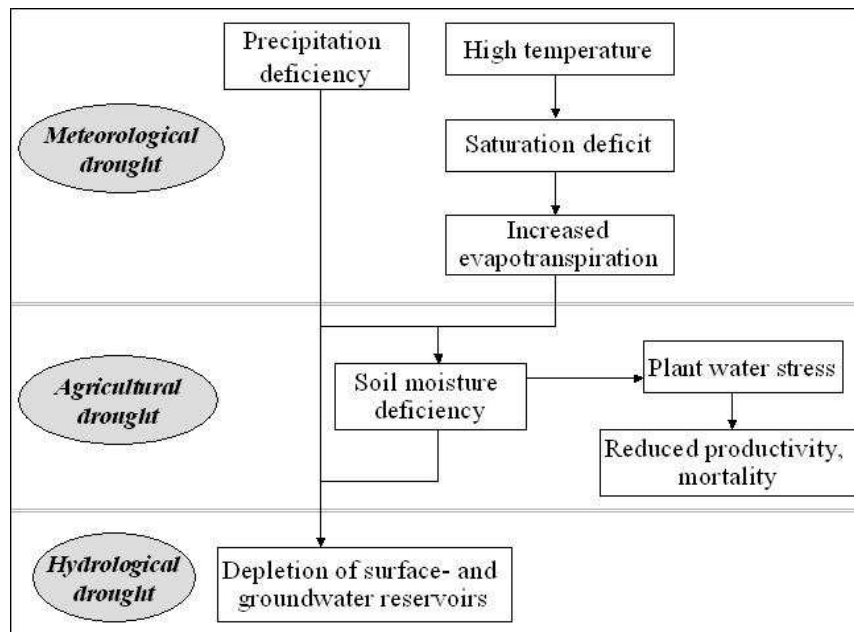


Figure 3. Sequence of droughts (modified after NDMC⁶)

Meteorological droughts develop, if the precipitation deficiency is large, relative to the long term mean of the analysed region. Other climatic factors such as high temperature, high wind and low relative humidity can significantly increase severity. Definitions of meteorological drought are region specific since the atmospheric conditions that result in deficiencies of precipitation are highly variable among regions.

Agricultural droughts occur if precipitation shortage causes soil moisture deficits. Available soil moisture can be also reduced by the increased evapotranspiration due to higher saturation deficit of air, which is induced by the higher temperature (Figure 3). The high potential evapotranspiration rate and/or the lack of available soil moisture leads to water stress of plants, reduced photosynthetic activity and crop production, or in extreme cases to mortality

⁶ <http://www.drought.unl.edu/>

(Szász 1988, Vig 2002, Bréda et al. 2006). For forests, available precipitation and soil moisture are the most important factor in the growing season. In the absence of winter precipitation, the soil does not fill up with water, which can induce earlier and much more severe summer droughts (Vig 2002).

Hydrological droughts are associated with the effects of precipitation deficiency on surface or subsurface water supply. They usually occur later than meteorological and agricultural droughts since it takes longer for precipitation deficiencies to show up in components of the hydrological system such as soil moisture, streamflow, and ground water and reservoir levels⁷. Although climate is a primary contributor to hydrological droughts, physical soil properties or changes in land use (e.g. deforestation) can affect their frequency and severity via altering the infiltration and runoff rates.

Characteristics of droughts. Droughts can be characterised by frequency, duration and severity. Frequency gives information about the number of occurrences in the investigated time period. The longer duration increases the impacts of droughts. Severity can be described by the magnitude of the precipitation and soil moisture deficits as well as of the environmental impacts. The most severe droughts develop, if large precipitation deficit occurs together with extremely high temperatures.

Drought as abiotic stress. The increased probability and severity of climatic extremes through climate change as well as the abrupt changes of the meteorological parameters lead to stress in vegetation. Changes of the extremes challenge the adaptability much more than the slow changes of the climatic means. Therefore these extremes are important limiting factors of the vegetation distribution. Response to water stress depends on the severity and duration of droughts as well as on the resilience, the adaptive and reproductive capacity of the plant species (Láng 2002). Severe drought as abiotic stress can lead to further biotic and abiotic damages, which will be discussed in Sect. 2.2.2 more in detail.

Drought indices

Severity and spatial extent of droughts can be investigated using several indices and functions, analysing satellite images or calculating the hydrologic water balance. Numerous studies deal with the review, characterization and classification of the drought indices (e.g. Tuhkanen 1980, Bussay et al. 1999, Maracchi 2000, Dunkel 2009). They are classified mostly based on their complexity or input parameters, the precipitation, temperature, evapotranspiration and soil moisture conditions. Many of them are suitable only in special circumstances or for special plant species. Therefore the application of these indices for other regions or species as well as the spatial comparison of the results are limited.

In this section an overview about indices is given, with focus on the commonly used ones in the agricultural and forestry sectors and which will be referred to in the later investigations.

Indices of precipitation anomalies provide information about the meteorological drought by calculation of the deviation from a normal precipitation value. These are the simplest drought indices that need only precipitation as input parameter. The *relative precipitation anomaly* index, which will be also used in the present work allows the spatial and temporal comparison of droughts.

⁷ <http://www.drought.unl.edu/>

It can be calculated as

$$\frac{P - \bar{P}}{\bar{P}} * 100 \quad (1)$$

where P [mm] is the precipitation sum in the investigated time period and \bar{P} [mm] is the long term climatic mean of precipitation.

The *Standardized Precipitation Index (SPI)* (McKee et al. 1993) was the first index, which could be applied to quantify the precipitation deficit for multiple time scales. SPI is well suitable for analysis of the duration and severity of agricultural and hydrological droughts over Europe (Bussay et al. 1999, Szalai and Szinell 2000, Lloyd-Hughes and Saunders 2002), since it shows a strong correlation with the discharge and the groundwater level.

The other very commonly used and accepted index is the *Palmer drought severity index (PDSI)* (Palmer 1965). It considers monthly precipitation, evapotranspiration, and soil moisture conditions to measure the departure of the moisture supply. Using the PDSI, the comparisons of soil moisture content and severity of droughts between months and between regions with different climate are possible (Dunkel 2009).

The *Pálfai Drought Index: PAI* (Pálfai et al. 1999) is suitable under Hungarian climate conditions to characterize the severity of droughts. Additionally to the precipitation and temperature conditions, the ground water level is considered.

Aridity indices describe the relation of the energy and water budgets. They are used to characterize agricultural and hydrological droughts and the climatic limits of the distribution of the ecosystems. The simplest indices give information about the aridity (or humidity) of the region or time period determining the ratio of the precipitation to potential evapotranspiration (Varga-Haszonits 1987).

Index based on remotely sensed parameters. In practice, the normalized difference vegetation index (NDVI) is often used as drought index since stress induced by water shortage results in altered spectral reflectance of vegetation (Wilhite and Glantz 1985).

The commonly used drought indices are not sufficient to represent drought conditions for forests, because drought sensitivity and tolerance of these ecosystems are different from agricultural plants. For application in the forestry, forestry aridity indices have been developed considering temperature and precipitation weighted for the month, in which these climatic conditions are especially important for the growth and production. In most of these indices soil moisture content is also taken into account.

The *Ellenberg-index (EQ)* (Ellenberg 1988) is commonly applied to model the distribution of zonal tree species (e.g. beech, *Fagus sylvatica*, L.; hornbeam, *Carpinus betulus* L.; sessile oak, *Quercus petraea* L.) over Europe (Standovár and Kerekes 2003, Jensen et al. 2004, Franke and Köstner 2007, Czúcz et al. 2010). It can be calculated based on the annual precipitation sum (P_{ann} [mm]) and the temperature mean in July (T_{VII} [°C]) as

$$EQ = \frac{T_{VII}}{P_{ann}} * 1000 \quad (2)$$

To describe the drought tolerance limit of beech in Hungary, a *beech tolerance index (TI_B)* has been developed (Berki et al. 2007). Considering the weighted precipitation sum and temperature mean for summer, the index corresponds to the special climatic needs of this tree

species. Under a critical threshold value, drought leads to mortality of beech. TI_B can be determined as

$$TI_B = \frac{0,2 * P_{III.} + 0,5 * P_{IV.} + P_{V.} + P_{VI.} + P_{VII.} + 0,8 * P_{VIII.}}{(T_{VI.} + T_{VII.} + T_{VIII.}) / 3} \quad (3)$$

where P [mm] is the precipitation sum and T [°C] is the temperature mean for the certain months. TI_B is also suitable to investigate the changes of beech distribution due to the increased drought probability projected for the future.

Contrary to the TI_B , the *forestry drought index* (*FAI*; *Führer and Járó* (2000)) is primary designed to simulate the effect of drought on the production. It can be applied also for other zonal tree species. The *FAI* be calculated as

$$FAI = \frac{T_{VII.-VIII.}}{P_{V.-VII.} + P_{VII.-VIII.}} * 100 \quad (4)$$

where P [mm] is the precipitation sum and T [°C] is the temperature mean for the corresponding months. Physiological water stress in forest-hydrology models is commonly described by the ratio of the actual and potential transpiration (*Federer et al.* 2003, *Zierl* 2007).

2.2.2 Drought vulnerability of the xeric forest limit

The xeric limit concept

For all zonal tree species the lower limits of distribution are ecologically very important. This limit is called xeric forest limit, which may be defined as “low altitude and low latitude limits of species distribution areas along a moisture balance gradient” (*Mátyás et al.* 2009, *Mátyás* 2010). It extends along the forest steppe and woodland ecotones of the Mediterranean, Southeast Europe, South Siberia and North America.

Whereas the upper forest limit is determined by the temperature conditions (called thermal limit), on the lower margin, presence of forests is primary limited by the climatic aridity (*Mátyás* 2009). Here, extent of the climatically suitable area of the certain tree species is determined by the frequency, severity and duration of droughts rather than by the climatic means. Small increase of the frequency of extremes can lead to drastic effects (growth decline or mortality of forests) in these regions (*Mátyás et al.* 2008). Therefore the study of long-term tendencies of droughts at the xeric limit becomes even more important with the projected climate change.

Hungary has special climatic conditions regarding forest vegetation zonation. Here, many of the zonal tree species have their lower limit of distribution, which are especially sensitive and vulnerable to the consecutive and severe dry periods.

Drought trends in Hungary in the 20th century and its effects on the xeric limit

Droughts are a recurrent feature in Hungary’s climate (*Szinell et al.* 1998). Due to the high annual variability of precipitation the relatively dry and warm weather events have a very high probability in this country.

Similar to global and continental trends, annual mean temperatures became higher during the second half of the 20th century, in particular, summers were warmer in the last 15 years (1990–2004) compared to the climate period 1961–1990 (figure 4). Precipitation decreased in the last century, the strongest negative trend appeared in spring (Szalai et al. 2005). The number of days with precipitation of more than 1mm decreased, whereas the intensity of precipitation events increased, leading to severe droughts and floods (Bartholy and Pongrácz 2007).

At the end of the 20th century a significant increase in drought frequency has been observed. Between 1983 and 1994, a continuous, extraordinarily dry period with severe droughts occurred in the Carpathian Basin (figure 4). Based on the Pálfai Drought Index (PAI) the Great Plane was the most affected region (Pálfai 1994). The PDSI values showed also a decrease, which refers to dryer conditions especially in the East Hungarian regions (Szinell et al. 1998, Bussay et al. 1999). The higher temperatures and the lower amount of precipitation led to decrease of the soil moisture content (Jankó Szép et al. 2005 Makra et al. 2002). This tendency seemed to continue in the first years of the 21st century. Impacts of droughts depend also on the sensitivity and vulnerability of the affected system. Bella et al. (2005) developed a method to define the drought vulnerability on regional scale, which consider the meteorological, hydrological, relief and soil properties of a certain area. Due to the unfavourable soil conditions over the Great Plane, pound water and drought occur often in the same year.

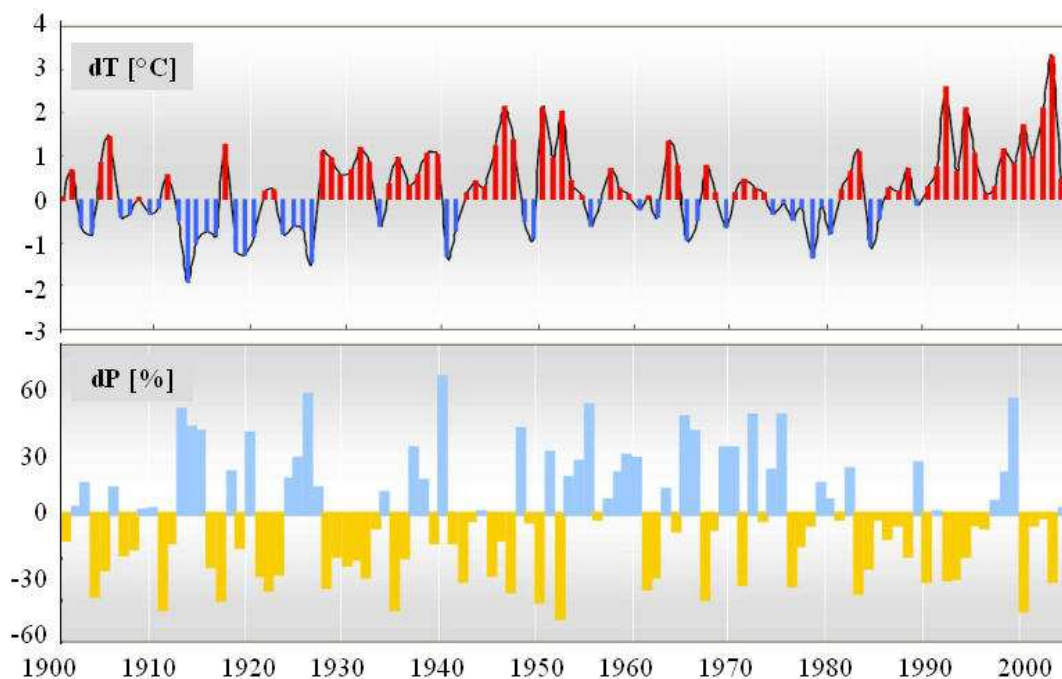


Figure 4. Average temperature (dT ; top) and precipitation (dP ; bottom) anomalies for summer 1900–2000 relative to the mean of 1961–1990 (after Szalai et al. 2005)

Observed impacts of droughts on forests

Several studies are dealing with the drought-related forest damages and mortality throughout the world (e.g. Breda et al. 2006, McDowel et al. 2009, Allen 2009). Droughts have been showed to have a major influence on the health conditions of zonal tree species in Hungary. Recurrent droughts at the end of the 20th century resulted in loss of vitality (Mátyás et al. 2007, Berki et al. 2009), and triggered the severe insect outbreaks and the appearance of pests

and pathogens in the beech and oak stands at the forest/steppe limit (Csóka 2007, Molnár and Lakatos 2007). Also the drought damages of forests reported by the National State Forest Service are very high in this time period (figure 5).

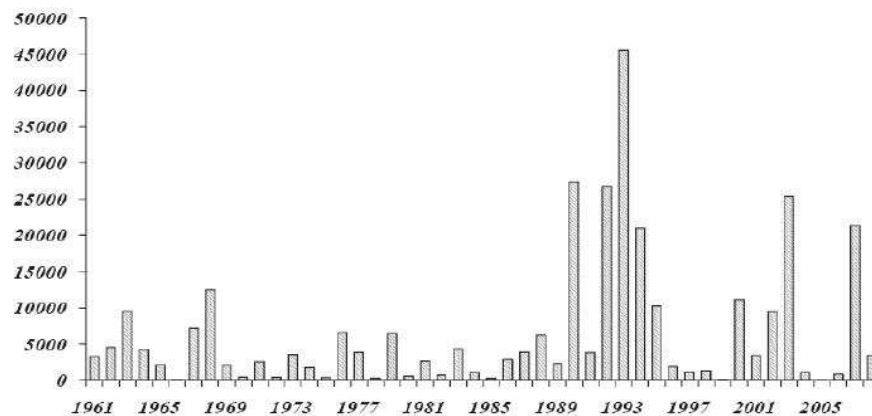


Figure 5. Reported drought damages in hectares 1961-2005 (Source: National State Forest Service)

In the southwestern regions of Hungary, after the extreme dry periods 1992-1994 and 2000-2004, an increasing decline of beech forests has been observed (Berki et al. 2007). Figure 6 visualises that decrease of the climatically favourable area for beech is the largest in this area relative to the beginning of the 20th century. It can be related to the decreasing trend of summer precipitation during the last century, which is stronger, than in other part of the country (Szalai et al. 2005).

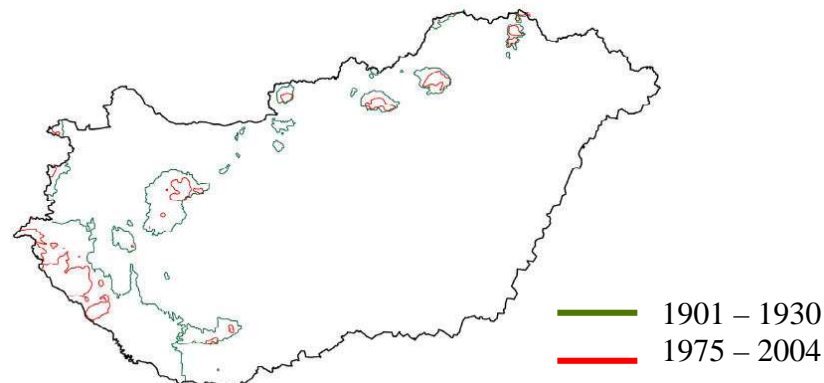


Figure 6. Change of climatically favourable area for beech (prepared by Rasztovits and Móricz)

Projected impacts of droughts on forests for the future

Climatic sensibility and shift of the lower forest limit in Hungary has been investigated and modelled first by Mátyás and Czimmer (2004) assuming different temperature and precipitation scenarios. If the probability and severity of climatic extremes increase in the future, zonal beech may almost disappear from Hungary (Berki et al. 2007, Czúcz et al. 2010). Effects are predicted to occur first at the xeric limits of the distribution causing health decline and mortality of the tree species. Here, open woodlands could potentially replace a significant part of present-day closed forests (Mátyás et al. 2008). Shifts triggered by current and future climatic changes are too fast compared to spontaneous natural processes (Mátyás et al. 2009) that underline the urgent need of adaptation and mitigation strategies to help the maintenance of these ecosystems.

2.3 Feedback of forests on climate

2.3.1 Climatic role of forest ecosystems

Terrestrial ecosystems interact with the atmosphere through exchanges of energy, moisture, momentum, mineral aerosols, carbon-dioxide and another trace gases. Effects of land surface on climate, which are referred as *feedbacks* in this work, can be divided into two categories: biogeophysical and biogeochemical. Vegetation affects the physical characteristics (e.g. colour, roughness, water conductivity) of the land surface (*biogeophysical effects*), which control the partitioning of available energy at the surface between sensible and latent heat, and the partitioning of available water between evapotranspiration, soil water and runoff. Through *biogeochemical effects*, ecosystems alter the biogeochemical cycles, thereby change the chemical composition of the atmosphere (Betts 2001, Bonan 2002, Pitman 2003, Bonan 2004, Feddema et al. 2005). These land-atmosphere interactions can enhance or weaken the climate change signal.

This chapter is focusing on the role of land surface, particularly forests, in the

- surface energy balance,
- surface hydrologic cycle,
- vertical turbulent exchanges.

Surface energy balance

The energy balance at the land surface can be written as

$$R_n = (1 - \alpha) * S \downarrow + (L \downarrow - L \uparrow) = H + \lambda E + G + F \quad (5)$$

R_n [W m^{-2}] is the net solar radiation absorbed by the ground surface after accounting for reflection of solar radiation and emission of net long-wave radiation. An amount of energy ($S \downarrow$ [W m^{-2}]) reaches the Earth's surface and some is reflected, depending on the albedo α . Long-wave radiation is also received ($L \downarrow$ [W m^{-2}]) and emitted ($L \uparrow$ [W m^{-2}]) by the Earth's surface, depending on the temperature and emissivity of the land and atmosphere. R_n is balanced by sensible heat (H [W m^{-2}]), latent heat (λE [W m^{-2}]), heat storage (G [W m^{-2}]) and the chemical energy (F [W m^{-2}]) stored during photosynthesis and released by respiration (Pitman 2003, Bonan 2004, Bonan 2008b).

Albedo (α) is defined as the fraction of incoming solar radiation that is reflected by a surface (Bonan 2004). The surface albedo influences the short wave radiation budget, hence the energy availability at Earth's surface (Betts 2001, Bonan 2002). It strongly depends on the wavelength of the solar radiation and on the surface properties. Surface albedo varies not only spatially but also temporally with the solar angle, vegetation phenology and with snow and ice cover. Albedos generally range from 0.05 to 0.15 for coniferous, 0.15-0.2 for deciduous forests and 0.16-0.26 for grasslands (Bonan 2004). In the regions, where forests have lower surface albedo (are darker) than grasslands, they receive more incoming solar radiation, which leads to the increase of net radiation and higher temperatures of the vegetation surface. This process, which is called *albedo-effect*, is one of the basic biogeophysical feedbacks of vegetation on climate and is typical in boreal regions (Bonan et al. 1992, Brovkin 2002, Kleidon et al. 2007).

Vegetation also influences the absorption of energy by the surface via modification of the surface albedo, thus alteration of energy partitioning between sensible and latent heat.

Sensible heat flux in the atmosphere is a flux of energy, which heats the surface without evaporating a liquid from it. **Latent heat** is the energy required to evaporate water from the evaporating surface. When water evaporates, energy is absorbed from the evaporating surface without a rise in temperature, which is the latent heat of vaporisation (Bonan 2008b). The latent heat flux cools the surface because of the large amount of energy required to evaporate water.

The sensible heat flux is directly proportional to the temperature difference between the surface and air, whereas the latent heat flux is directly proportional to the vapour pressure difference between the surface and air (Bonan 2004). Both are dependent from the surface roughness length and the wind speed.

The processes related to the surface energy and water balance are basically determined by the ratio of sensible heat flux (H [W m^{-2}]) to latent heat flux (λE [W m^{-2}]), which is called **Bowen-ratio** (BR).

$$BR = \frac{H}{\lambda E} \quad (6)$$

When the magnitude of BR is less than one, a greater proportion of the available energy at the surface is passed to the atmosphere as latent heat than as sensible heat. In this case, evapotranspiration is not limited by the soil water, the boundary layer is cooler and moister, which should increase instability and should lead to more convective clouds (Kleidon 2004). The converse is true for values of BR greater than one.

Surface hydrologic cycle

Land-atmosphere interactions related to the energy and water cycle are linked by the processes of **evapotranspiration**. Evapotranspiration is a collective term for all the processes, by which water in the liquid or solid phase at or near the earth's land surfaces becomes atmospheric water vapour (Dingman 2002). It is the sum of transpiration, interception, bare soil evaporation and evaporation from open water and snow.

Transpiration is the vaporization of water from the saturated interior surfaces of leaves to the surrounding air via microscopic pores called stomata (Hungate and Koch 2003). Stomata open and close in response to environmental factors such as light, temperature, CO_2 concentration and soil water. **Interception** and its hydrological role is introduced and discussed more in detail in Sect. 2.3.2. **Bare soil evaporation** is the vaporization of water directly from the mineral soil surface. It is only a small amount under forests because of the litter on the ground (Hewlett 1982).

Vegetation is basically influencing the water budget through interception and transpiration, which are affected by the leaf area and the rooting depth of the plants.

Leaf area index (LAI) is defined as a one sided green leaf area per unit ground area (Bonan 2008b). It affects the radiative transfer process within the canopy and evapotranspiration from the plant surface. LAI varies temporally with age and phenology. Its value differs strongly among plant communities. Measurements by Járó (1959) showed the large variability of LAI (from 2.5 to 8.4) in different Hungarian forest types depending on age and site conditions.

Forests have larger leaf area compared to other vegetated surfaces. Larger LAI warms the surface due to lower albedo. But larger LAI also results in larger roughness length thus higher

evapotranspiration rate in forests (Betts et al. 1997), which influences the exchange of both latent and sensible heat fluxes. The increase of the latent heat flux through transpiration is the major contributor to the cooling of the surface. The process is called *evaporative cooling effect*, which is the other basic biogeophysical feedback of forests on climate. It dominates primarily on the tropical regions leading to cooler and moister atmospheric boundary layer that may feed back to increased precipitation by affecting the larger-scale circulation (Brovkin 2002, Kleidon et al. 2007).

Vertical profile of leaf area in the forest canopy affects the distribution of radiation in the canopy. Larger leaf area increase the canopy shading, which leads to cooler air temperatures in the stem area, decrease of net radiation at the soil surface, therefore less bare soil evaporation in summer (Pitman 2003, Chang 2006).

Due to the higher evaporation rate, forests may increase the amount of precipitation. Chang (2006) summarizes the arguments and counterarguments to the possible precipitation-increasing role of forests. It is often assumed that forests enhance the precipitation formation increasing the effective height of mountains, which leads to an increase of the orographic precipitation. The higher transpiration rate of forests can lead to the increased vapour content of the air, which promotes the condensation and precipitation formation in the forested area. The basic counterargument is that the horizontal distribution of precipitation is mainly affected by the general circulation and topographic characteristics rather than by forests. For the precipitation formation water vapour content is not enough (Chang 2006).

The amount of precipitation, which reaches the ground surface infiltrates into the soil. Rooting depth and the soil texture determine the amount of water that can be stored in the soil, which is potentially available to the vegetation for transpiration (Kleidon and Heimann 1998). Available water holding capacity can be defined as the difference between field capacity (the amount of water after gravitational drainage) and wilting point (the amount of water in the soil when evapotranspiration ceases; Bonan 2004). Rooting depths have a large variability depending on plant species soil texture and soil water conditions.

Deep roots increase the water uptake and the amount of transpiration. It is an important characteristic in dry spells when moisture of advective origin diminishes. If there is enough moisture in the soil to continue evapotranspiration, local evapotranspiration can be an important contributor to precipitation. This is defined as precipitation recycling (Bisselink and Dolman 2009), which is a land-atmosphere feedback process from local evapotranspiration to local precipitation that acts as a mechanism in central-Europe to keep precipitation at stable level.

Vertical turbulent exchanges

Surface roughness affects the turbulence activity close to the ground surface. The intensity of the mixing is determined by the roughness of the surface and the strength of surface winds. Taller vegetation like forests are rougher and have lower aerodynamic resistance than shorter vegetation. It creates more turbulence increasing the transfer of sensible and latent heat away from the surface (Bonan 2004, Betts 2007), enhance evapotranspiration, which promotes the cloud- and precipitation formation.

Vegetation height determines the thickness of the layer above the ground surface, in which the microclimatic effect of vegetation is sensible. On local scale it is an important parameter, especially for forests, which can be characterised by their own microclimate in the crown and

stem area. The energy and matter exchange between the atmosphere and the upper crown is often completely different than those between the lower crown and the trunk space and the soil (Foken 2008). So in forests, characteristic profiles for temperature, humidity and wind can develop, which influence the atmospheric boundary layer climate. In atmospheric models, vegetation has mostly no height but the sensitivity of the simulation results of this value on both global and regional scale is unknown.

2.3.2 Interception and its hydrologic role

Forests can greatly affect the hydrologic budget at the surface through the interception of precipitation (Brutsaert 2005). Forest catchments generally evaporate more water than those covered with shorter vegetation (Bosch and Hewlett 1982), mainly due to the greater rainfall interception loss from forest. The process of interception and the most important measurement methods and interception models are overviewed in Móricz et al. (2009).

Basic definitions

In the literature there are several definitions for interception (e.g. Hewlett 1982, Dingman 2002, Brutsaert 2005, Chang 2006), which are often inconsistent with each other. Here, definitions related to the process of interception are introduced, which are applied in this work. Interception occurs from rain and from snow. In this chapter only the rainfall interception is introduced.

In forests, only a fraction of the precipitation reaches the soil surface. The other part evaporates from the vegetation during and after the precipitation event, which is the **interception loss**. In a forest stand interception loss is the sum of the crown interception loss and the litter interception loss (Dingman 2002; figure 7).

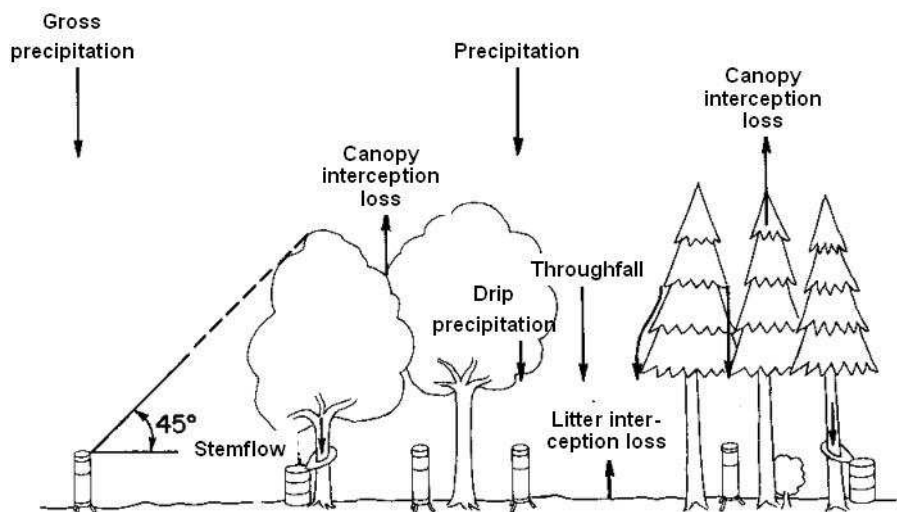


Figure 7. Precipitation in forests (modified after Hewlett 1982)

In the process of interception are not only losses but also wins by condensation and sublimation processes as vapour, dew, rime and fog (Balázs and Führer 1990-91, Führer 1994, Brutsaert 2005).

Interception loss will be referred as *interception* in this work. It can be determined as the difference of the precipitation in the open air place (*gross precipitation*) and the *stand precipitation* in forest, which is the sum of throughfall, drip precipitation and stemflow.

Throughfall is the precipitation that falls directly to the forest floor without touching the canopy (*figure 7*). From the vegetation, precipitation drips to the ground (*drip precipitation*), or flows down along stems and major branches, which is the *stemflow* (*figure 7*).

Canopy storage capacity is the amount of water left on the canopy at the end of the storm, under conditions of zero evaporation. The maximal storage capacity is reached when surface elements are fully saturated (*Brutsaert 2005*). It is the one of the most crucial parameters that basically determines the potential amount of water, which is available for evaporation. Storage capacity ranges from 0.5 to 4 mm in needleleaf evergreen forests and up to 2.6 mm in broadleaf deciduous forests (*Hörmann et al. 1996*). In modelling studies it is also called *skin reservoir content*. In the simulations, precipitation falls to the soil surface only after the skin reservoir is filled (when the amount of precipitation is larger than the maximal storage capacity).

Process of interception and the determining meteorological conditions and canopy factors

In nature, during and after the rainfall event the processes related to interception can be divided into the following phases (*Aston 1979*):

- *Wetting phase*. At the beginning of the rainfall event canopy storage starts to fill and due to the intense evaporation the vapour content of the air strongly increases. Nearing to the reach of the saturation of the air, increase of the evaporation becomes slower and wetting of the canopy intensifies.
- *Saturation phase*. The crown is fully saturated, the maximal storage capacity of the canopy is reached.
- *Drying phase*. After precipitation has ceased the canopy surface gets dry. Evaporation is continuing depending on the meteorological conditions.

Amount of interception is influenced by the actual weather conditions and canopy characteristics.

Meteorological conditions are

- *Duration, intensity and frequency of the precipitation event*. In case of a brief, intense storm, the canopy wets once and interception is limited primarily by the canopy storage capacity. For a low intensity storm with longer duration, the canopy stays wet and the interception loss (limited primarily by the actual weather conditions) can be larger (*Horton 1919, Zeng et al. 2000*). Evaporation is the largest at the beginning in the wetting phase so higher frequency of the rainfall events (higher wetting frequency) leads to the larger amount of the stored and intercepted precipitation. These emphasise the role of the small precipitations with low intensity in the total interception amount (*Kucsara 1996*). Consequently, changes of the frequency and intensity of the precipitation events under future climate conditions may affect the interception.
- *Energy balance* (radiation energy, air temperature). Warmer temperature results in more intense evaporation thus larger interception (*Hewlett 1982*).
- *Vapour content of the air*. Higher water vapour content in the air leads to the decrease of the saturation deficit therefore weakens evaporation.
- *Wind*. Higher wind velocity enhances evaporation, which results in larger interception rate. On the other side precipitation is shaken from the canopy by wind and the amount of the drip precipitation increases (*Hörmann et al. 1996*).

Canopy characteristics are

- *Leaf area index (LAI)*. Larger leaf area enables larger amount of precipitation stored on the canopy surface, which is available for evaporation.
- *Type of vegetation*. Coniferous forests have larger leaf area index and have foliage year-round, therefore intercept more precipitation annually than deciduous forests. The difference between them can be 5-10% (Járó 1980, Führer 1984, Kucsara 1996). Amount of interception also varies among tree species: annual mean of interception amount is 37% for spruce, 28% for beech and 25% for sessile oak under Hungarian conditions (Führer 1994). The smaller interception of beech can be explained by its smaller storage capacity and larger stemflow compared to spruce.
- *Canopy density and closure*. The denser the foliage the greater amount of water can be stored.
- *Age and vitality of the canopy*. The older canopies have larger leaf area but also larger crown closure, which leads to smaller throughfall rates (Balázs and Führer 1990-1991).
- *Bark characteristics*. Smooth barks have greater stemflow than rough barks (figure 8). For Hungary, beeches can be characterised by the largest stemflow rate (> 8%) turkey oak and poplars have 4-8%, whereas spruces have < 4% (Führer 1984; Kucsara 1996).
- *Stem area index (SAI)*. In the case of smooth trunks, larger stem area enhances the amount of stemflow. But for rough trunks, the larger storage capacity enables larger amount of evaporation.



Figure 8. The smooth trunk of beech (left) and the rough trunk of alder (right)

- *Branching patterns*. Upright branches support stemflow compared to horizontal branches.
- *Leaf shape and orientation*. Leaves which are concave and elevated horizontally above the pare are able to contribute to stemflow (Crockford-Richardson 2000).

In Hungary, interception measurements in forest ecosystems have been carried out since the 1970th (Führer 1984, Járó 1980, Koloszár 1981, Kucsara 1996, Simonffy 1978-79; Sitkey 1996). The same methods are also applied in this study (Sect. 5.4).

Interception amount varies from 10 to 40% of gross precipitation depending on numerous parameters like tree species, forest density, canopy structure, vegetation physiology and site

conditions. The variability of interception within the tree species (depending on age or location) can be larger than its variability between the tree species. Sufficient measurements for the canopy properties are seldom available, therefore in the models these properties are mainly adopted based on local experiences.

Since interception is site-specific and its spatial variability is large, the spatial extrapolation of results of interception functions for other sites and the comparison between different forest ecosystems is quite difficult. It can be only achieved if not only the effects of the climatic and precipitation conditions but also the morphological properties of the investigated canopy are known (*Führer* 1984). For adequate description of interception in large areas it is necessary to include both the effects of spatial variability of canopy storage and rainfall.

Modelling of interception

In climate- and forest hydrology models the process of interception is described quite simplified because of the large spatial and temporal variability of the process. There are functions and models developed for interception only, which will be overviewed in this section, but it is impossible to include all of these parameters and processes in models designed for simulation of complex atmospheric processes over larger areas.

Modelling via regression analysis. Early studies assumed a linear function between the amount of precipitation and interception loss. Interception loss was described as a function of the storage capacity of the plant surface, the duration of the precipitation and the evaporation rate during the precipitation (*Horton* 1919). But this approach does not give any correct result for small precipitations and in the early wetting phase.

Amount of available water for evaporation from the vegetation surface strongly depends on canopy storage capacity, which cannot be measured directly. *Führer* (1984) applied saturation functions to determine this variable. Based on his assumption, interception is the function of precipitation and storage capacity, if evaporation during the rainfall is neglected. For this approach, weakly measurement of stand precipitation in the forest is sufficient.

According to *Kucsara* (1996) stand precipitation should be measured and interception should be calculated for each precipitation event rather than averaged over longer time period. After classification of precipitation events by their amount it was concluded that the role of small-precipitations in the total interception amount is quite important. He determined canopy storage capacities for different forest ecosystems applying exponential precipitation-interception functions (allowing evaporation during the whole process), which describe the process and amount of interception more realistic in the investigated canopies (*Kucsara* 1996). In the development of these functions was an important criteria that they should be based on data, which are available from measurements.

Physically-based models require the measurement of gross- and stand precipitation on larger temporal resolution (mostly in hourly time step). The first conceptual, physically-based model for interception was developed by *Rutter et al.* (1971). Evaporation is calculated based on a potential evapotranspiration rate for wet canopy using the Penman-Monteith equation with a canopy resistance zero. If actual canopy storage exceeds the storage capacity, evaporation takes place at the potential rate, else evaporation is reduced in proportion to actual canopy storage and the storage capacity. This approach is simplified by *Gash and Morton* (1978) and modified by *Valente* (1997) for the application to sparse canopy. In the later the area of interest is partitioned into the fraction covered by a forest canopy and the open fraction. The canopy storage is filled by rainfall and emptied by drainage and evaporation. Drainage from the canopy occurs when the canopy storage capacity is exceeded.

For studying interception on local scale in this work the hydrologic model BROOK90 has been selected, which uses a simplified version of the Rutter-model.

Limitation of these models is that they are unable to represent the spatial variability of the hydrologic processes and parameters. Furthermore, there is a general lack of data to parameterise these models and the relative large spatial variability in those data that are available.

Interception has a crucial role in the water budget of forest ecosystems. This amount of water does not reach the ground surface, is not available for transpiration. But it can evaporate in the potential rate enhancing the vapour content of the air and the evaporative cooling effect of forests. In forests evaporation of intercepted water occurs at rates several times greater than for transpiration under identical conditions. Thus intercepted water disappears quickly and interception loss replaces transpiration only for short time periods (*Dingman 2002*).

2.3.3 Climatic effects of land cover change

Climate change and anthropogenic land use are the two main driving factors of land cover- and land use change. At regional to global scales, changes in the land cover affect the water- and energy balance, thus have an influence on the natural climate variability (*Grassl 2003, Pitman 2003*). Recent research projects (e.g. iLEAPS⁸) aim the understanding of processes and feedbacks in the land-atmosphere interface even more frequent. So far, much of our understanding of how forests affect global or regional climate comes from atmospheric models and their numerical parameterisations of Earth's land surface (*Bonan 2008b*). In the last two decades several studies investigated the sensitivity of these models to change of a single land surface parameter as well as the climatic impacts of land cover change (mostly afforestation and deforestation) for the past (e.g. *Pongratz et al. 2009*) and for the future (e.g. *Sánchez et al. 2007*).

One of the most cited global scale sensitivity studies for land cover change was prepared by *Kleidon et al. (2000)*. The maximum effect of vegetation changes on the global climate has been investigated by assuming complete afforestation ('green planet') on the Earth and compared this to the complete deforestation ('desert world') experiment. In the presence of the 'green planet', land surface evapotranspiration more than tripled, land precipitation doubled and near surface temperatures was lower by as much as 8 K.

Based on the global model studies the effect of vegetation is not the same around the globe. In this chapter, studies are selected and introduced, which represent the differences of the climatic feedbacks of forest cover change among regions and research methods.

Researches on climate-vegetation interaction are mostly concentrated on regions, where the interaction is the most pronounced: the mid- and high latitude forests in the northern hemisphere (boreal forests), subtropical deserts and semideserts in North Africa (Sahara/Sahel region), tropical rainforest in South America (Amazon forest) and the Mediterranean area.

Boreal forests have the greatest biogeophysical effect of all biomes on annual mean global temperature, which is larger than their effect on the carbon cycle. They warm both winter and spring air temperatures compared to tundra vegetation or bare ground due to the albedo-effect. The darker coniferous forest masks the snow cover resulting in lower surface albedo when snow is present. This leads to an earlier springtime warming, which accelerates snowmelt and

⁸ Integrated Land Ecosystem-Atmosphere Processes Study; <http://www.ileaps.org>

extends the growing season, which is in turn favourable for the presence of forests (Bonan et al. 1992, Brovkin 2002, Kleidon et al. 2007, Bonan 2008a).

The northwards shift of the upper tree line due to global warming is a positive feedback to the climate change, especially in winter and spring. For Siberia a possible change of vegetation from tundra to boreal forest leads to a warming of up to 1°C (Göttel et al. 2008). Consequently, the biogeophysical feedback of deforestation in the boreal region leads to higher surface albedo thus cooler temperatures (Brovkin et al. 1999), which may offset the forcing from carbon emission (Bonan 2008a).

Tropical forests maintain high rates of evapotranspiration also during the dry season. In this region, surface warming arising from the low albedo of forests is offset by the strong evaporative cooling. Additionally to the relative strong carbon sequestration of these ecosystems, it is a positive effect that reduces global warming (Bonan 2008a).

Numerous climate model studies confirm that large-scale conversion of Amazon forest to pasture creates a warmer, drier climate. The biogeophysical consequences of the deforestation are the increase of surface albedo, reduction of net radiation, decrease of the rooting depth, roughness length and leaf area index, which alter the water-, energy-, and momentum exchange between the surface and the atmosphere (Pielke et al. 1998, Chase et al. 2000). These changes lead to the change of the moisture availability, the decrease of evapotranspiration and smaller evaporative cooling effect of forests.

Based on the results of global climate model simulations, replacement of these forests to degraded pastures would cause the decrease of the mean annual evapotranspiration by 30%, the decrease of the mean annual precipitation by 25% and increase of mean surface temperature by 1-2.5°C (e.g. Shukla et al. 1990, Stich et al. 2003).

Temperate forests. Whereas results of model simulations agree quite well in the biogeophysical effects of boreal and tropical forests, the net climate forcing and benefit of temperate forests is highly uncertain (Bonan 2008a, Jackson et al. 2008). Reforestation and afforestation may sequester carbon, but the albedo and evaporative forcings are moderate compared with other forests and the evaporative influence is unclear, they can enhance or dampen the climate change signal (Bonan 2008a).

A number of climate model studies suggest that replacing forests with agriculture or grasslands in temperate regions cools the surface air temperatures (e.g. Bonan, 1997, Bounoua et al. 2002, Oleson et al. 2004). Consequently, trees warm surface temperature relative to crops due to their lower albedo. For North American climate, Oleson et al. (2004) found that natural needleleaf evergreen and broadleaf deciduous vegetation maintained a warmer summer climate compared to the present-day crops, which can be characterised by larger evaporative cooling in the growing season than forests. This study agrees with the conclusions of Bonan (1997) for the same region. Crops as the present vegetation cover caused not only the cooling of daily mean temperature but also a reduction in the diurnal temperature range. In these studies the albedo of the land surface seems to play the determining role in the simulated climate. Results refer to the climatic conditions above the canopy rather than to the microclimatic effects within the forest stand, which are not considered in the simulations.

Other studies show the opposite, that temperate forests cool the air compared with grasslands and croplands. Copeland et al. (1996) investigated the climatic effects of the land use change also in the USA. Converting of forests to cropland resulted in the increase of the Bowen ratio and increase of temperatures by up to 0.22°C. In spite of the albedo increase, changes in the

partitioning of that between latent and sensible heat flux determined the feedback of the land use change on the temperature.

For the Canadian woodland-prairie border *Hogg et al. (2000)* also found that the presence of deciduous forests affect the energy and water balance, resulting in cooler temperatures and higher precipitation rate in the forested area. The leaf phenology has a strong control over the land-atmosphere interaction influencing on seasonal patterns of temperature and precipitation. Consequently, the effect reaches a maximum during the summer season.

For Western Australia, reforestation (i.e. from grassland or crops to forest) reduces warming caused by the enhanced greenhouse gas concentrations in the middle and at the end of the 21st century (*Pitman and Narisma 2005*). The cooling effect was the result primarily of the increase in leaf area index and the enhancement of the turbulent exchange of energy that led to a corresponding increase in the latent heat flux.

This study also points out that significant change of climatic variables occurred in areas where land cover was changed, with the exception of precipitation. Precipitation has more complex spatial behaviour, changes can occur also remote from the location of the land surface modifications due to the long-distance transport of moisture (*Zhao et al. 2001, Brovkin 2002, Pitman and Narisma 2005, Sánchez et al. 2007*).

Quite few studies investigate vegetation-atmosphere interactions in Europe. The most of them concentrate on the *Mediterranean region*, which has been extensively deforested over the past 2000 years. Based on global climate model simulations *Dümenil Gates and Ließ (1999)* concluded that complete deforestation in the Mediterranean region leads to a cooling at the surface due to the albedo-effect. Historical land use change seemed to contribute the dryness of the current climate through the reduced precipitation amount during the summer.

Detailed analyses of the spring and summer months showed opposite results (*Heck et al. 2001*). Using regional climate model simulations, climatic conditions under the natural, potential vegetation cover (i.e. without human influence) have been compared to the present-day conditions. For potential vegetation cover (mainly forests), in the period from April until mid-July evapotranspiration increased causing cooler and moister conditions. In mid-July, a soil moisture value dropped below the critical value and transpiration was almost completely inhibited (for August, evapotranspiration was 25% lower with forests than with present-day vegetation), which resulted in dryer and warmer summer. In northern Europe, moistening effect of forests dominated over the whole time period, but had smaller amplitude.

Sánchez et al. (2007) investigated the sensitivity of the climate as well as climate change signal (2070-2100 vs. 1960-1990) to different vegetation descriptions over Europe, concentrating on the Mediterranean area. The results indicate a high sensitivity of summer precipitation processes to vegetation changes. Vegetation types dominated by trees led to larger amount of evapotranspiration and precipitation compared to the grass dominated types both for the past and the future time periods. But for the Mediterranean region climate change signals are robust and not critically sensitive to the proposed vegetation descriptions (different vegetation descriptions resulted in different future summer climates for Europe but produce similar climate change impacts).

For eastern Hungary, *Mika et al. (2006)* showed the effects of the documented land cover change on the radiation balance of the surface-atmosphere system, but in this study the corresponding changes of temperature and precipitation on regional scale still remained an open question. Based on mesoscale simulations for the Carpathian Basin (*Drüszler et al. 2009*), land use change during the 20th century (especially urbanisation) resulted in increase of temperature and decrease of relative humidity. For precipitation conditions no significant changes occurred.

2.4 Models as research tools for studying climate change

A *model* is an abstraction of reality, represents complex systems in a simplified way. Models have been constructed for various purposes on different scales, to investigate and understand the spatial and temporal processes and impacts, not only in the environmental sciences.

2.4.1 General aspects of climate modelling

The past and future evolution of the climate system can be described by numerical models. The climate system can be characterized by a high complexity of exchange processes (mass, energy, impulse) and interactions. In climate models a fictive grid is determined over the Earth surface, and the atmosphere (and ocean) is divided into discrete layers. Within each grid box of these three dimensional grid the new climate variables are computed integrating a set of prediction equations for each time step.

Climate models are essential research tools for providing valuable insight into the atmospheric processes. They can be used for simulation of the present and future climate tendencies.

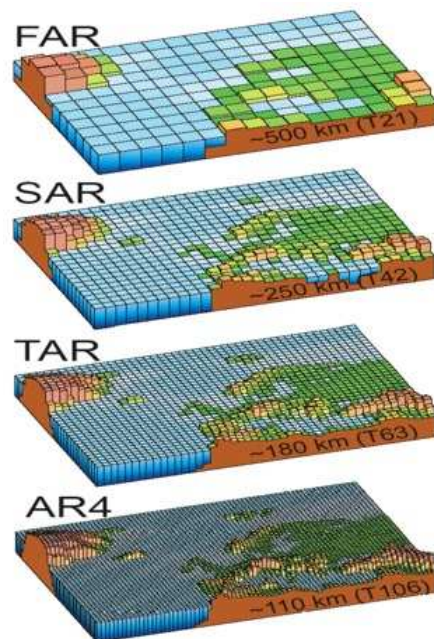


Figure 9. Horizontal resolutions applied in the simulations for the first (FAR), second (SAR), third (TAR) and fourth (AR4) IPCC assessment reports

General Circulation Models (GCMs) are applied for simulation of the entire climate system over the Earth, the general evolution of the circulation due to changes in the chemical composition of the atmosphere. They are able to represent fairly realistically and comprehensively many aspects of the global circulation over long time periods (i.e. several hundred years). The horizontal grid spacing varies between 110 and 500 km (*figure 9*).

GCMs can be run either for the atmosphere only, or as a coupled atmosphere-ocean model.

2.4.2 Regional climate modelling

Regional climate models differ in complexity and character from the general circulation models. The horizontal resolution of GCMs is not fine enough to resolve small-scale atmospheric circulations, which are affected by orography or details of the land surface. To produce detailed climate simulations for a selected region, a limited-area model can be nested within a global GCM (*figure 10*). The technique is like zooming on the area of interest, which has finer horizontal resolution within the global model. Such nested models are the regional climate models (RCMs) (*McGregor 1997*).

Nesting methods: the dynamical downscaling of GCMs is usually carried out in one-way mode, which means large-scale meteorological fields from GCM runs provide initial and time-dependent lateral boundary conditions for the high-resolution simulations, and there is no feedback from the RCM to the large scales. Recently, also two-way nesting methods have been developed and applied (e.g. *Lorenz and Jacob 2005*). Here, the circulations produced by the nested regional model feed back to the global model.

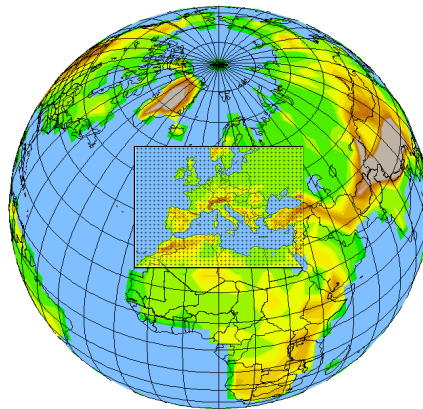


Figure 10. Illustration of the concept of nested models with finer resolution

Advantages and applications of RCMs

Many responses to climate change will be regional (e.g. change of the water availability, land use change) and local. Society is interested in regional consequences of global changes, since they have to decide for the best adaptation and mitigation strategies.

Regional climate models (e.g. *Christensen et al. 1996, Giorgi and Mearns 1999, Jacob et al. 2001, Lenderink et al. 2003, Vidale et al. 2003*), are useful tools for the analysis of regional energy and water cycles as well as for the long-term prediction of climatic changes on regional scale (*Jacob et al., 2001, 2007, Hagemann et al. 2004, Déqué et al., 2005*). The fine horizontal resolution allows more detailed description of the land surface and small-scale atmospheric circulations, which are affected by orography and land cover. RCM in climate mode has the advantage that mesoscale phenomena, which are not present in the driving fields due to the coarse horizontal resolution and which are initiated through a more detailed land surface representation in the regional model, can develop within the simulation domain (*Jacob 2001*). Studies comparing simulation results of GCMs and RCMs (*Déqué et al., 2005, Hagemann et al. 2008*) concluded that the RCMs are producing detailed distributions of precipitation and temperature, which are also in better agreement with observations.

Regional modelling with high horizontal resolution is essential and their advantages can be utilised

- for regions, where regional climate tendencies differs from the global ones, or are especially affected by climate change (e.g. coastal zones),
- for regions, which modify the global climate change signal (e.g. Arctic),
- for analysing extreme events (e.g. hurricanes, floods, droughts, storms) on country scale, which cannot be resolved by the GCMs,
- for regional and local impact assessment, especially on regions with complex topography and high elevation (e.g. Alpine region, since mountain ranges can strongly influence the spatial patterns of precipitation change through the orographic precipitation shadowing effect) as well as on areas with heterogeneous land cover (e.g. agriculture, forestry mosaics).
- for the projection of future changes in the individual components of the water and energy cycles through climate- and land cover change.

Numerical weather prediction is basically different from climate modelling. In a numerical weather forecast weather events should be exactly forecasted for short time periods (i.e. 3-5 days). Whereas for long-term climate simulations it cannot be expected that every single weather event is calculated realistically in time and space. Only the climate, the long-term tendencies (e.g. climatic means, probability of extremes) will be represented (*Jacob 2001*). It is also valid for the simulation of the land surface-related processes: due to the large variability of the surface–atmosphere interactions it cannot be expected that all site-specific processes are described in full complexity. But the RCMs are well suitable to simulate the order of magnitude and the direction of the feedbacks for longer time periods.

General characteristics of regional climate models

In this section the most important characteristics of RCMs are introduced, which will be referred to in *Sect. 4.1* by describing the applied model and the experimental set-up.

The climatology of a regional atmospheric model is determined by the dynamical equilibrium between two factors: the information provided by the **lateral boundary conditions** and the internal model physics and dynamics (*Giorgi and Mearns 1999*).

RCMs are initialised and driven at the lateral boundaries using data from (re)-analysis products or global model output. Re-analyses are referred to as ‘perfect boundary conditions’ (*Jacob 2001*). They describe the state of the atmosphere close to reality, since they are based on the observed state of the atmosphere. Re-analyses experiments (e.g. reanalysis product provided by ECMWF (European Center for Medium-Range Weather Forecasting; *Uppala et al. 2005*) are also used to validate the RCM simulations.

The smaller the **model domain**, the closer is the selected region to the lateral boundaries and the larger is the influence of the lateral boundaries on the simulation results. Choice of a domain, in which the area of interest is far as possible from the lateral buffer zone allows the full development of the model’s internal circulation and minimizes the effect of the coarse resolution lateral forcing (*Giorgi and Mearns 1999*). **Horizontal resolution** is primarily determined by the scientific question of the research or the available datasets.

During the **initialisation** process, special interpolation methods are used, to avoid possible discontinuities of some variables (such as surface temperature, subsoil temperature and moisture) at topographic interfaces (e.g. boundaries of different vegetation types; *McGregor 1997*).

Simulation length. The advantages of continuous long-term simulations are (Giorgi and Mearns 1999) that the model can reach an internal dynamical balance, the own internal circulations of the model can develop, and a better equilibrium can develop between the model climate and the surface hydrologic cycle.

The memory of the initial conditions in the model is slowly lost over time as the atmosphere and land come into equilibrium. The *spin-up* time of model is the adjustment process, during which the model approaches its equilibrium solution (Bonan 2008b). In long time climate simulations model results are affected by the initial values of the atmosphere only in the first 2-3 weeks. But for the soil variables longer spin-up time (1 year) is needed (Giorgi and Mearns 1999).

A broad spectrum of sub-grid scale processes occur at the surface and in the boundary layer, which have an important effect in long-term climate studies. Physical processes that are too small to be explicitly calculated by the model, are *parameterised* (e.g. exchanges of heat, moisture and motion between the surface and lower atmosphere, cloud radiation processes, turbulent transports, soil and vegetation types, sub-surface processes).

Investigation of the dependence of model results on lateral boundaries, simulation domain size, horizontal resolution, initial conditions, and physical parameterisations (Jacob and Podzun 1997) underlines, that regional climate modelling is essentially a boundary value problem. Considering long-term simulations, the role of the initial conditions and horizontal resolution become less important compared to the lateral boundary conditions.

Uncertainties in the climate model simulations

The quality of the regional climate simulations is very sensitive to the lateral boundary forcing, i.e. by the quality of the global model simulations and reanalyses products as it has been shown in the PRUDENCE project⁹. The basic types of uncertainties (e.g. uncertainties of the emission scenarios, internal model variability) of the global climate model simulations are listed in the recent IPCC report (2007).

Limitations can also be caused by the uncertainties of the surface station data (e.g. station distribution and density, length, quality and inhomogeneity of the time series). Uncertainties can be reduced by analyses of long time series as well as spatial and temporal averages or applying ensembles of simulations (e.g. ENSEMBLES project¹⁰)

Summer drying problem (SDP) is related to the investigated region of this work. The too dry and too warm simulation of climate over Central and Eastern Europe during the summer is a special model feature that is typical for many regional climate models, and to a less extent is visible in some general circulation models (Machenhauer et al. 1998, Hagemann et al. 2001). It is known from previous modelling studies in the frame of MERCURE¹¹ (Hagemann et al. 2004) and PRUDENCE projects (Christensen and Christensen 2007, Hagemann and Jacob 2007, Jacob et al. 2007). It is related to the model parameterisation, but it is too complex, it cannot be solved from only one research direction. In the EU-project CLAVIER¹² the possible reasons for this phenomenon have been investigated from many aspects (e.g. model dynamics, weather patterns, energy balance, moisture transport through the lateral boundaries,

⁹ <http://prudence.dmi.dk>

¹⁰ <http://ensembles-eu.metoffice.com>

¹¹ <http://www.pa.op.dlr.de/climate/mercure.html>

¹² <http://www.clavier-eu.org>

soil moisture capacity). The SDP is still an open issue and is a substantial part of ongoing model development.

2.4.3 Land surface models

In order to project future climates, the way that the Earth's surface interacts with the atmosphere and the ways that this interaction changes as a result of both human activity and natural processes, must be represented in the climate models (Pitman 2003). An appropriate land surface scheme in climate models is important to understand

- the role of the land surface in simulating climate and climate variability in climate models,
- the impact of changes in the land surface processes on climate,
- the role of the land surface in climate change and climate sensitivity.

Sect. 2.3.1 introduced the climatic role of forest ecosystems, their influence on the surface energy and water balance. This chapter summarises how the basic processes and the characteristics of vegetation are included in the land surface models in different stages of development. It must be emphasized that the role played by the land surface within climate and climate models is different from the role played by the land surface in microclimatology, mesoscale meteorology, and weather. Land surface models are not meant to be detailed models of forest meteorology but rather simplified treatments of surface heat fluxes that reproduce at minimal computational costs the essential features of land-atmosphere interactions important for climate simulation (Bonan 2008a)

Pitman (2003) provided an overview from simple first-generation models to complex third-generation schemes. *First generation models* used simple prescription of albedo, surface roughness and soil water without explicitly representing vegetation or the hydrologic cycle. Water storage in the soil is represented using a simple bucket model (Manabe et al. 1965).

In the *second generation models* (e.g. Biosphere-Atmosphere Transfer Scheme: BATS, Dickinson et al. 1986; Simple Biosphere Model: SiB Sellers et al. 1986) the vegetation-soil system interacts with the atmosphere, rather than being passive. Vegetation, which is treated as a single layer 'big leaf' (Deardorf 1978) and the underlying soil are characterized by their own surface energy fluxes and hydrologic cycles. Second generation models have been applied to study the impact of tropical deforestation on the climate (Dickinson and Henderson-Sellers 1988).

In contrast to the second generation models, *third generation models* use a photosynthesis-stomatal conductance model (Bonan 1995, Sellers et al. 1996). Through modelling of photosynthesis, simulation of atmospheric CO₂ in climate models is possible (Bonan 1995).

Dynamic global vegetation models (e.g. DGVM, Potter and Klooster 1999; LPJ, Stich et al. 2003) simulate the effects of future climate change on natural vegetation and its carbon and water cycles. Ecosystems are represented as mixtures of plant functional types, which are defined by key physiological and life history characteristics that determines vegetation dynamics. The linkage among climate, biogeophysics, biogeochemistry, phenology and vegetation dynamics allows spatial distribution of vegetation as well as the species and structure of plant community change as climate changes (*figure 11*). Using these models it is possible to study the interaction between biological and physical processes at the land surface and their feedback on climate. However, the combined carbon cycle and biogeophysical effect of vegetation, their status as carbon sinks, interactions of fires, aerosols, and reactive gases

with climate, and the effects of small scale deforestation on clouds and precipitation are key unknowns in the current generation of models (Bonan 2008b).

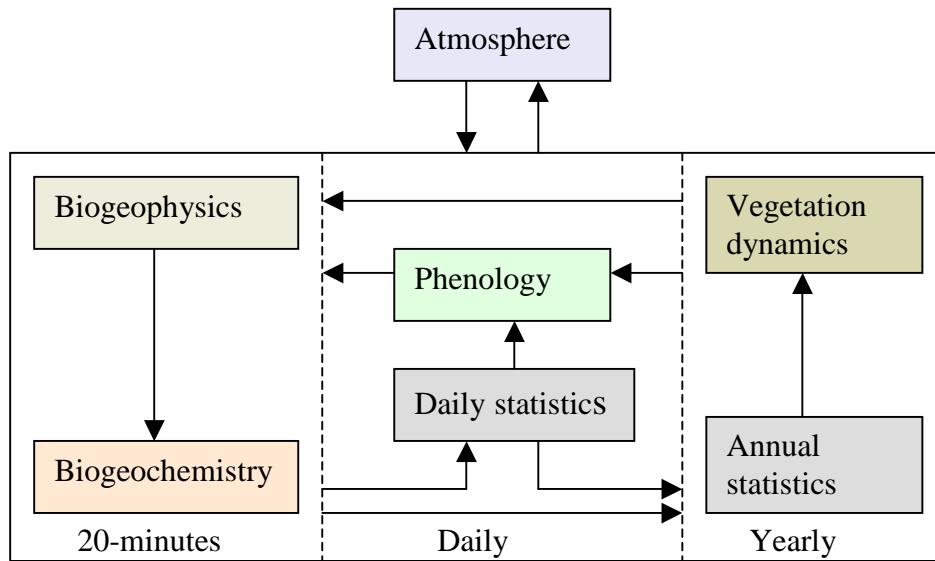


Figure 11. DGVM architecture (simplified after Bonan et al. 2003)

Representation of spatial variability of land cover on the model's grid. Land surface in climate models is described by various land cover types. Associated with each type, a set of specified properties (e.g. roughness length, leaf area index, albedo) is allocated. In early land surface models, each grid box is characterised by the dominant vegetation type, which is assumed to be uniformly distributed over the grid cell. Surface heterogeneity can be represented by the *mosaic approach*. Based on this concept each model grid cell is divided into a number of smaller patches of homogenous vegetation or soil (Avissar and Pielke 1989). Each patch is individually modelled and has its own surface climate. The grid cell average is the weighted average of these patches.

So far, land surface models have been coupled to global climate models (Foley et al. 1998, Levis et al. 2004). There are only a few, mostly off-line coupling experiments with regional climate models (e.g. Göttel et al. 2008). Dynamic representation of vegetation in regional climate models is an ongoing research question, which is essential for studying land-atmosphere interactions and feedbacks on finer scale (i.e. for the assessment of the climatic impact of land use change as well as for the climate change adaptation strategies). On finer resolution, description of the vegetation related processes gets more complex due to the heterogeneous land cover. Applying the few predefined global vegetation types, this heterogeneity, the region specific characteristics of the land surface and its feedbacks get lost. Therefore not only downscaling of global processes but also the upscaling of fine scale datasets (observations, flux tower measurements, satellite monitoring of vegetation) would be important.

2.5 Discussion and research needs

In this section, results of the recent studies introduced in *Chapter 2* are discussed and research needs are pointed out, which can explain the relevance of the dissertation.

In case of Europe, it is likely that the increase of annual mean temperature will exceed the global warming rate in the 21st century. For precipitation, there are huge spatial differences in the climate change signals among the European regions. The projected increase of the inter-annual variability of temperature and precipitation, the more intense hydrological cycle can lead to the increase of the probability of climatic extremes (e.g. heat waves, droughts, heavy precipitations and floods). The change of the spatial and temporal distribution of precipitation can have severe ecological, economical and social impacts and consequences in the natural ecosystems.

Forest/steppe limits are especially sensitive and vulnerable to increase of the frequency of extremes, therefore effects of climate change in these regions can be much more severe than in other areas. So far, research activities and publications are concentrating on the shift of the upper limit of forest distribution (at high latitudes and altitudes) due climate change (e.g. *Bonan 1992, Vygodskaya et al. 2007*), where increase of temperature prolongs the growing season, improves the growth, reproduction and survival. Xeric limits are seldom addressed in the literature (e.g. *Jump et al. 2009, Mátyás 2010*), although their shift is an important indicator of climate change. This emphasises the need of regional scale information about the future tendencies of probability, severity and duration of droughts and their spatial distribution, which are essential for projecting the effect of climate change on forests and preparing for the adaptation in the forestry practice.

Vegetation feedbacks have much more weaker influence on atmospheric circulation in comparison with the greenhouse-gas forcing (*Betts 2007, Göttel et al. 2008*). However there are regions, where regional climate changes are significantly affected and altered by land-atmosphere feedbacks thus land use and land cover changes. The direction of regional change differs, which has been also shown by *Pitman et al. (2009)*.

Results of the introduced studies show that climatic feedbacks of temperate forests differ strongly among regions, they can cool or warm the regional climate. A possible reason for it can be the large spatial variability of the climatic and soil conditions as well as the physical characteristics of vegetation, which let to dominate either the albedo-effect or the evaporative cooling. Different feedbacks for the same regions can be the result of the different experimental set-up (i.e. model domain, resolution, time period) as well as of different land surface parameterisations in the climate models.

Quite few studies have addressed vegetation-atmosphere interactions for Europe, there is a lack of information about the climatic impacts of land cover and land use for smaller European regions. ***For Hungary***, results of mesoscale model studies showed that land cover change in the 20th century alter weather and climate (*Drüszler et al. 2009*). But ***so far, the climatic effect of forests for longer, consecutive, future time periods, on regional scale has not been investigated.***

To study the feedback of land cover change on the regional climate, regional climate model simulations are essential. So far, there isn't any regional climate model running coupled to a dynamical vegetation model for longer climate periods. Only test simulations have been done to study climate-vegetation interactions in fine horizontal resolutions (e.g. *Göttel et al. 2008*), the fully coupling is one of the ongoing research topics in regional climate modelling.

The study by *Rechid et al. (2006)* emphasizes the importance of the realistic description of land surface characteristics and processes in regional climate simulations especially over Eastern Europe and the Hungarian lowland. These regions characterised by continental climate, are shown to be much more sensitive to the altered vegetation description than the western European areas close to the sea.

One of the most important forest-related processes is the interception. Its hydrologic role increases if there are frequent low intensity rainfall events. The temporal distribution of precipitation is projected to change under future climate conditions, which can alter the interception rate, thus the evaporative cooling effect of forests. Therefore its appropriate representation in the hydrologic and climate models is essential.

3. Objectives and research questions

In order to achieve the four main scientific goals of the analysis of forest-climate interactions (*Chapter 1*), the following research questions are raised:

Climate change and drought trends

- How accurately can the regional climate model REMO simulate past dry events?
- What are the projected tendencies of temperature means and precipitation sums in the 21st century?
- Will climate change have an effect on probability and severity of droughts in the future?
- Which region can be characterised by the largest tendency of warming and drying?

Feedback of forest cover change on the regional climate

- What is the climatic effect of forest cover in Hungary on regional scale?
- How big are the climatic feedbacks of maximal afforestation in the region characterised by the largest possible increase of forest cover?
- How does the interaction of the main climatic forcings of afforestation change during the summer months?
- Has the potential afforestation survey an effect on the regional climate?

Climate change altering effect of afforestation (investigated by synthesising the previous results of the dissertation)

- Are there any spatial differences in the forest-climate interactions in Hungary?
- How big is the effect of maximal afforestation on the summer precipitation compared to the climate change signal?
- Can probability and severity of droughts be reduced by maximal afforestation?
- Can projected climate change be influenced by the extent of the present forest cover?
- Are the feedbacks of maximal afforestation different under moderate and enhanced climate change?
- Are there any regions, in which deforestation enhances climate change?

Measuring and modelling of interception on local scale

- How accurately can the one dimensional hydrologic model BROOK90 simulate the amount of interception in the Hidegvíz-Valley?
- Has the intensity of precipitation an effect on the simulated interception?

4. Data and methods

To answer the research questions related to climate change and the forest-climate interactions (*Sect. 3*), the regional climate model REMO (*Jacob 2001, Jacob et al. 2001*) has been used. In the dissertation the model was a research tool, the aim was not the further development of the model parameterisation.

- Climate change and drought trends have been investigated partly by analysing existing model results, partly by carrying out simulations (*Sect. 4.1.2*).
- To study the feedback of forest cover change on the climate, three different land use change scenarios have been prepared, which have been used as land cover input for the climate simulations (*Sect. 4.1.3*).

The process of interception has been investigated on local scale through field measurements and with the hydrologic model BROOK90 (*Federer et al. 2003*).

This chapter introduces the two models and the forest research site with respect to the objectives of the present study, furthermore the data and methods applied by the analyses.

4.1 Simulation of climate change and forest-climate interactions applying the regional climate model REMO in Hungary

4.1.1 The regional climate model REMO

General characteristics

REMO (*Jacob and Podzun, 1997, Jacob 2001, Jacob et al. 2001, Jacob et al. 2007*) is a regional three-dimensional numeric atmospheric model. It is based on the ‘Europamodell’, the former numerical weather prediction model of the German Weather Service, DWD (*Majewski 1991*).

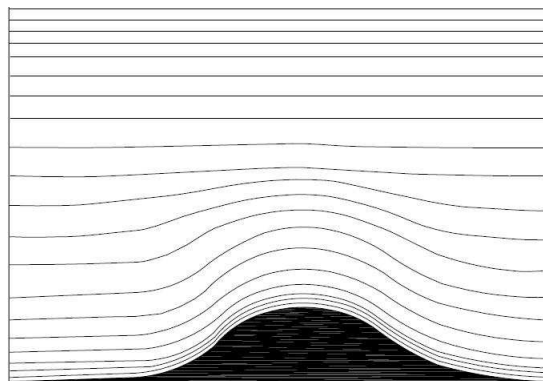


Figure 12. Illustration of the hybrid vertical coordinates

Dynamical scheme. The lateral boundary conditions as input variables are provided by analysis/reanalyses products or GCM outputs (*Sect. 2.4.2*). The prognostic variables of REMO are surface pressure, temperature, horizontal wind components, specific humidity and cloud liquid water. Their calculations are based on the hydrostatic approximation. The model equations are formulated in a rotated spheric coordinate system. The equator of the rotated system crosses the middle of the model domain, which is to maintain a regular grid spacing in

the model area. The vertical levels in REMO are represented in a hybrid coordinate system (Simmons and Burridge, 1981). Hybrid coordinates are following the surface orography in the lower levels and become independent from surface orography in higher atmospheric model levels (figure 12).

REMO can be integrated in forecast as well as in climate mode. In climate mode the model runs continuously for long time periods with updates of the lateral boundaries every 6 h (Jacob 2001).

Modified ECHAM4-physics. For the same dynamical scheme REMO has two different physical parameterisation schemes. The original one called DWD¹³-physics. Additionally, physical parameterisations from the global climate model ECHAM4 (Roeckner et al. 1996) were implemented at the Max Planck Institute for Meteorology in Hamburg. In the present study simulations will be carried out using REMO with ECHAM4-physics (DKRZ 1993, Roeckner et al. 1996) including recent modifications of the original scheme.

In the original ECHAM4 parameterization a model grid box consisted of only one single surface type. The **fractional surface cover concept** was implemented by Semmler (2002) including subgrid fractions for each of the three basic types (land, water, sea ice). These fractions are not assumed to be located in a specific area of a grid box but do simply cover a certain percentage of the total grid box area, summing up to a total of 100% (tile approach, figure 13). The land fraction is further divided into a part covered by vegetation and a bare soil fraction. Kotlarski (2007) extended the tile approach and introduced a fourth surface fraction (glacier ice) in the grid box.

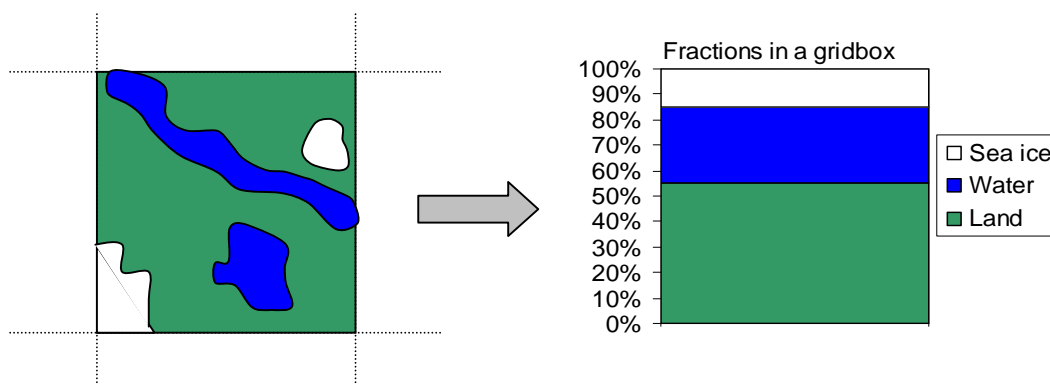


Figure 13. Illustration of the tile approach
(example for a gridbox covered by 55% land, 30% water and 15% sea ice)

During the model integration, each surface fraction is characterised by its own land surface parameters. In order to aggregate them over the model grid box in the given horizontal resolution, vegetation parameters can be linearly averaged, weighted by the fractional areas of the component land cover classes (Feddes et al. 1998). The only exception is the roughness length due to vegetation, which has to be logarithmically averaged at a so-called blending height (Mason 1988; Annex II).

Based on these characteristics, the turbulent surface fluxes and the surface radiation flux are calculated separately for each fraction and are subsequently averaged within the lowest atmospheric level using the respective areas as weights.

¹³ Deutscher Wetterdienst

Land surface parameterization

Land surface processes in REMO are controlled by physical vegetation properties like leaf area index, fractional vegetation cover, background albedo, surface roughness length due to vegetation, forest ratio and soil water holding capacity. For each land cover type these parameter values are allocated in the global dataset of land surface parameters LSP (Hagemann et al. 1999) and in its improved version LSPII (Hagemann 2002).

These datasets include the major ecosystem types according to the classification list of Olson (1994a,b). Their global distribution were derived from AVHRR¹⁴ data at 1 km resolution supplied by the International Geosphere-Biosphere Program (Eidenshink and Faundeen 1994) and constructed by the U.S. Geological Survey (1997, 2002; figure 14). The LSPII dataset has been validated and used for the application in regional (Hagemann et al. 2001, Rechid and Jacob 2006, Rechid et al. 2008a) as well as in global climate models (Hagemann et al. 2000).

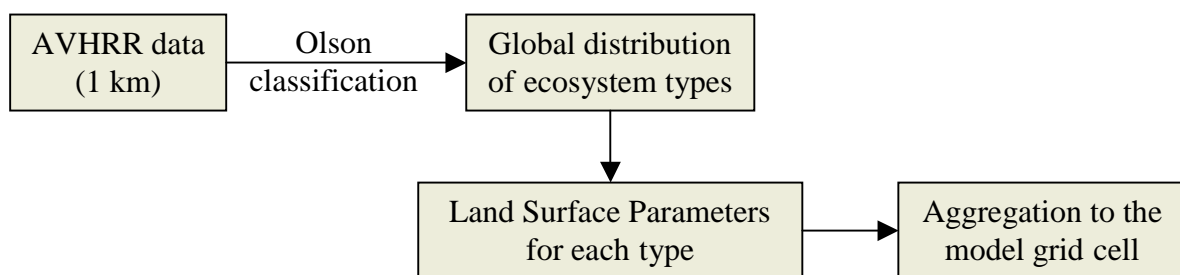


Figure 14. Steps of derivation of land surface parameters in the gridboxes

In the current model version the vegetation phenology is represented by the monthly varying values of the leaf area index and vegetation ratio. The mean climatology of the annual cycle of background albedo is also implemented (Rechid and Jacob 2006, Rechid et al. 2008a, 2008b). The other land surface parameters remain constant throughout the year.

Leaf area index (LAI) in the model influences evapotranspiration through stomatal conductance and defines also the canopy storage capacity (the size of the skin reservoir). In REMO vegetation has no height, therefore vegetation density (e.g. canopy layers in forests) is represented by LAI and fractional vegetation cover.

The **fractional vegetation cover (c_v)** determines the fraction of grid area where vegetation properties take effect on surface exchange processes.

In the LSP database (Hagemann et al. 1999) maximum and minimum values of LAI and c_v are allocated to get growing- and dormancy season, respectively. For representation of the annual vegetation cycle, monthly varying fields of LAI and c_v have been provided (Hagemann 2002) based on the maximum and minimum values of these two variables (Hagemann et al. 1999), and a monthly growth factor f_i . In low and mid-latitudes water availability is the limiting factor of growth. In these regions the monthly values of FPAR¹⁵ (Knorr 1998) is used to define the global field of f_i , which represents the local climate and determines the growth characteristics of the vegetation at 0.5° resolution. In high latitudes, the growth of the vegetation is mainly limited by temperature. Here, f_i is determined according to the monthly 2m-temperature climatology (Legates and Wilmott 1990).

¹⁴ Advanced Very High Resolution Radiometer

¹⁵ Fraction of Photosynthetically Absorbed Radiation

Using f_i , the monthly variation of LAI (LAI_i) between minimum and maximum values (and analogous $c_{v,i}$) can be estimated as

$$LAI_i = LAI_{\min} + f_i * (LAI_{\max} - LAI_{\min}) \quad (7)$$

In REMO the background **albedo**, α is the albedo of a snow-free surface. Influencing the net radiation budget, the surface albedo has an impact on the simulated vertical energy exchange at the earth's surface and modifies the surface heat fluxes and temperatures.

By *Rechid et al. (2008a)* an advanced parameterisation of the snow-free land surface albedo for climate modelling has been developed, which describes the temporal variation of surface albedo as a function of vegetation phenology on a monthly time scale. Based on remotely sensed MODIS¹⁶ products of the white-sky albedo for total short-wave broadband and absorbed photosynthetically active radiation, vegetation canopy albedo has been separated from the underlying soil albedo, applying a linear regression method. The separated soil and vegetation albedo are applied to compute the annual surface albedo cycle from the monthly varying leaf area index.

The total background albedo (α) results from the vegetation albedo (α_{canopy}), where vegetation is present, and the albedo of the soil (α_{soil}), where the underlying surface is visible.

The total background albedo can be described as follows (*Rechid et al. 2008a*):

$$\alpha = \alpha_{soil} * e^{-0.5*LAI} + \alpha_{canopy} * (1 - e^{-0.5*LAI}) \quad (8)$$

Processes in the surface boundary layer are strongly influenced by the roughness length of the surface. In the models, the turbulent exchange of momentum, energy and moisture between the surface and the atmosphere is calculated as a function of **roughness length** (z_0 [m]). The roughness length consists two parts: a roughness length due to orography ($z_{0,oro}$ [m]) and a roughness length due to vegetation and therewith land use ($z_{0,veg}$ [m]). According to *Tibaldi and Geleyn (1981)* z_0 is computed as

$$z_0 = \sqrt{z_{0,oro}^2 + z_{0,veg}^2} \quad (9)$$

Forest ratio (c_f) is the fractional cover of trees, regardless whether they are photosynthetically active or not. In REMO c_f is used to account for the different behaviour of snow albedo in forested and non-forested areas.

Soil water holding capacity (W_{cap}) influences the soil water content. The plant available water holding capacity (W_{ava}) is the maximum amount of water that plants may extract from the soil before they start to wilt. The difference of W_{cap} and W_{ava} is called the permanent wilting point, which can also be expressed as volumetric wilting point (f_{pwp}) defined by *Eq 10*.

$$f_{pwp} = \frac{W_{cap} - W_{ava}}{W_{cap}} \quad (10)$$

W_{ava} is climatologically important because it defines the maximum soil moisture that is potentially available to the atmosphere due to the transpiration of plants. W_{cap} is necessary in establishing the mass conservation of the hydrological cycle, thereby in determining the

¹⁶ MOderate-Resolution Imaging Spectroradiometer

turnover of precipitation into evaporation, and in controlling runoff and drainage processes (Hagemann and Gates 2003).

Allocation of soil water holding capacity for each land cover type may not be very realistic, since the soil water capacities depend also on the texture of the soil, which is not as highly correlated with a land cover type as a pure vegetation parameter. W_{ava} is primarily influenced by root depth, which depends largely on the land use type (Dunne and Wilmott 1996). Therefore in the LSP dataset W_{ava} has been assigned to each ecosystem classes. The construction is based on the optimized rooting depths (Kleidon and Heimann 1998) and f_{pwp} was derived from data of Patterson (1990).

Evapotranspiration in REMO

In REMO total evapotranspiration over land is the sum of four fractions: transpiration, evaporation from the water stored on the canopy surface (interception), from bare soil and from snow.

Rainwater and melting snow that reach the vegetation surface goes into the skin reservoir. The maximum skin reservoir content (W_{lmax} [m]) is the function of the LAI, the fractional vegetation cover (c_v) and the maximum amount of water (W_{lmax} [m]) that can be held on one layer of leaf or bare ground. W_{lmax} is taken to be $2 \cdot 10^{-4}$ m, but simulation results are not sensitive to this value (Hagemann ex verb.). W_{lmax} [m] can be calculated as

$$W_{lmax} = W_{lmax} * ((1 - c_v) + c_v * LAI) \quad (11)$$

Based on W_{lmax} and the prognostic variable for the skin reservoir content (W_l [m]), the wet skin fraction (C_l) can be determined as

$$C_l = \min\left(1, \frac{W_l}{W_{lmax}}\right) \quad (12)$$

Over the fraction of the grid box, which is completely wet (the skin reservoir or snow), evaporation takes place at its potential rate (Eq. 13)

$$E_l = \rho * C_h * |v_h| * (q_v - q_s) \quad (13)$$

where E_l [mm] is the potential evaporation, ρ is the air density [kg m^{-3}], C_h is the transfer coefficient for heat and v_h [m s^{-1}] the horizontal velocity. q_v [kg kg^{-1}] is the specific near-surface humidity and q_s [kg kg^{-1}] is the saturation specific humidity at surface temperature and surface pressure.

From dry surfaces in the grid box (no water in skin reservoir), moisture can reach the atmosphere via bare soil evaporation or transpiration.

Evaporation from bare soil E_d [mm] is calculated as a function of the relative humidity (h) at the surface, which is assumed to be related to the water content of the soil (Eq. 14).

$$E_d = \rho * C_h * |v_h| * (q_v - h * q_s) \quad (14)$$

For transpiration E_v [mm] (i.e. evaporation from dry vegetated areas), the potential evapotranspiration is reduced proportional to the evaporation efficiency e as

$$E_v = e * \rho * C_h * |v_h| * (q_v - q_s) \quad (15)$$

Based on *Sellers et al. (1986)*, the evaporation efficiency is expressed as a function of the stomatal resistance of the canopy (*Annex III*). The stomatal resistance is depending on the *LAI*, the photosynthetically active radiation and the water stress factor. Water stress factor is an empirical function of the available water in the root zone (*Roeckner et al. 1996*).

Application of REMO

REMO is used for simulating climate processes to analyse mean climate and extreme weather events for the past and future time periods (*Lorenz 1999, Semmler and Jacob 2004, Jacob et al. 2007, Gaertner et al. 2007, Bülow 2009, Tomassini et al. 2009*) as well as for studying land cover change (*Göttel et al. 2008, Frenger 2008, Paeth et al. 2009*) and air pollution (*Teichmann 2009*). Horizontal grid spacings between 0.088° and 0.44° are currently used for simulations corresponding to horizontal resolutions of ~ 10 km and ~ 50 km, respectively.

Many studies are dealing with the validation of the model, especially of its hydrologic cycle (*Jacob et al. 2001, Hagemann et al. 2004, Hagemann and Jacob 2007*). Sensitivity of REMO to domain size, horizontal resolution, initial conditions and lateral boundaries have been investigated by *Jacob and Podzun (1997)*.

REMO has been successfully tested and validated in many regions: Europe, Arctic, Antarctic, Siberia, Indonesia, India, Brazil, Peru, Africa, North America, Baltic Sea, North Sea, North Atlantic, Pacific. For Hungary, REMO has been adapted, validated (*Szépszó and Horányi 2008*) and used for future climate projections (*Szépszó and Horányi 2008, Jacob et al. 2008, Gálos et al. 2007, Radvánszky and Jacob 2008, 2009*).

The atmospheric model REMO is coupled to three different hydrology models and three ocean/sea-ice models. The coupling to a dynamical vegetation model is in progress (*Wilhelm ex verb.*).

4.1.2 Simulation of climate change and drought trends in Hungary

Climate change experiments have been carried out using the regional climate model REMO over two domains with different horizontal resolutions. The first simulation domain covered Europe (*figure 15*). The horizontal grid resolution was 0.44° (corresponding to 50 km) with 109×121 grid boxes, the grid specification has been adopted from the RCM set-up used in the EU-project ENSEMBLES.

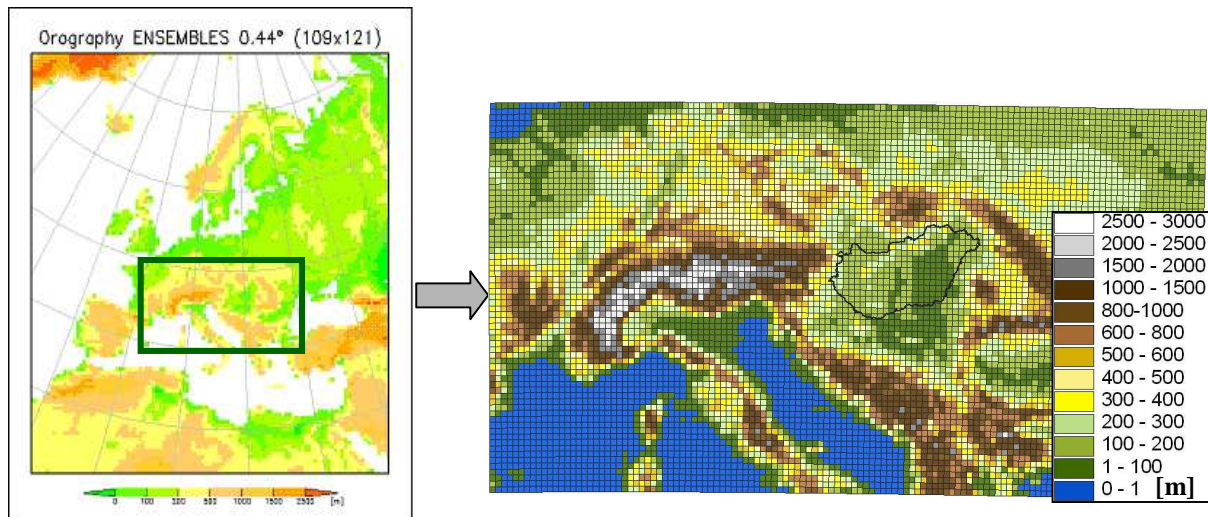


Figure 15. Simulation domains (0.44° horizontal resolution left and 0.176° right)

The following three types of REMO simulations have been studied on 0.44° horizontal resolution (*table 1*):

- *Validation simulation for the past* (1961-2000): lateral boundaries provided by ERA-40 re-analyses (Uppala et al. 2005) have been used to drive REMO. Initializing and forcing the model with reanalysis data ensures that the model results represent the real observed climate in the best possible way.
- *Reference (control) simulation for the past* (1951-2000): lateral boundary conditions of REMO are taken from the coupled atmosphere-ocean GCM ECHAM5/MPI-OM (Roeckner et al. 2006, Jungclaus et al. 2006). This is the reference simulation for the scenario simulations.
- *Emission scenario simulations for the future* (2001-2100): lateral boundaries to drive REMO are taken again from ECHAM5/MPI-OM GCM. Three scenario simulations were available for the analyses, which are based on three different IPCC-SRES emission scenarios: B1, A1B and A2 (IPCC 2001; Annex I).

Applying a double nesting procedure, these REMO 0.44° simulations were used to initialize and drive the REMO simulations with 0.176° (~ 20 km) horizontal resolution. The simulation domain covered Middle-Europe (*figure 15*) with 121×65 grid boxes and 27 vertical levels. A reference simulation for the past (1961-1990) and two emission scenario simulations for the future (2021-2050 and 2071-2100) were performed based on the A1B IPCC-SRES emission scenario (*table 1, Annex I*).

The main steps of the data analyses

- Validation of the model for temperature, precipitation and droughts
- Investigation of the climate change signal for temperature and precipitation means

- Analysis of the probability and severity of droughts
- Investigation of the spatial differences in the drought trends

Monthly precipitation sums and 2m-temperature means were studied for Hungary, using simulation results and observed data (*table 1*). In this dissertation the months May, June, July and August have been selected for the analyses and called ‘*summer*’, because in this part of the year water availability is especially important for the vegetation growth.

Table 1. Analysed data and time periods

Time period	Model and data	Horizontal resolution	Lateral boundaries
1961-2000	data from OMSZ-VITUKI ^a	station data	-
	CRU data ^b	0.5°	-
	REMO ^c validation simulation	0.44°	ERA-40 ^d re-analyses
1951-2000	REMO reference simulation	0.44°	ECHAM5/MPI-OM ^c
1961-1990		0.176°	REMO 0.44°
2001-2100	REMO scenario simulations B1, A1B, A2	0.44°	ECHAM5/MPI-OM
2021-2050	REMO scenario simulation A1B	0.176°	REMO 0.44°
2071-2100			

^a Data of 87 precipitation and 31 temperature stations from the Hungarian Weather Service (OMSZ) and from the Hungarian Environmental Protection and Water Management Research Institute (VITUKI)
^b Gridded station data (*Mitchell et al. 2004; CRU: Climatic Research Unit*)
^c REgional climate MOdel (*Jacob 2001, Jacob et al. 2001*)
^d ECMWF (European Centre for Medium-Range Weather Forecasts) re-analysis product (*Uppala et al.2005*)
^e General circulation model (*Roeckner et al. 2006, Jungclaus et al. 2006*)

Validation. To get information about the accuracy of the model, results of the validation simulation have been compared against observations for the past. Here, gridded station data (CRU¹⁷ 0.5° horizontal resolution; *Mitchell et al. 2004*) and observed data of 87 precipitation and 31 temperature stations in Hungary (OMSZ¹⁸-VITUKI¹⁹) have been used for validation (*table 1*).

Using REMO in climate mode it is possible to simulate statistical characteristics of meteorological quantities, but it cannot be expected that every single weather event is calculated realistically in time and space: individual years, which are dry in observations, can be different from those in the simulation.

Emission scenarios. *Figure 16* visualises the simulations and time periods (in coloured squares) selected for investigation of climate change. The arrows marked with capital letters show the compared experiments. Climate change signal for temperature and precipitation has been determined both for the middle (*figure 16; A*) and the end (*figure 16; B*) of the 21st century, calculating the difference between the results of the scenario simulations (2021-2050 and 2071-2100, respectively) and reference experiment (1961-1990). These 30-year periods have been selected to be comparable with the results of international projects.

¹⁷ Climatic Research Unit

¹⁸ Hungarian Weather Service

¹⁹ Hungarian Environmental Protection and Water Management Research Institute

To study the dependence of the projected climate change signal on the resolution, simulation results of 0.44° and 0.176° horizontal resolutions have been compared to each other.

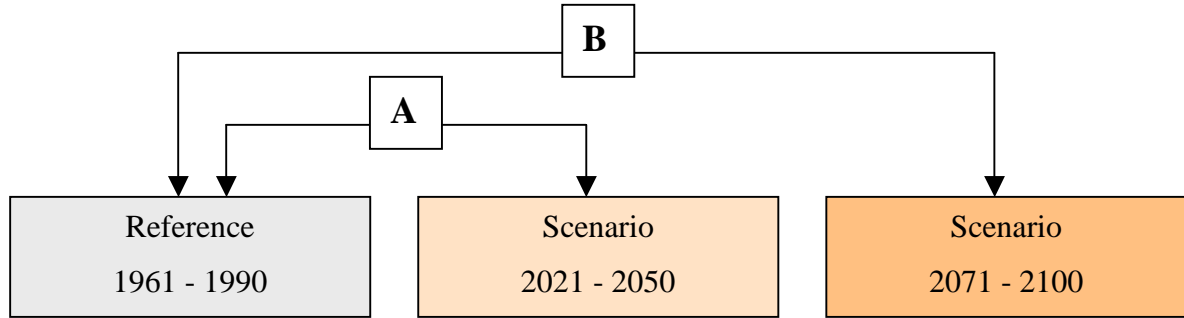


Figure 16. Simulations and time periods selected for analysing climate change

Droughts. For the three emission scenarios in 0.44° horizontal resolution, simulation results were available for the whole 21st century (table 1). Including longer time periods and more dry events in the analyses, the drought trends are more representative. Therefore the 21st century was divided into two parts: each 50 years long (2001-2050; 2051-2100) and a 50-year reference period (1951–2000) were determined in the 20th century, too. Simulated frequency and severity of droughts have been validated for 1961-2000, because reliable, continuous observations for the 87 precipitation and 31 temperature stations were available for this period.

The dissertation aims to analyse the long-term tendency and the spatial distribution of droughts from meteorological point of view, without considering its effect on the health status and distribution of vegetation. Therefore instead of the application one of the existing drought indices, a new definition and classification of dry events has been developed according to monthly precipitation and temperature values from model results and observations (Gálos et al. 2007). This has been used to analyse the tendencies of drought probability and severity for Hungary in the 21st century.

In the new approach a summer is called dry if it can be characterised with low precipitation conditions with relative to a reference period. Here, relative precipitation anomalies (dP) and temperature anomalies (dT) for summer have been calculated from the time period 1961-1990 (Eq. 16, 17), which is the most commonly used reference period in this kind of analyses.

$$dP[\%] = \frac{P_i - \sum_k^n P/30}{\sum_k^n P/30} * 100 \quad (16)$$

$$dT[^\circ\text{C}] = T_i - \sum_k^n T/30 \quad (17)$$

where P [mm] is the summer (from May to August) precipitation sum, T [°C] is the summer temperature mean, i varies from 1951-2100, $k = 1961$, $n = 1990$.

The following categorisation was developed and applied: considering relative precipitation anomalies, two main groups have been determined:

- extreme dry summers (EDS): $dP \leq -25\%$
- moderate dry summers (MDS): $-25\% \leq dP < -15\%$

According to dT further categories have been created within these groups:

- for EDSs: $dT \geq 1^\circ\text{C}$ or $dT < 1^\circ\text{C}$
- for MDSs: $dT \geq 0.5^\circ\text{C}$ or $dT < 0.5^\circ\text{C}$

The thresholds are based on the dPs and dTs of extreme/moderate dry summers in Hungary for the past and characterise the Hungarian circumstances quite well.

The number of events in each category has been determined in REMO and in the observations too. (Simulated droughts have been identified relative to the simulated reference period, droughts from the observed data have been determined relative to the reference period from the observations). The total number of dry summers is the sum of EDSs and MDSs. For analysing the severity of droughts, dPs and dTs of all dry summers have been averaged, and the results for simulated and observed dry periods have been compared. Finally, the results of the three emission scenario simulations (B1, A1B, A2) have been studied for the 21st century, and for country means, the tendencies of frequency and severity of droughts have been analysed.

Spatial differences in drought trends. Using simulation results with finer horizontal resolution (0.176°), spatial distribution of the future climate conditions have been investigated in Hungary. The region has been determined, in which both positive temperature anomalies and negative relative precipitation anomalies are largest in the period 2071-2100 relative to 1961-1990. Here, the drought trends have been studied more in detail.

An investigation of the uncertainties of this analysis due to internal model variability would require an ensemble of simulations. Nevertheless, only one realisation for the control run and each of the three emission scenario simulations were available.

4.1.3 Simulation of feedback of forest cover change on the regional climate and the climate change altering effect of afforestation in Hungary

Application of the regional climate model REMO in this study has the advantage that the feedback of forest cover change on the climate can be investigated for long continuous time periods. To obtain this aim, three different land use change scenarios have been prepared:

- *Maximal afforestation scenario:* the whole vegetated surface of Hungary is assumed to be forest. Additional forested areas are all deciduous.
- *Deforestation scenario:* the whole forested area in Hungary is replaced by grassland.
- *Potential forest cover:* based on a survey of ecological potentials for afforestation in Hungary (Führer 2005), marginal agricultural croplands were replaced by deciduous and coniferous forests.

These land use change scenarios have been used as land cover input for the regional climate model REMO to estimate the effect of forest cover change on the regional climate under future climate conditions.

Land cover data

To determine the present distribution of land cover types in Hungary the CORINE Land Cover (CLC2000) vector database²⁰ was used at scale 1:100000. The database has been produced by computer assisted visual interpretation of ortho-rectified Landsat Thematic Mapper satellite images. CLC2000 defines 44 classes. On the map objects larger than 25 ha and wider than 100 m are represented²¹.

The advantage of this vector database is the exact representation of the area and location of the polygons and it has more region-specific land use types than the climate models. The limitation of its application for climate modelling is, that in models land cover is described by physical parameters (e.g. albedo, leaf area index, roughness length), which are not allocated to the CORINE categories.

In the frame of this study a method has been worked out to represent the CLC2000 database on the model grid and to build it in into REMO according to the following steps:

- The model grid and the CLC2000 database have been merged using ArcView (ESRI 1996) and DigiTerra (DigiTerra Map 2004) softvers (figure 17).

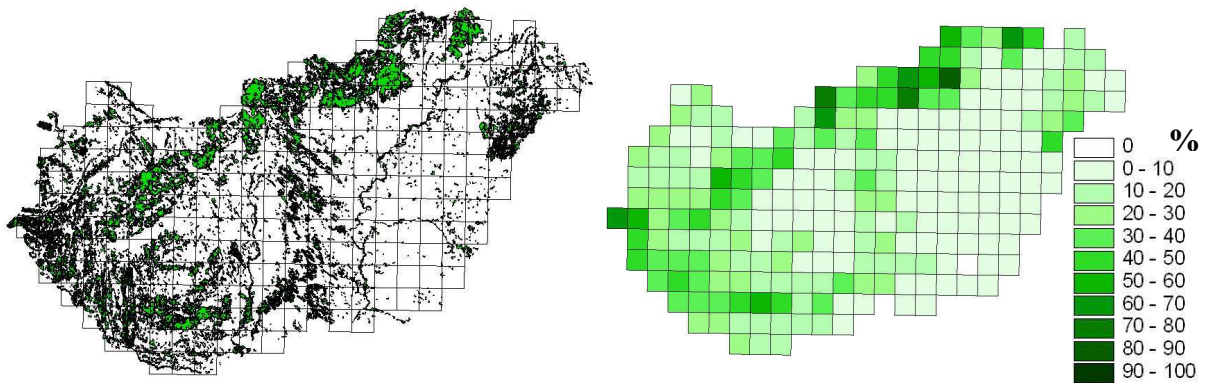


Figure 17. Forests based on the CORINE Land Cover (CLC2000) database (left) and merged with the REMO grid (right)

- Each CLC2000 type has been related to a global ecosystem type defined by *Olson* (1994a, 1994b; *Annex IV*). Reason: for all of the Olson-classes a land surface parameter set is specified (*Hagemann et al. 1999, Hagemann 2002*), which are required as input parameters for REMO (*Sect. 4.1.1*). For each Olson-land cover type existing in Hungary, the parameter values applied in the simulations can be found in *Annex IV*.
- In all grid boxes the fractional area of the Olson-ecosystem types has been determined.
- Land surface parameters have been aggregated over the gridboxes in the applied resolution: they were linearly averaged (excepting roughness length due to vegetation), weighted by the fractional area of the component land cover types, as described in *Sect. 4.1.1*.

This parameter-set represents the present land cover for Hungary, which has been used as reference in the model simulations.

²⁰ <http://dataservice.eea.eu.int/>

²¹ http://www.fomi.hu/corine/clc2000_hun.html

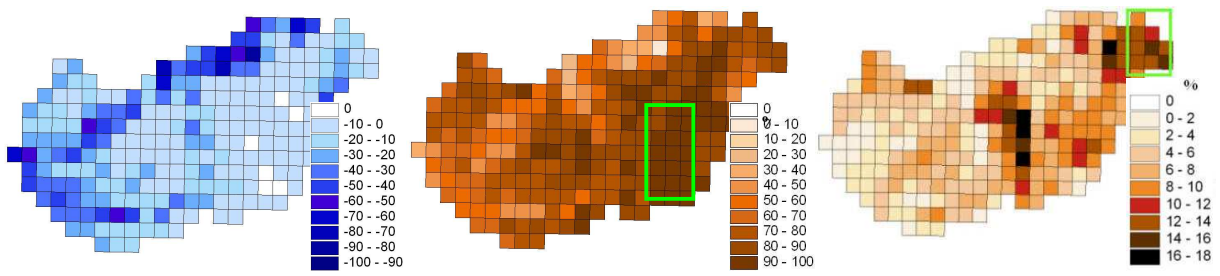


Figure 18. Changes of the forest cover for the deforestation (left), maximal afforestation (middle) and potential afforestation (right) experiments compared to the reference. Regions, which are analysed more in detail, are marked with squares.

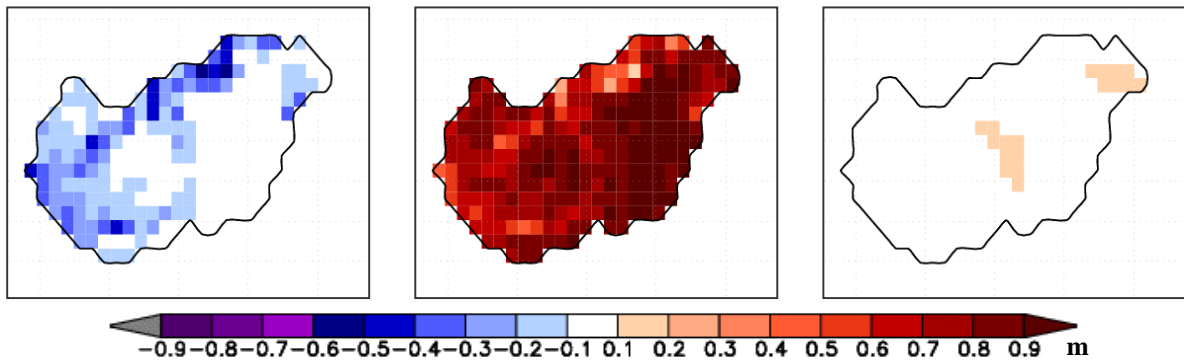


Figure 19. Changes of the roughness length for the deforestation (left), maximal afforestation (middle) and potential afforestation (right) experiments compared to the reference.

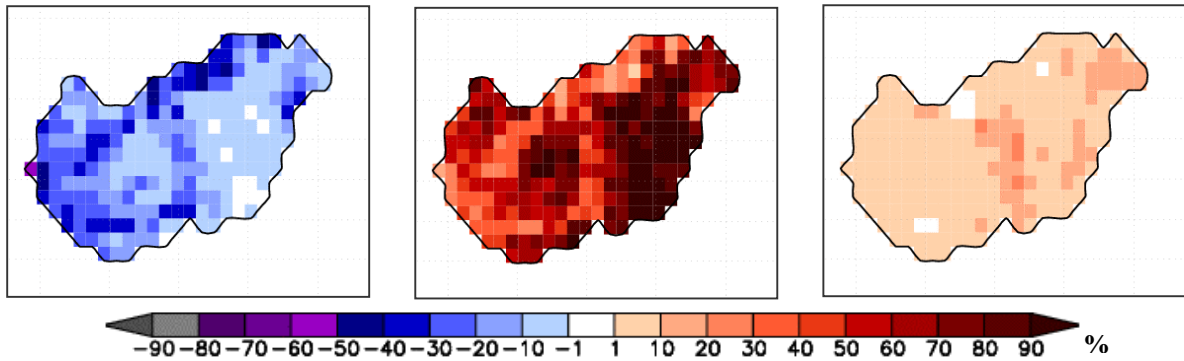


Figure 20. Changes of the leaf area index for the deforestation (left), maximal afforestation (middle) and potential afforestation (right) experiments compared to the reference.

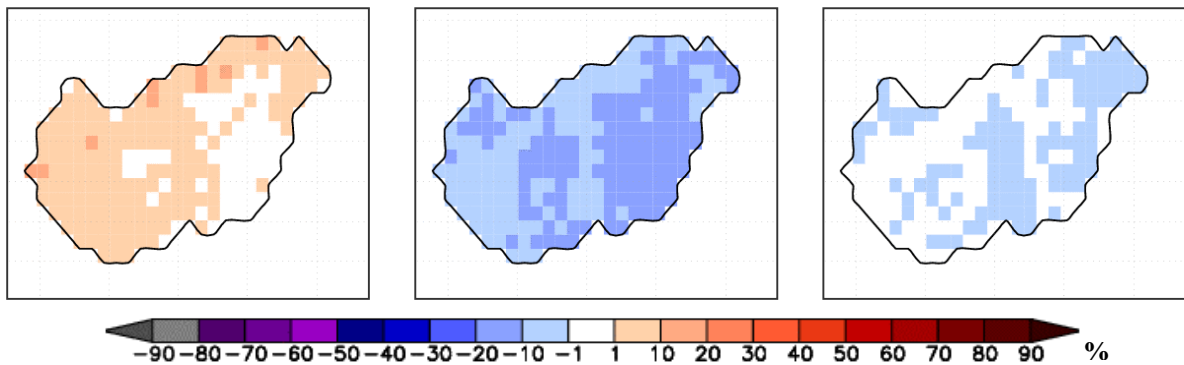


Figure 21. Changes of the albedo for the deforestation (left), maximal afforestation (middle) and potential afforestation (right) experiments compared to the reference.

Land cover change in REMO can be implemented by modification of the characteristic parameters. For the sensitivity studies in all grid boxes the new distribution of land cover categories has been determined, and for each experiment a new surface parameter set has been calculated. It has been found that for land use change studies with REMO, the prescribed vegetation- and soil albedo map (Rechid et al. 2007) have to be replaced based on the modified values (an appropriate method is under development, Rechid ex verb.).

For the maximal afforestation and deforestation sensitivity studies, forest cover change and the corresponding changes in the land surface parameters are shown on figures 18-21.

The increase of the forest ratio in Hungary (figure 18) caused a significant increase of roughness length (figure 19) and LAI (figure 20). Forests are darker, have smaller albedo (figure 21) than other vegetated surfaces. For the deforestation scenario, decrease of LAI, and roughness length and increase of albedo can be observed. The bigger changes are localised in the regions with larger loss of forested area.

Future afforestation survey in Hungary

In the potential future afforestation survey of Hungary, forest cover is suggested to increase in areas, which are less suitable for arable cropping (Führer 2005). For the 50 forest regions (Danszky 1963) the fraction of the less agriculturally fertile areas has been determined that could be potential afforested. This means 7% increase of forest cover (6.3% deciduous and 0.7% coniferous) for Hungary until the near future (figure 22). The exact location of the additional forest area within the region is not determined.

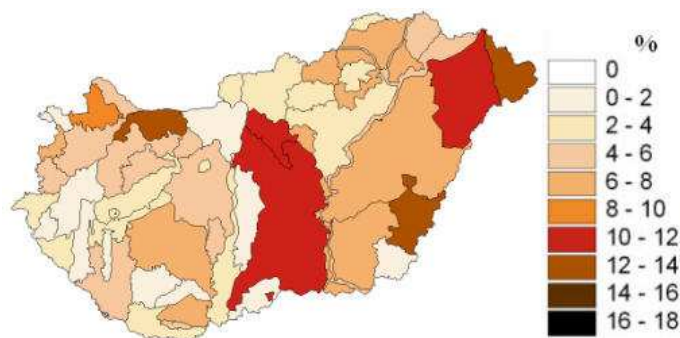


Figure 22. Potential increase of forest cover for the 50 forest regions (the map is prepared based on the data from Führer 2005)

Steps for building in this survey into REMO:

- The forest regions the REMO grid and the CLC2000 dataset have been merged.
- The gridboxes in the 50 forest regions have been identified and the area of crops in each box was determined.
- It is assumed that in all gridboxes, which belong to a selected forest region and have crops, the fraction of crops should be reduced as prescribed for that region in the potential afforestation survey. This is equivalent to the forest cover increase in that region.
- Adding the increase to the CLC2000 reference forest cover, the potential forested area has been allocated for all gridboxes (figure 18).
- Finally the new parameters were calculated as described in the previous section.

This scenario can be characterised by only a small increase of *LAI* (*figure 20*) and almost no changes in albedo (*figure 21*) and roughness length (*figure 19*). The reason for it is that a relative small fraction of crops has been replaced by forests and the differences between the parameters of forests and crops are also comparatively small (*Annex IV*).

Model simulations, experimental set-up

The following sensitivity experiments have been performed (*table 2*):

- *Emission scenario simulations* for the future (2021-2050, 2071-2100) with present land cover applying A1B IPCC-SRES emission scenario (*Annex I*). These are the references to the sensitivity studies.
- *Maximal afforestation experiments* for 2021-2050 and 2071-2100
- *Deforestation experiment* for 2071-2100
- *Potential forest cover* for 2021-2025

Table 2. Analyzed data and time periods

Experiment	Reference simulation	Maximal afforestation	Deforestation	Potential forest cover
Characteristics	Present forest cover	Forest over all vegetated area	Grassland over all forested area	Some agricultural areas replaced by forest
Time period	1961-1990 2021-2050 2071-2100	2021-2050 2071-2100	2071-2100	2021-2025
GHG^a forcing	IPCC-SRES ^b emission scenario A1B ^c			
Horizontal resolution	0.176°			
Lateral boundaries	REMO ^d 0.44°			
^a GHG: Greenhouse gas ^b IPCC-SRES: Intergovernmental Panel on Climate Change – Special Report on Emission Scenarios ^c description can be found in <i>Annex I</i> ^d REgional climate MOdel (<i>Jacob 2001, Jacob et al. 2001</i>)				

The simulation domain covered Central-Europe (*figure 15*), the horizontal grid resolution was 0.176°, with 121x65 grid boxes and 27 vertical levels, the same as used for the climate change simulation studies in *Sect 4.1.2*. For all simulations a double nesting procedure has been applied (*Sect. 2.4.2*). From the selected domain, forest cover has been changed only in Hungary.

The main steps of the data analyses

The analyses are concentrated on the Carpathian-basin and on the summer months (May, June, July and August), because the largest effect of forests on the climate is expected in this part of the vegetation period. After skipping the first year for model spin up, 5- and 30-year time periods (2021-2025, 2021-2050 and 2071-2100) have been determined and investigated. The simulation results of the maximal afforestation-, deforestation-, and potential forest cover experiments (*figure 23* in squares) have been compared to the reference simulations from the corresponding time period as shown by the arrows marked with capital letters on *figure 23*.

- For 2071-2100 the effects of maximal afforestation and deforestation on evapotranspiration, surface temperature, 2m-temperature and precipitation have been investigated (*figure 23; D, E*).
- The region, characterised by the largest climatic effect of maximal afforestation has been determined.
- The region with the largest possible increase of forest cover is selected (*figure 18*), in which the feedback of maximal afforestation on heat, evapotranspiration, temperature and precipitation conditions have been analysed more in detail.
- In the selected region, interaction of the main climatic forcings of afforestation has been studied during the summer months.
- For 2021-2025 the climatic effects of maximal and potential afforestation is compared to each other (*figure 23; F, G*) for the area characterised by the larger increase of forest cover in the potential afforestation scenario (*figure 18*).

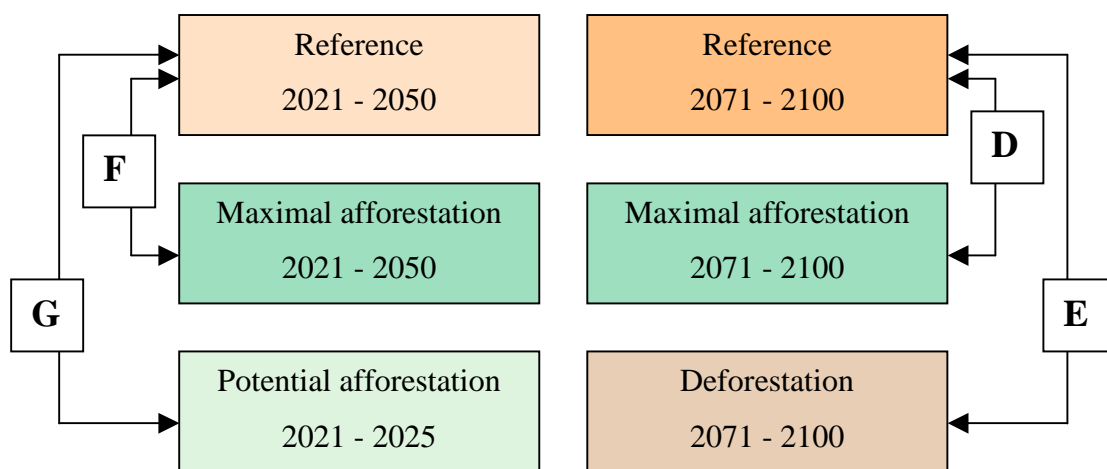


Figure 23. Analysed simulations and time periods

Climate change altering effect of maximal afforestation have been analysed based on the following steps:

- Spatial differences in the forest-climate interactions have been investigated. Based on the results of the previous sections, three regions have been selected: the most drought affected one, the area with the largest amount of afforestation and the region characterised by the largest precipitation-increasing and temperature-decreasing effect of maximal afforestation. Each of them cover 15 gridboxes ($\sim 300 \text{ km}^2$).
- For precipitation, magnitude of the climate change signal and the climatic feedback of maximal afforestation is compared to each other for three selected regions (*figure 24; B, D*).
- Effects of maximal afforestation on the probability and severity of droughts have been investigated for the period 2071-2100.
- Climate change signal for precipitation has been studied for 2071-2100 relative to 2021-2050 with and without forest cover increase (*figure 24; C, H*) in order to get information about the influence of the extent of forested area on the projected climate change.
- Dependence of the afforestation feedback on the magnitude of climate change has been analysed: for the middle and the end of the 21st century, effects of maximal afforestation on precipitation have been compared to each other (*figure 24; D, F*).

- Regions were determined, where deforestation enhances the climate change signal (figure 24; E).

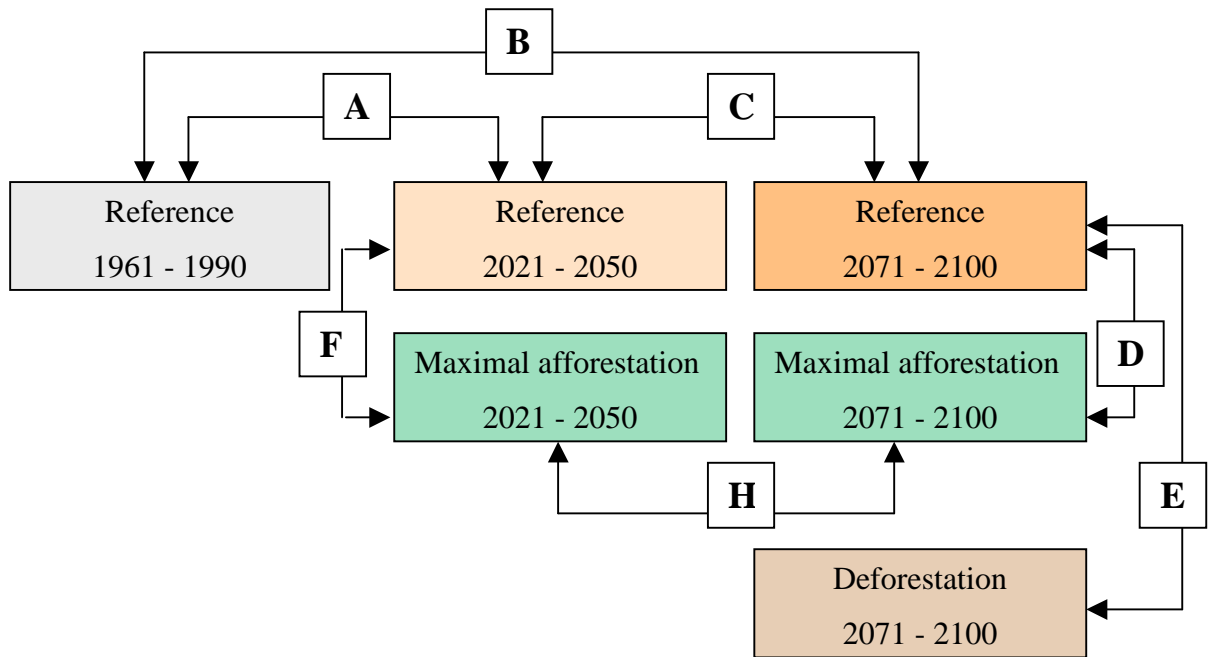


Figure 24. Analysed simulation results and time periods

4.2 Measuring and modelling interception on local scale

On local scale, hydrological processes in forest have been investigated in the Hidegvíz-Valley forest hydrological research area. For the beech site the hydrologic model BROOK90 (Federer et al. 2003) has been adapted and applied for the simulation of interception. Results have been validated with field measurements.

4.2.1 The Hidegvíz-Valley forest hydrological research area

The *research site* is situated in the Sopron Mountains, west of Sopron (Hungary) in the watershed of the Rák-stream (figure 25). The beech forest sub-compartment is 510 m above sea level. The bedrock is schist covered by sediments. The genetic soil type is acidic non-podzolised brown forest soil, the physical type is loam. The site can be characterised by 8-8.5°C annual mean temperature and 917 mm annual precipitation sum (Kalicz 2006). In the investigated forest sub-compartment the dominant tree species is beech (*Fagus sylvatica* L.) admixed with only single individuals of hornbeam (*Carpinus betulus* L.) and sessile oak (*Quercus petraea* (Mattuschka) Liebl).

The general research aim in the area is to study the water- and energy balance of the beech forest stand (Vig 2004, 2007), and to explore and model the water cycle of the forest covered catchment (Gribovszki et al. 2006, 2008, Kalicz et al. 2007).

In the dissertation, regarding to the available, complete, reliable dataset, which was needed for the analyses, the year 1997 was selected for the investigations. In this year the stand was 39 years old, 15 m high, the diameter at breast height was 0.14 m and the canopy closure 100% (Vig 2002).

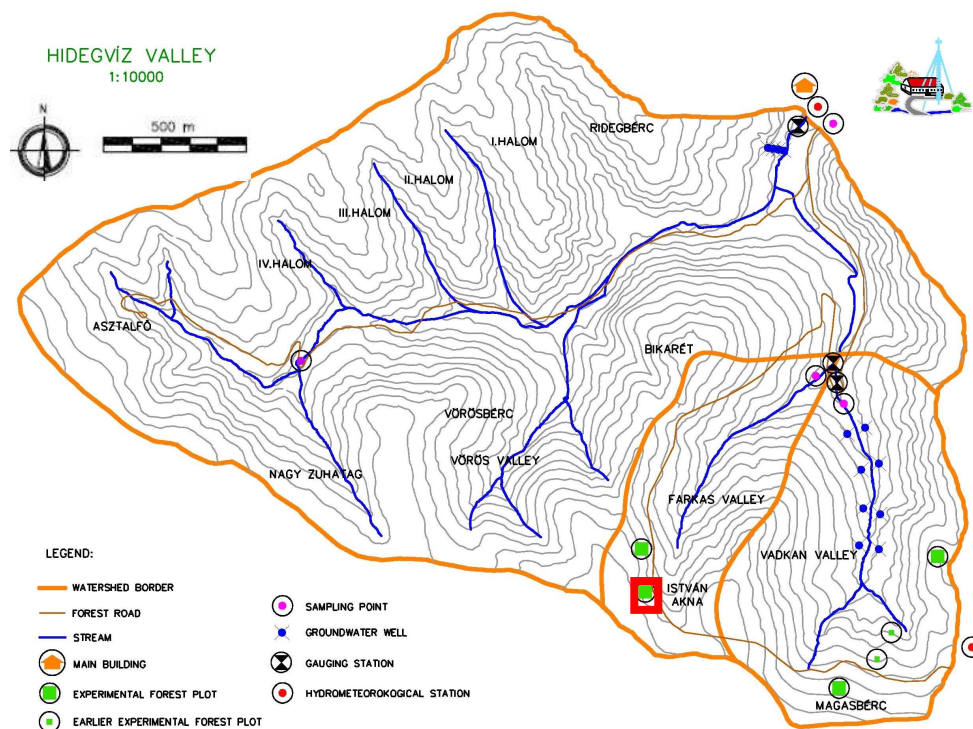


Figure 25. Location of the beech site (marked with red square) in the Hidegvíz-Valley forest hydrological research area (adapted from Kalicz 2006)

4.2.2 The hydrologic model BROOK90

General characteristics

BROOK90 (Federer et al. 2003) is a deterministic, process-oriented, lumped parameter hydrologic model that can be used to simulate most land surfaces at a daily time step year-round. It is a parameter-rich model designed primarily to study evapotranspiration and soil water movement for a single location or for a small, uniform watershed.

Input variables. Meteorological input variables are: maximum and minimum temperatures, solar radiation, vapour pressure and wind speed on daily scale and precipitation at daily or shorter intervals. These parameters can be measured either above the canopy of interest or in a weather station nearby. Further input parameters are needed about location (latitude, aspect), infiltration and drainage, soil (e.g. thickness, water content and water potential at field capacity for each layer), and canopy (e.g. maximum leaf area index and leaf conductance, stem area index, albedo, relative root density, roughness of the ground surface below the canopy). Canopy is assumed to have one layer.

Output for the surface and subsurface hydrological processes are provided on daily time scales or for precipitation intervals.

Basic processes. Water is stored in the model as intercepted rain, intercepted snow, snow on the ground, soil water in from one to many layers, and groundwater.

Validation. The model can be validated with interception or soil moisture measurements.

Evapotranspiration in BROOK90

In BROOK90 evapotranspiration is the sum of five components: evaporation of intercepted rain and snow, snow and soil evaporation, and transpiration. Potential evaporation rates are obtained using the *Shuttleworth and Wallace* (1985) modification of the Penman-Monteith approach (*Annex V*).

Shuttleworth and Wallace (1985) applied the Penman-Monteith equation separately for the canopy and for the soil surface to give separate estimates of transpiration and soil evaporation (*Annex V*). This method provides a potential transpiration estimate based primarily on maximum leaf conductance reduced for humidity, temperature, and light penetration. Aerodynamic resistances are modified from *Shuttleworth and Gurney* (1990). They depend on leaf area index (*LAI*), which can vary seasonally, and on the canopy height, which determines stem area index (*SAI*). Soil evaporation resistance depends on soil water potential in the top soil layer. Actual transpiration is reduced below potential when water supply to the plant is limited by plant resistance, rhizosphere resistance, and minimum (critical) leaf water potential.

Interception

Potential interception rate is defined as the evaporation that would occur from any given land surface in given weather conditions if all surfaces were externally wetted as by rain. It is calculated from the Shuttleworth-Wallance equations with a canopy resistance of zero (*Annex V*) and aerodynamic resistances based on canopy height, coupled with a canopy capacity and an average storm duration. Potential interception rate is determined separately for daytime and

for nighttime and the results are weighted by the day length. Its amount is considered to be constant throughout the daily time step.

In the model there are two ways to simulate actual interception (the same symbols are applied as in the model):

Precipitation input is more than once a day (*Annex VI*). The model calculates the rate of precipitation, which is caught by the canopy, the remaining part is throughfall. Until the maximum storage capacity is reached, the maximum catch rate (*CATCH* [mm]) is assumed to be a constant fraction of rainfall and is linear function of *LAI* and *SAI*. It can be determined as

$$CATCH = (FRINTL * LAI + FRINTS * SAI) * RFAL \quad (18)$$

where *RFAL* [mm] is the rainfall rate, *FRINTL* and *FRINTS* are intercepted fractions per unit *LAI* and *SAI*, respectively. The maximum amount of water that can be hold on the canopy (maximum storage capacity; *INTRMX* [mm]) increases linearly with *LAI* and *SAI*. It is calculated as

$$INTRMX = CINTRL * LAI + CINTS * SAI \quad (19)$$

where parameters *CINTRL* [mm] and *CINTRS* [mm] are the maximum interception storages of rain per unit *LAI* and *SAI*, respectively (similarly to the four interception parameters for rain, there are also four parameters allocated for snow). After *CATCH* reaches the maximum storage capacity, no more water can be stored on the canopy, which is available for evaporation.

In BROOK90 it is assumed, that at the beginning of the time-step the storage of the canopy is *INTR* [mm]. Its value differs from zero, if in the previous time-step the amount of evaporated water was smaller than the amount of the stored water. If it is raining during the time-step, water caught on the canopy evaporates in the potential rate (*PINT* [mm]). At the end of the precipitation interval time-step (*DTP*) the new storage (*NEWINT* [mm]) is determined as

$$NEWINT = INTR + (CATCH - PINT) * DTP \quad (20)$$

For each precipitation time-step the net catch rate (*RINT* [mm]) and the evaporation rate of intercepted water (*IRVP* [mm]); called interception in this work) are determined in the three cases:

- The canopy wets during the time-step, interception occurs in the potential rate. If the canopy capacity is reached and the new storage exceeds the maximal capacity, *RINT* can be calculated as

$$RINT = PINT + (INTRMX - INTR) / DTP \quad (21)$$

- If the canopy wets but does not reach the maximal capacity, the net catch rate has its maximal value (*RINT* equals to *CATCH*) and increases linearly (*Eq. 18*).
- If the canopy dries during the time-step, or stays dry, *RINT* equals to *CATCH* and the interception, which is smaller than the potential rate is determined as

$$IRVP = (INTR / DTP) + CATCH \quad (22)$$

Interception from daily precipitation input (*Annex VI*). Amount of interception is strongly depending on the intensity of precipitation, which is calculated from the duration of the storm. There is an input parameter that specifies the average hourly duration of precipitation for each

month of the year. The amount of interception is determined based on the duration and the average potential interception rate for the day.

Limitations related to interception processes are:

- There is no allowance for non-green leaves, which can intercept precipitation and radiation but do not transpire.
- Reduction of leaf area index after prolonged water stress is neglected.
- The canopy is considered to be either completely wetted or completely dry. Partial canopy wetting and drying is not treated.

General application of the model. BROOK90 is a fairly complex water budget model against which simpler models can be tested. It can be also used for predicting climate change effects. The model can be applied as a water budget model for land managers, as a research tool to study the water budget and water movement on small plots and as a teaching tool for evaporation and soil water processes (e.g. *Imbery* 2004, *Schwärzel* et al. 2006).

4.2.3 Application of BROOK90 for interception in the Hidegvíz-Valley

For adaptation of the model to the beech stand, it requires measured data for estimation of the fix parameters (*calibration*) as well as for testing the acceptance of the output variables (*validation*).

Meteorological data. Since 1995 micrometeorological measurements have been carried out in the beech stand by Vig using an AANDERA 2700 AVS automatic meteorological station (Vig 2002; figure 26). Net radiation budget, temperature, relative humidity and wind velocity are determined in 19 m (above the canopy surface), 14 m (effective height), 10 m (crown - stem area boundary) and 2 m (stem area) above ground surface. These datasets have been used as meteorological input for the BROOK90 model in daily and hourly time steps. (In 2005 a new meteorological station was located and the measurement heights were adjusted to the actual height of the stand – Vig ex verb.)



Figure 26. Microclimate tower (left) and interception garden (right) in the beech stand

The further input parameters related to site conditions (e.g. soil and flow parameters) as well as to canopy characteristics (e.g. maximum leaf area index and leaf conductance, albedo, relative root density, canopy height and density) have been allocated based on literature values and local experiences (Vig, Kovács ex verb.).

Measuring of interception. Interception cannot be measured directly, it can be calculated from the amount of gross precipitation in the open and stand precipitation in the forest. Data for interception have been collected for 20 years continuously in different forest stands in the Hidegvíz-Valley (figure 26), in which I also participated to during my PhD work.

Gross precipitation is measured in the highest (500 m above sea level in Új-Hermes using Hellmann-ombrograph) and in lowest (370 m above sea level) part of the watershed as well as in the beech stand 20 m above ground surface.

Throughfall precipitation is collected in 8 throughfall gages systematically located below the canopy (figure 27), each of them has 0.2 m² area.

For measuring *stemflow*, beech trees in the 400 m² research site were classified based on their diameter at breast height. Representative number of trees per classes has been determined, on which stemflow measurements are carried out using circular cuffs secured on the bark

(method: *Kucsara* 1996). The collected stemflow from these is then led to containers for volume measurements (*figure 27*).



Figure 27. Throughfall (left) and stemflow measurement (right) in the beech stand

Stand precipitation is measured in the vegetation period, as far as possible after each rainfall event. From the measured precipitation data interception is calculated based on the following steps (*Kucsara* 1996):

- From the 8 gages (P_{THi} [l]) an averaged throughfall amount (P_{TH} [l]) is calculated and determined for 1 m² area as

$$P_{TH} = \frac{\sum_{i=1}^n P_{TH_i}}{n * A_g} \quad (23)$$

where n is the number and A_g [m²] is the area of the gages.

- Stemflow (P_S [l]) is calculated by the weighted sum of the average stemflow of the sample trees (P_{Si} [l]) in the 6 diameter classes and determined for 1 m² area as

$$P_S = \frac{\sum_{i=1}^k \varepsilon P_{Si}}{A} \quad (24)$$

where ε is the weighting parameter, which equals the number of the trees in the individual classes k is the number of the diameter classes, and A [m²] is the area of the beech research site.

- Interception (I) is the difference between the measured gross precipitation (P_G [l]) and stand precipitation for 1 m² area. The later is the sum of the throughfall (P_{TH}) and stemflow (P_S) for 1 m² area.

$$I[l/m^2] = P_G - (P_{TH} + P_S) \quad (25)$$

$$I[\%] = \frac{P_G - (P_{TH} + P_S)}{P_G} * 100 \quad (26)$$

The main steps of the local scale research

- Calibration of the model.
- Validation of the simulation results with measurements.
- Investigation of the sensitivity of the interception output to the change of meteorological and canopy parameters.

In this work BROOK90 has been used only for estimation of interception, the other hydrological processes have not been analysed. Therefore calibration and validation were done for the interception-related meteorological and canopy parameters (e.g. soil and flow parameters have no effect on the simulated amount of interception, so their accuracy have not been tested, the predefined values have been accepted and used). Calibration and sensitivity studies were carried out for 1997, because for this year complete meteorological input dataset was available and the stand was young-aged with 100% closure and no forestry interventions. To simulate interception in the beech site, BROOK90 has been applied with hourly precipitation inputs using the INTER subroutine (*Sect. 4.2.2; Annex VI*).

Calibration of the model. The best fit of the model has been achieved by calibration of the maximal storage capacity (*CINTRL*) and the intercepted fractions of rain per unit leaf area (*FRINTL*) to the measured interception data for the period June-September 1997.

For **validation** of the interception outputs, measured data from the same time period has been selected, which have not been used for the calibration. The simulated and measured interception have been compared to each other and the model bias has been determined. If no interception measurement was available for the precipitation event, simulated as well as measured precipitations and the corresponding interceptions have been summarised over longer time periods.

Sensitivity studies for precipitation intensity. It has been tested whether the more accurate determination of the duration of the rainfall event have an influence on the simulated interception. Two sensitivity studies have been prepared:

- *HourlyP*: interception has been simulated using hourly precipitation measurements as input (INTER subroutine; *Sect. 4.2.2*).
- *DailyP*: the model run with daily precipitation input and an average hourly duration of rainfall for each month (INTER24 subroutine; *Sect. 4.2.2*). The monthly mean hourly rainfall duration has been calculated from the hourly precipitation measurements.

For both cases the simulated interception has been compared to the measurements.

5. Results

5.1 Climate change and drought frequency

For precipitation and temperature, the term ‘climate change signal’ refers to the difference between the simulated future and present conditions. Detailed description on of the applied emission scenarios can be found in *Annex I*. In *Sect. 5.1*, temperature (T) means the 2m-air temperature.

5.1.1 Validation of the regional climate model REMO for temperature, precipitation and droughts

For the climate period 1961-1990 simulated results have been compared against observations (OMSZ-VITUKI) and gridded station data (CRU).

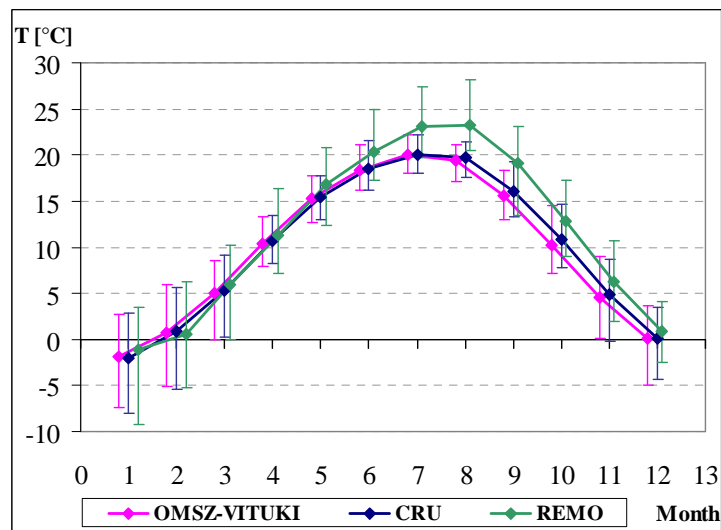


Figure 28. Validation for the monthly temperature (T) means (Hungarian mean, 1961-1990). Bars represent the spread of values within the 30-year period.

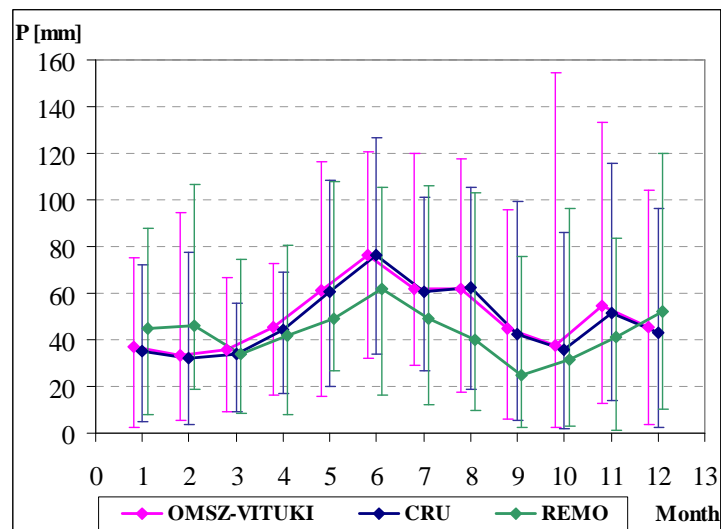


Figure 29. Validation for the monthly precipitation sums (Hungarian mean, 1961-1990). Bars represent the spread of values within the 30-year period.

The 30-year temperature means for winter and spring month are simulated by REMO almost perfect with respect to the CRU and OMSZ-VITUKI dataset in Hungary (*figure 28*), but from July to September simulation results show a strong warm bias. REMO simulates not only higher temperatures in the summer months but also the variability of the modelled values is larger than observed. The increased variability of summer temperatures in the validation simulation was also discussed by *Schär et al. (2004)* and *Seneviratne et al. (2006)*.

For precipitation, the difference between model results and observations are rather small from October to April. In summer, precipitation amount is underestimated by REMO, especially in August and September (*figure 29*).

Results of the validation show that the summer drying problem (i.e. the too warm and too dry simulation of climate in the Central European countries during the summer; introduced in *Sect. 2.4.2*) is present also in these simulations. To eliminate this kind of uncertainty, ‘delta change approach’ has been used, which means, changes of climatic variables were analysed rather than absolute values calculated by the model. This approach is based on the assumption that model biases do not change under climate change conditions (*Jacob et al. 2008*).

It is also supposed that the frequency of observed dry summers relatively to the observed mean (1961-1990) should be the same as the frequency of simulated dry summers relatively to the simulated mean, despite of the dryer and warmer bias of the model.

Validation for droughts. Dry summers defined in *Sect. 4.1.2* have been classified, and for each category the number of events has been determined (*table 3*). *Table 3* shows that for 1961-2000 the frequency of simulated and observed moderate (MDS) and extreme (EDS) dry summers agree rather well almost in all categories and in total (EDS+MDS) too. Only the number of droughts characterised by larger than 25% negative relative precipitation anomaly (dP) and 1°C temperature anomaly (dT) is overestimated by REMO. Dry summers occurred in more than one third of the analysed 40-year period from these every second summer was extremely dry. More than half of the extreme dry events can be characterised with high positive temperature anomalies.

Table 3. Number of dry summers in the period 1961–2000

	Extreme dry summers (EDS)			Moderate dry summers (MDS)			EDS+MDS
	$dP \leq -25\%$		Total	$-25\% \leq dP < -15\%$		Total	Total
	$dT \geq 1^{\circ}\text{C}$	$dT < 1^{\circ}\text{C}$		$dT \geq 0.5^{\circ}\text{C}$	$dT < 0.5^{\circ}\text{C}$		
OMSZ-VITUKI	4	3	7	5	3	8	15
CRU	4	3	7	4	3	7	14
REMO	9	3	12	3	3	6	18

Figure 30 represents the dP and dT values of the individual summers (1961-2000) relatively to the climatic mean (1961-90). Corresponding to *table 3*, the amount of extreme dry and warm events, therefore the severity of droughts in the model is higher compared to observations. REMO simulates not only more extreme dry and warm summers, but also more extreme wet and cold ones (*figure 30*). This means that in the summer months the variability of the simulation results is larger than observed. For dTs the difference between the highest and lowest model result is 5°C , in the observations it is less than 3.5°C . REMO simulates 6 summers with dT above 2°C , whereas there are none in the observations. Also for dPs there is a larger variability in the model than in the observations, but this difference is not so large as for temperature. (*Figure 29* does not show this because it represents absolute precipitation values for each individual month.)

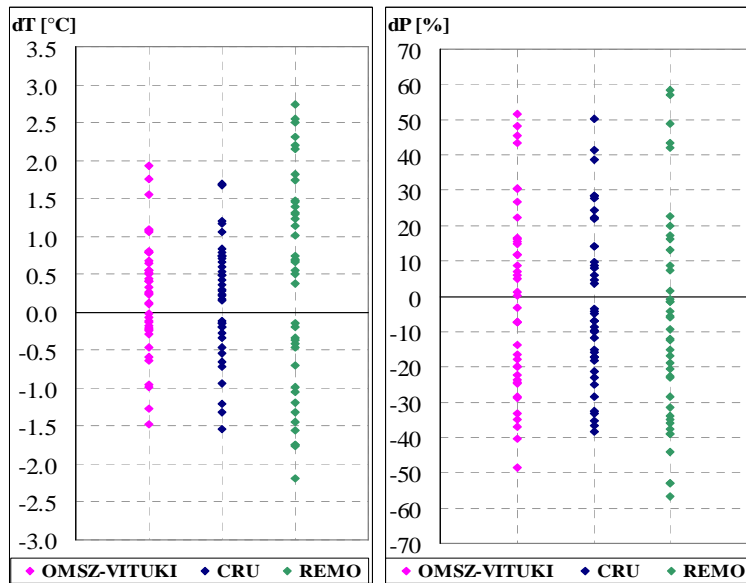


Figure 30. Temperature (dT ; left) and precipitation (dP ; right) deviations in all summers for 1961-2000

Based on the validation results REMO is well suitable for projecting temperature, precipitation and drought tendencies for the 21st century in the selected region.

5.1.2 Projected temperature and precipitation tendencies for the 21st century

Climate change signal for 2021-2050 and 2071-2100 has been studied based on the results of three emission scenario simulations (B1, A1B, A2) relatively to the reference period 1961-1990. In the near future (2021-2050) for A1B scenario the summer months (May, June, July, August) can be 0.5-1.5°C warmer in average than at the end of the 20th century (*figure 31*). Results of the three investigated scenario simulations are very similar (*Annex VII*). The increase of temperature is the largest in West-Hungary. Precipitation is projected to be 5-10% lower on the western part of the country and 5-10% higher on the eastern part (*figure 31*). For the A2 scenario, 5-15% precipitation increase is projected for the whole country (*Annex VII*), maybe due to the high aerosol concentration in the air, which can lead to the easier cloud- and precipitation formation.

For the second half of the 21st century, warming and drying of summers are more significant in the whole country. Based on the A1B scenario, summer temperatures may increase 3-4°C compared to the mean of the period 1961-1990 (*figure 31*). At the end of the 21st century decrease of the 30-year mean of summer precipitation sum can reach the 30-35% relative to reference period in the past in all investigated scenarios (*figure 31, Annex VII*), especially South-Hungary is affected by drying. Between 2021-2050 and 2071-2100 the largest precipitation difference can be detected in the southern part of the Hungarian lowland: in the first part of the 21st century this area can be characterised with the largest increase of precipitation and this seems to be one of the driest regions at the end of the century. These results underlines also that in the Carpathian basin the warming and drying of summers is much more stronger than the global trends. These findings are in good agreement with the analyses of different regional climate model simulations carried out in the EU-projects ENSEMBLES, PRUDENCE, CLAVIER and CECILIA²²

²² <http://ensembles-eu.metoffice.com/>, <http://prudence.dmi.dk/>, <http://clavier-eu.org/>, <http://www.cecilia-eu.org>

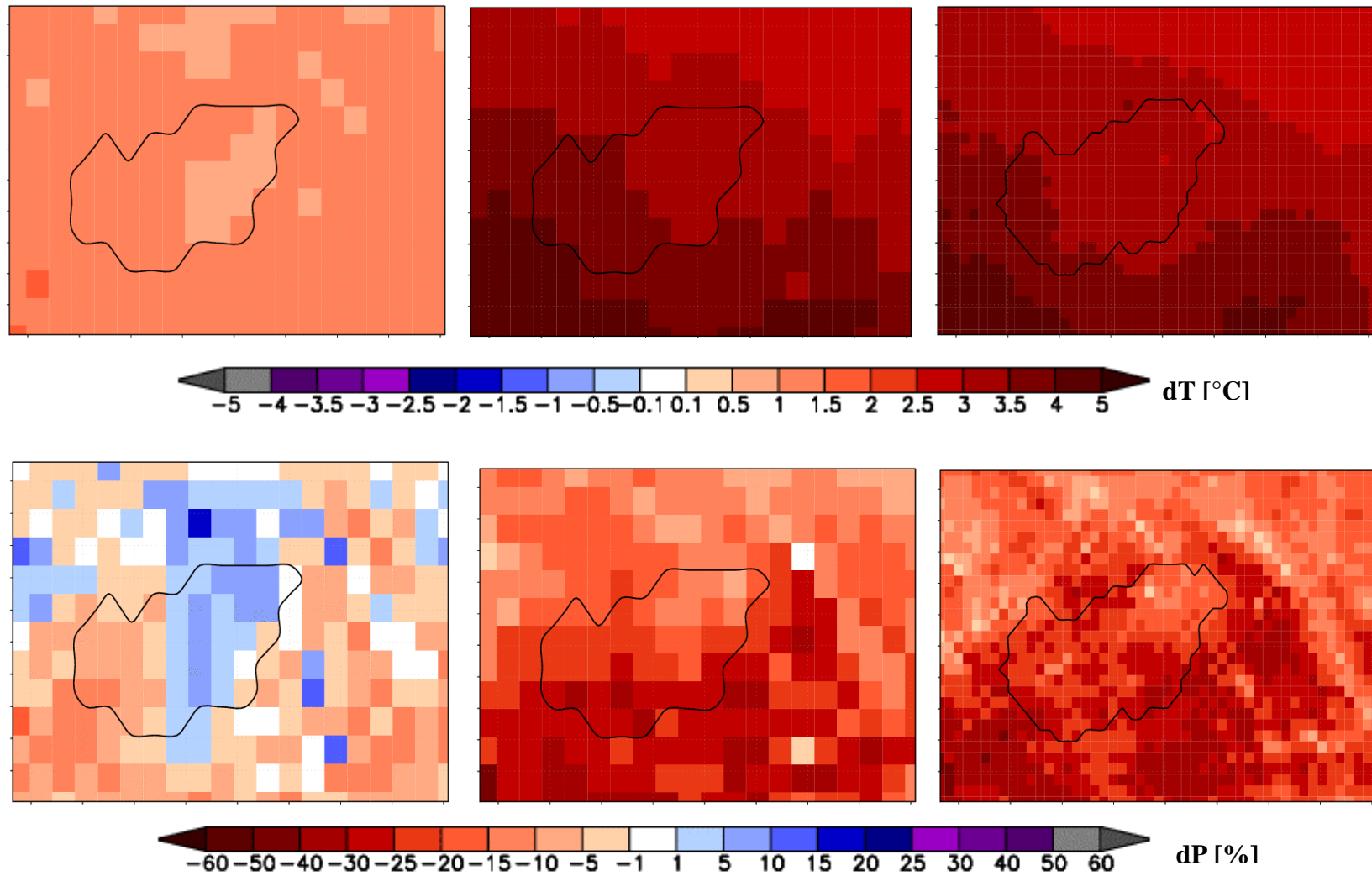


Figure 31. Climate change signal for summer temperatures (dT ; top) and precipitations (dP ; bottom) – emission scenario A1B. For 0.44° horizontal resolution, 2021-2050 vs. 1961-1990 (left) and 2071-2100 vs. 1961-1990 (middle). For 0.176° horizontal resolution 2071-2100 vs. 1961-1990 (right).

For A1B scenario dependency of climate change signal on horizontal resolution has been investigated. *Figure 31* visualises that projected changes of temperature and precipitation (2071-2100 vs. 1961-1990) are almost the same for both 0.44° and 0.176° resolution, although the finer scale provides more spatial details.

Probability distribution of the country mean summer temperature for the periods 1961-1990 and 2071-2100 shows that not only the climatic means but also the extremes are affected by climate change (*figure 32*).

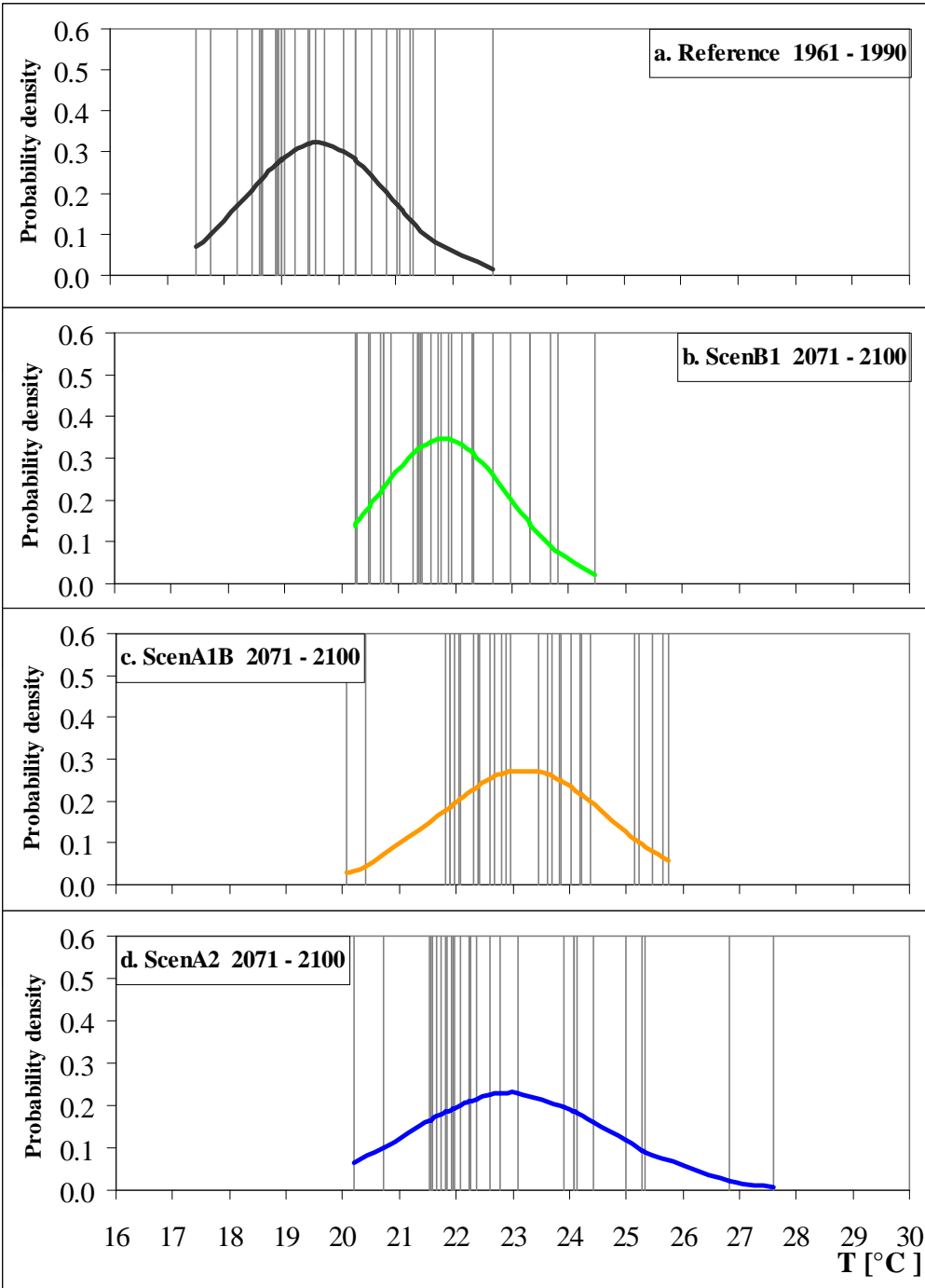


Figure 32. Probability distribution of the country mean summer temperature (*T*) for the reference simulation (a), and for the emission scenario simulations ScenB1 (b), ScenA1B (c) and ScenA2 (d). Grey lines represent the temperature values in the individual summers.

Distribution of temperature represented by the Gauss-curves are shifted in the warmer direction (similarly to *figure 1c*, IPCC 2001 and *Schär et al.* 2004). Based on the A1B scenario summer temperatures will be 3.6°C higher at the end of the 21st century than in the reference period. From the analysed scenarios B1 has the lowest future greenhouse gas emission rates, so that the smallest changes are also projected for the investigated period. The flatter and wider probability density functions mean that also the temperature variability, the probability and severity of extreme warm summers may increase under enhanced climate change.

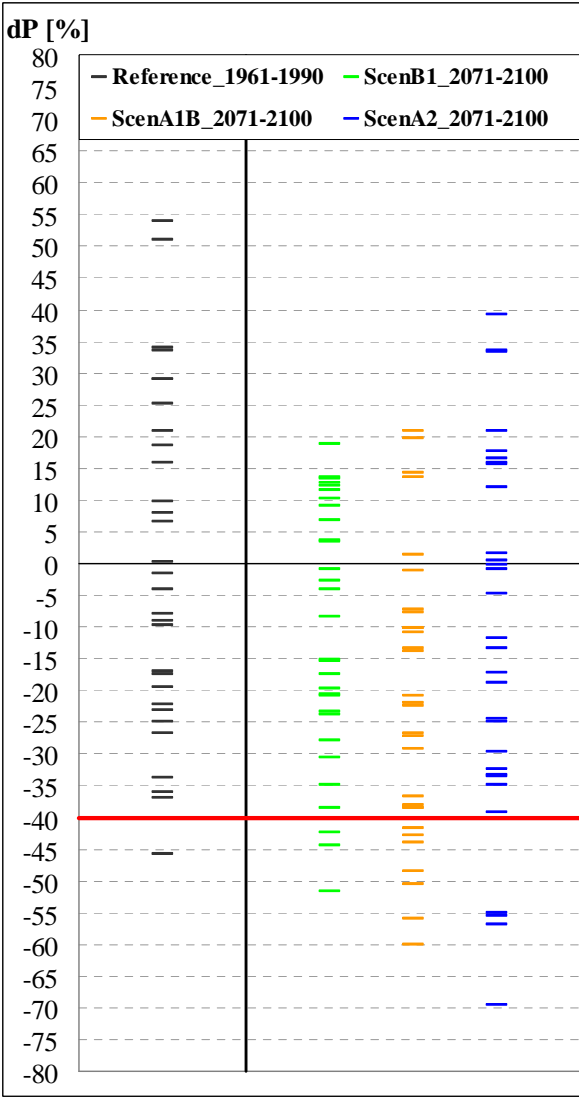


Figure 33. Relative precipitation anomalies (*dP*) of summers, for ScenB1, ScenA1B, ScenA2 emission scenarios. The 40% negative relative precipitation anomaly is marked with red line.

The country means of the relative precipitation anomalies also refer to the strong decrease of the summer precipitation for 2071-2100 (*figure 33*). At the end of the 20th century there were only one summer with larger than 40% precipitation anomaly, whereas at the end of the 21st century the probability of these events becomes higher. Similarly to the temperature, change of the 30-year mean of the summer precipitation sums is the largest for the A1B and the smallest for the B1 scenario. A2 scenario shows the largest variability for both temperature and relative precipitation anomalies. Tendencies introduced in this section can result in higher frequency and severity of droughts in the future.

5.1.3 Probability and severity of droughts in the 21st century

Probability of droughts. The country mean of the probability of dry events has been analysed considering the results of the three scenario simulations (B1, A1B and A2). The total number of droughts in the control simulation is the same as calculated with the CRU gridded station dataset (*figure 34*), which shows the excellent quality of the control simulation with respect to the analysed topic. *Figure 34* demonstrates that until 2050 the probability of the occurrence of dry summers can be lower in the A2 scenario. This relatively low frequency of droughts is probably caused by the stronger increase and higher level of SO₂ emission in this scenario compared to the other ones (IPCC 2007). It induces lower radiation and therefore lower temperature than for B1 and A1B scenarios. Also the higher aerosol concentration can play a role in the process that is favourable for the cloud- and precipitation formation (*Annex VII*), which can lead to the relative low frequency droughts.

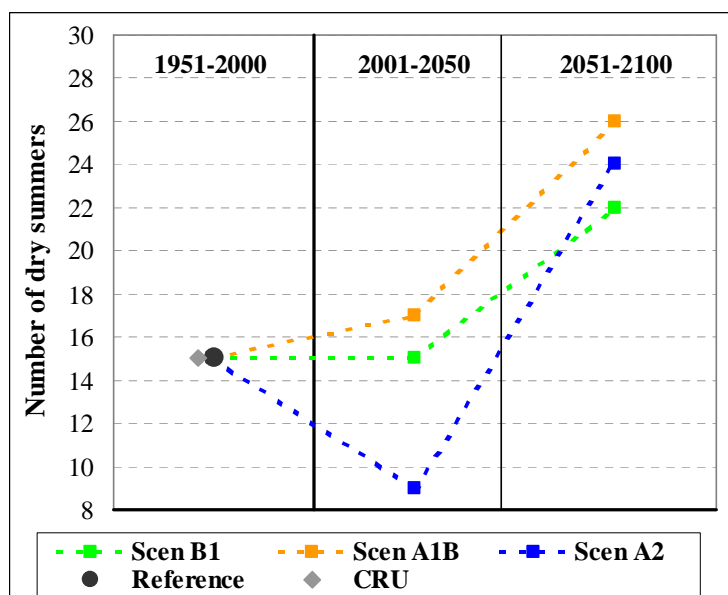


Figure 34. Total number of dry summers in Hungary for ScenB1, ScenA1B, ScenA2 emission scenarios. CRU: gridded station data.

For 2051-2100, the number of droughts increases significantly in all scenarios. In A1B, 26 droughts can occur, 11 more than in the period 1951-2000. This means that in the second half of the 21st century every second summer may be a dry one. The huge increase in the number of dry events may relate to the strong continuous increase of CO₂ emission and decrease of SO₂ emission during the second half of the 21st century. These lead to a higher radiation rate and the strong increase in temperature for all of the investigated scenarios (*figure 31, Annex II*). The decrease of the aerosol concentration can also support the high probability of droughts.

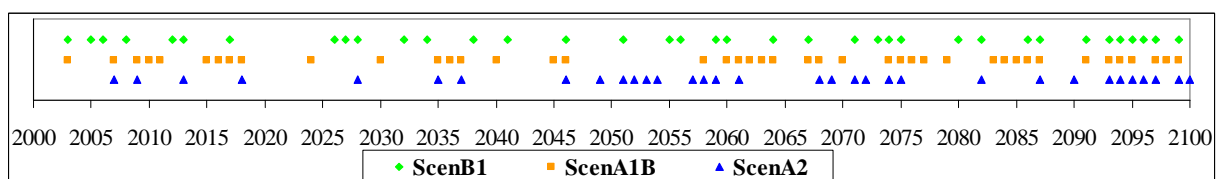


Figure 35. Consecutive dry periods in the 21st century. Each symbol represents a summer drought. ScenB1, ScenA1B, ScenA2: emission scenarios.

Consecutive dry periods. Not only the probability of dry summers, but also the length of consecutive dry periods is projected to increase in all scenarios after the middle of the 21st century (figure 35). Here, five or six droughts in sequence may occur compared to the two or three in the period 2001-2050. In the last 10 years of the 21st century almost all summers can be classified as dry.

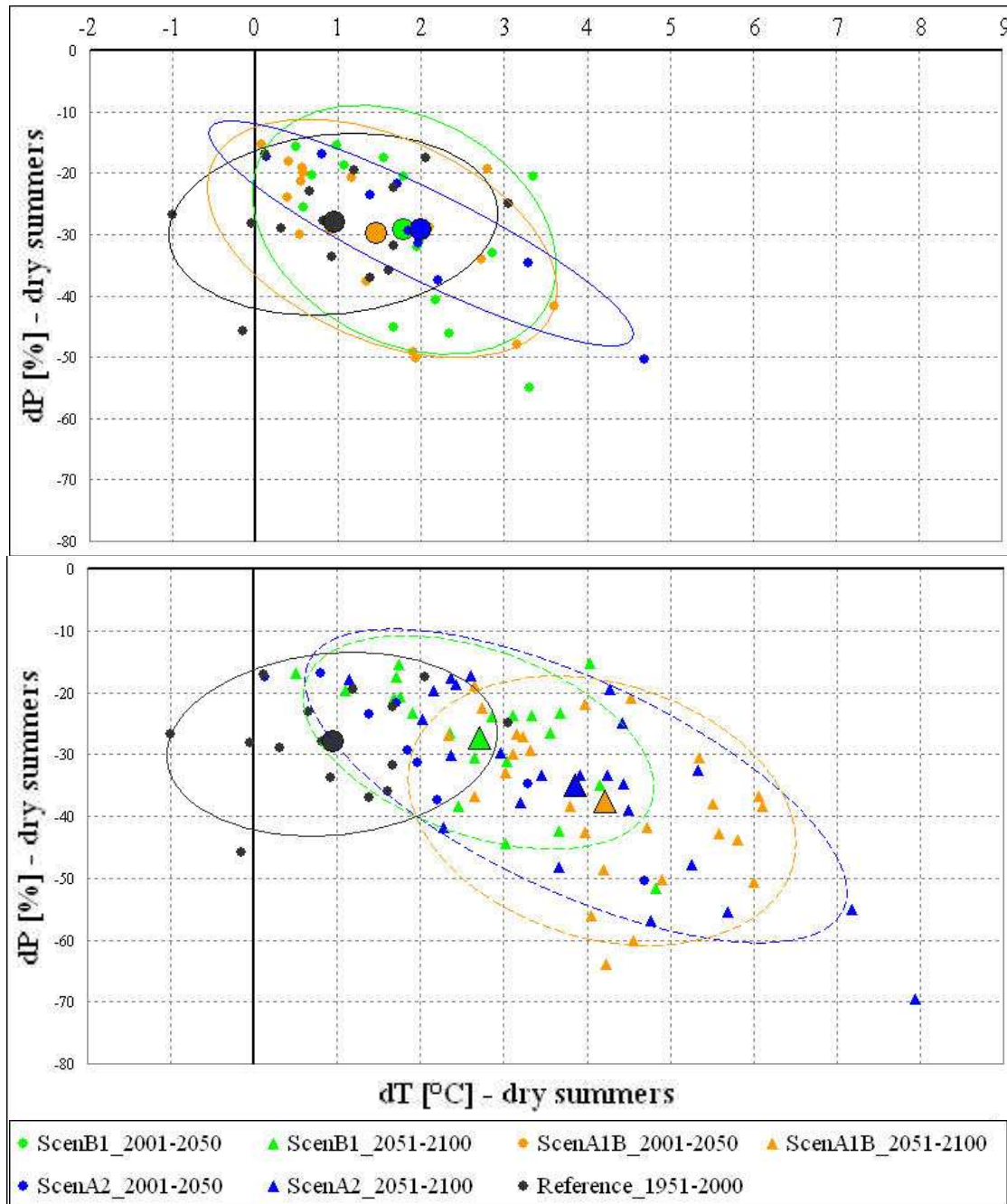


Figure 36. Severity of all dry summers for 2001-2050 (top) and 2051-2100 (bottom) for Hungary. The small symbols represent the individual dry events, the big ones the averages of the clusters. The ellipses describe the place of the different clusters with a 95% confidence level. *dT*: temperature anomaly, *dP*: relative precipitation anomaly for 2001-2050 vs. 1961-1990 and 2051-2100 vs. 1961-1990, respectively. *ScenB1*, *ScenA1B*, *ScenA2*: emission scenarios.

Severity of droughts. Changes of the drought severity in the future have been analysed based on the temperature- and relative precipitation anomalies of the dry summers (*figure 36*).

In the period 2001-2050 the average of *dPs* is almost the same in the three scenarios as in the control simulation, whereas their number in A2 scenario is significantly lower. The clusters visualised by the ellipses shift mainly to the direction of higher temperatures: *dT* is increased by about 1°C in A2 scenario relative to the reference simulation.

For 2051-2100 the clusters are moving to dryer and warmer conditions (*figure 36*), which means that the severity of droughts increases significantly in all scenarios. For A1B scenario in the second half of the 21st century the average negative *dPs* of dry summers will be almost 10% higher, the average *dTs* 3.2°C higher than in the control period. From the results of A1B and A2 scenarios it is clearly visible that summers with extreme low precipitation can be characterised in most cases with extreme high temperatures. The very dry and extreme warm summers become more frequent, as it was discussed in *Sect. 5.1.2*. From the analysed scenarios B1 shows the smallest changes relative to the reference period. In this scenario precipitation anomalies do not change significantly in the 21st century. The average of temperature anomalies of dry summers is 1.8°C in B1, whereas 3–3.5°C in the A1B and A2 scenarios.

5.1.4 Spatial differences in the drought trends

After the investigation of the drought trends for Hungarian mean, spatial distribution of the projected temperature- (*dT*) and relative precipitation anomalies (*dP*) has been analysed (2071-2100 vs. 1961-1990; *figure 37*). That area is assumed to be the most climate change affected, in which both positive temperature anomalies and negative precipitation anomalies are largest in the period 2071-2100 relative to 1961-1990. Thresholds applied to prepare the map are 20%-, and 25% negative relative precipitation anomalies and 3.0°C and 3.5°C temperature anomalies, respectively. In the southwestern part of Hungary is the projected tendency of warming and drying is the largest (*figure 37*). This area is characterised by 3.7°C higher summer temperature mean and almost 30% lower precipitation amount for 2071-2100 than in the period 1961-1990. The least affected are the northeastern areas.

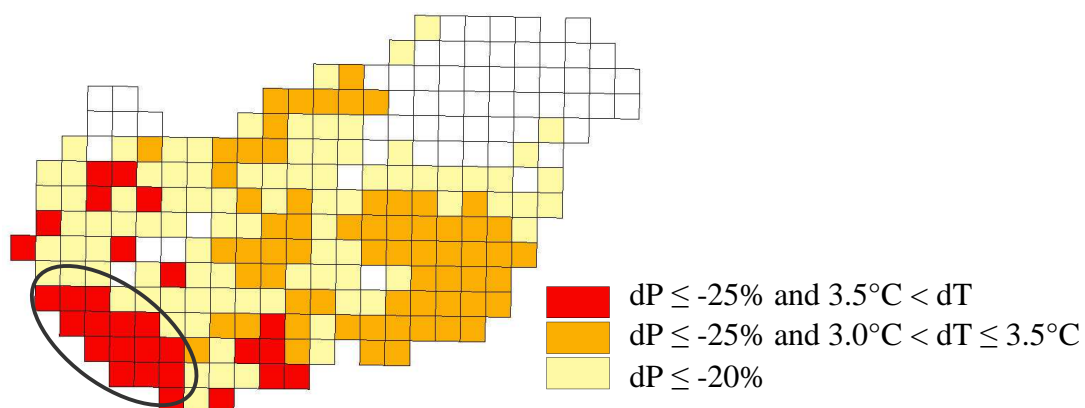


Figure 37. The spatial distribution of the climate change signal for precipitation (*dP*) and temperature (*dT*) in summer (2071-2100 vs. 1961-1990). The most drought affected region is marked with ellipse.

As discussed in *Sect. 5.1.3* for country means, number of droughts (MDS+EDS) almost doubles by the end of the 21st century compared to the second half of the 20th century. In this chapter the spatial differences of the increase of drought probability are studied, focusing on the change of the number of summers with larger than 40% precipitation decrease (2071-2100 vs. 1961-1990). The largest increase in their number is projected along the southern and western border of the country (*figure 38*).

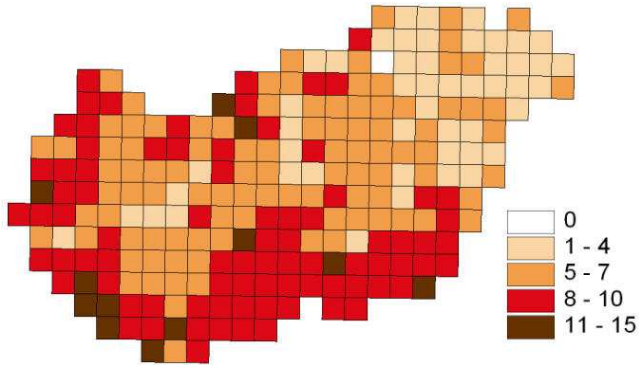


Figure 38. Change of the number of summers with negative relative precipitation anomaly $\geq 40\%$, 2071-2100 vs. 1961-1990 (unit: number of summers)

In the southwestern region (*figure 39*), the number of moderate dry summers does not change in the 21st century, whereas there is a huge increase in the probability of extreme dry summers (*figure 39*). Especially the number of summers characterised by larger than 40% negative relative precipitation anomaly increases: from 3 in the period 1961-1990 to 13 in 2071-2100, which is almost the half of the investigated period.

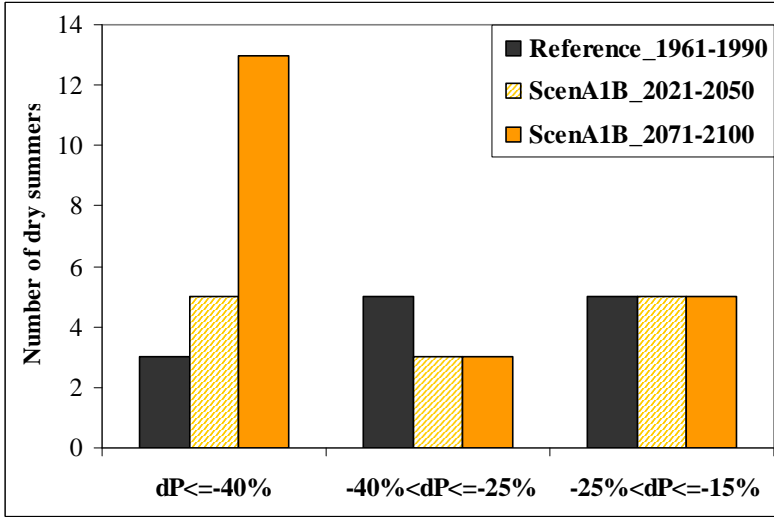


Figure 39. Frequency of dry summers on the most climate change affected southwest part of Hungary. *dP*: relative precipitation anomaly, ScenB1, ScenA1B, ScenA2: emission scenarios.

5.1.5 Summary

Regarding to the research questions the major findings of the analyses are as follows:

How accurately can the regional climate model REMO simulate past dry events?

- In summer a warm bias for temperature and a dry bias for precipitation has been detected compared to the observed data, which are related to the summer drying problem of the regional climate models.
- The statistical characteristics of dry summers can be represented realistically with REMO in comparison with observations. Simulated and observed data agree well in the frequency of droughts. Only the proportion and severity of extreme dry summers are overestimated by the model.
- Based on the validation results, REMO is well suitable for projecting the long-term tendencies of temperature and precipitation as well as the occurrence and severity of droughts for the 21st century in the selected region.

What are the projected tendencies of temperature means and precipitation sums in the 21st century?

- In the near future the climate change is moderate, results of the three investigated scenario simulations for temperature are very similar.
- For the second half of the 21st century warming and drying of summers are significant in the whole country. At the end of the 21st century, decrease of the 30-year mean of summer precipitation sum can reach the 30-35% relative to reference period in the past. Changes of the climatic means are the largest in A1B scenario, whereas A2 shows the largest variability for both temperature and precipitation values. From the analysed scenarios B1 has the lowest future greenhouse gas emission rates, so that the smallest changes are also projected for the investigated period.
- Projected tendencies of temperature and precipitation are the same for 0.44° and 0.176° horizontal resolution, which means that the magnitude of the climate change signal is independent from resolution. The finer horizontal resolution provides more regional details.

Will climate change have an effect on probability and severity of droughts in the future?

- For all scenarios, probability of droughts is not higher in the first half of the 21st century, their severity increases only through the higher temperature compared to the period 1951-2000.
- Under enhanced climate change (2051-2100), the number of dry events is significantly higher than for 1961-1990; in the A1B and A2 scenarios droughts may occur in every second summer. The consecutive dry periods will last longer compared to the first half of the 21st century. The severity of droughts increases significantly in all scenarios compared to the reference period.

Which region can be characterised by the largest tendency of warming and drying?

- The southwest part of Hungary is the most affected by warming and drying. It can be characterised by almost 30% precipitation decrease and 3.7°C temperature increase for summer (2071-2100 vs. 1961-1990). The expected increase of the probability of extreme dry summers is largest also in this area.

5.2 Feedback of forest cover change on the regional climate

5.2.1 Climatic effects of maximal afforestation and deforestation

For the time period 2071-2100 spatial distribution of evapotranspiration, surface temperature, 2m-temperature and precipitation have been analysed comparing the simulation results of the maximal afforestation as well as deforestation sensitivity experiments to the reference simulation. In the model, vegetation has no height, therefore surface temperature corresponds to the temperature of the vegetation surface and the 2m-temperature is the temperature 2m above the canopy.

Maximal afforestation. For the maximal afforestation scenario, the 30-year mean of the summer evapotranspiration rate is 10-15% higher than for the present forest cover (*figure 40*). In smaller areas this increase can reach the 20%. The difference of evapotranspiration between the maximal afforestation and reference simulation is larger in regions, which are characterised by larger increase of *LAI* and roughness length values (*figure 19-20*). Due to the cooling effect of the enhanced evapotranspiration rate, surface temperature is reduced by up to 1°C on the eastern part of the country, 0.3-0.5°C on the western part of the Hungarian lowland and in Southwest-Hungary, respectively, and 0.2-0.3°C over the mountainous areas (*figure 40*). A slight decrease of 2-m temperature (0.1-0.2°C) can be detected only in North-Hungary (*figure 40*).

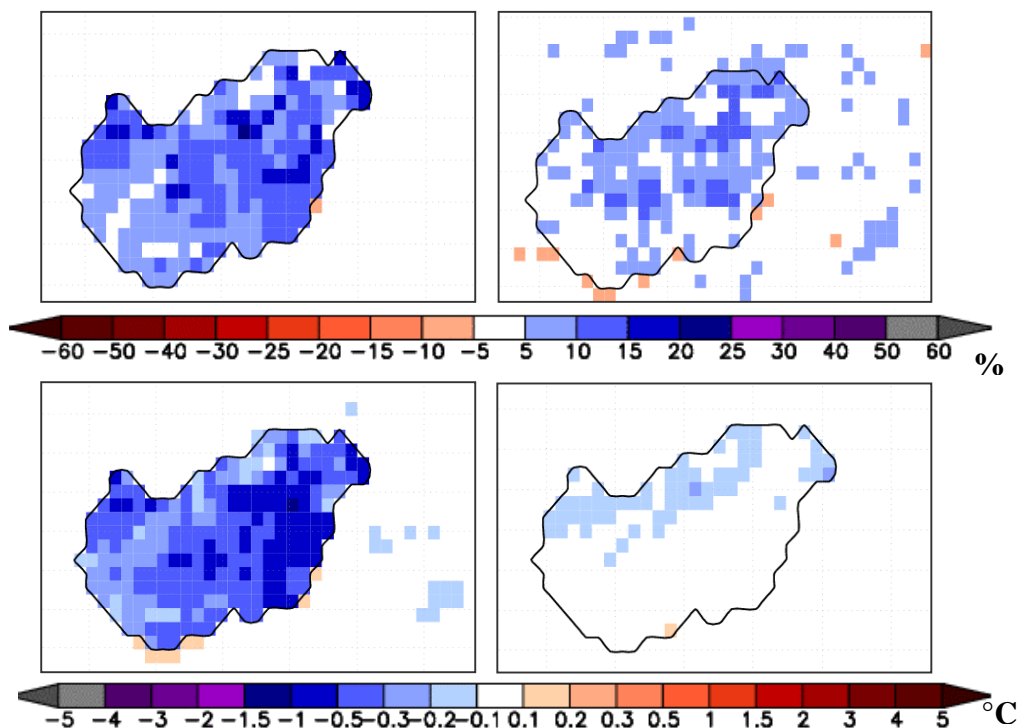


Figure 40. Changes of evapotranspiration (top left), precipitation (top right), surface temperature (bottom left) and 2m-temperature (bottom right); maximal afforestation vs. reference (2071-2100)

Changes of both evapotranspiration and surface temperature are localised in Hungary (corresponding to the changes of the land surface parameters), they are determined primary by local processes. On the contrary, precipitation has more complex behaviour, it is influenced also by large-scale atmospheric circulation, its changes are spread out over larger areas (*figure 40*). The 30-year mean of summer precipitation sum increased by up to 15% for the maximal afforestation simulation compared to the reference (*figure 40*). The moistened air seems to be

transported northwards, producing more precipitation also over the Carpathian Mountains. There are almost no changes on the southern and western part of the country. Over the mountainous areas 5-10% more precipitation is simulated with enhanced forest cover, although the afforestation rate was the smallest in these regions. Possible reasons for it can be the more humid air over mountains and the easier precipitation formation due to the orographic uplift as well as the characteristic large-scale circulation patterns and southwest wind in summer.

Similarly to the most climate change affected area (Sect. 5.1.4), the region has been determined, where both precipitation-increasing (dP) and temperature-decreasing (dT_{2m}) effect of maximal afforestation is the largest compared to the reference forest cover in the period 2071-2100 (figure 41).

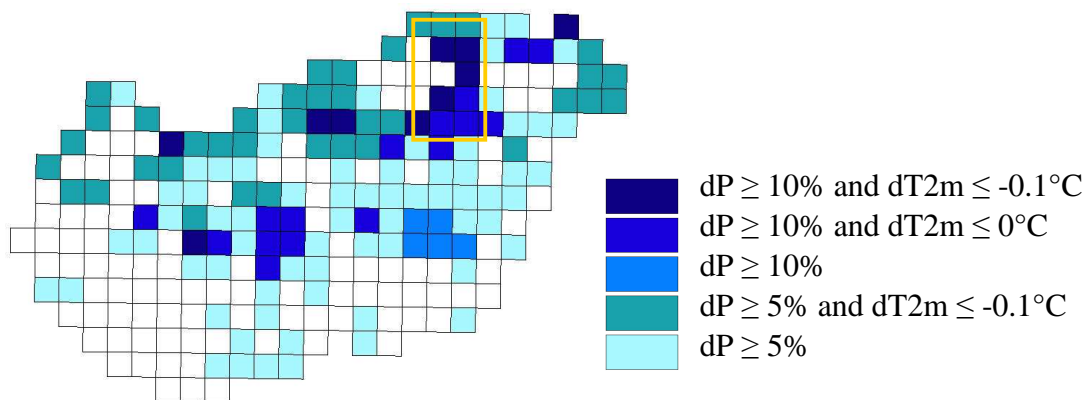


Figure 41. Spatial distribution of the effect of maximal afforestation on precipitation (dP) and 2m-temperature (dT_{2m}) in summer (2071-2100). The region, in which the climatic effect of maximal afforestation is the largest, is marked with yellow square.

Thresholds applied to prepare the map are 10%-, and 5% relative precipitation anomalies as well as -0.1 and 0°C temperature anomalies, respectively. Figure 41 shows that in the north-eastern part of Hungary is the climatic effect of the maximal afforestation the largest, which does not correspond to the area with the largest amount of afforestation. In the southern and western areas is the effect of maximal afforestation on precipitation and 2m-temperature quite small.

Deforestation. The opposite effect can be observed in the deforestation sensitivity study. The magnitude of the climatic feedbacks of forest cover change in this scenario is smaller. Evapotranspiration rate decreases 5-10% and surface temperature increases $0.3-0.5^\circ\text{C}$ in the regions where larger forest cover decrease has taken place (Annex VIII). There are no changes in the 2m-temperature and only a slight decrease in precipitation (Annex VIII). The weaker signal in this sensitivity study compared to the maximal afforestation scenario can be explained by the relative small fraction of forests in the gridboxes, which were replaced by grasslands. The forested area is 20% in Hungary, which appears mostly in small fragments rather than in larger continuous forest blocks. These forest-steppe mosaics are typical feature at the lower forest limit.

The spatial correlation between the magnitude of forest cover change and its effects has been investigated including all Hungarian gridboxes. Figure 42 visualises that the larger the increase/decrease of the forested area in the gridbox, the stronger the feedbacks on

evapotranspiration and thereby on surface temperature. For these two meteorological quantities, effects of maximal afforestation and deforestation are systematic.

In case of precipitation, afforestation results in wetter conditions for almost all Hungarian gridboxes, but for deforestation the opposite signal is not so clear (*figure 42*). Similarly to *figure 40*, this graph also shows that precipitation formation is influenced also by large-scale processes, therefore changes of its amount cannot be directly correlated to the magnitude of the forest cover change.

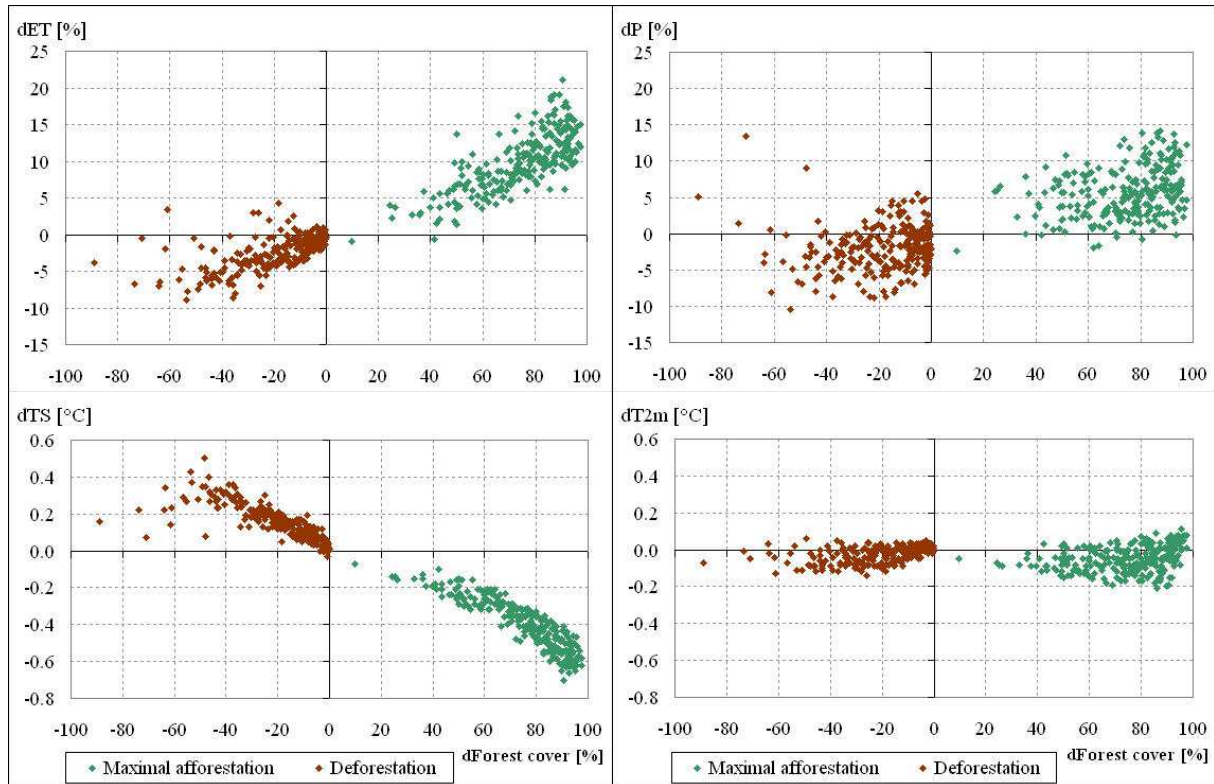


Figure 42. Correlation between the change of forest cover and the change of evapotranspiration (*dET*; top left), surface temperature (*dTTS*; bottom left), 2m-temperature (*dT2m*; bottom right) and precipitation (*dP*; top right) for all grid boxes in Hungary; maximal afforestation vs. reference (2071-2100)

5.2.2 Effect of maximal afforestation in the region characterised by the largest possible forest cover increase

For detailed analysis of the climatic effect of maximal afforestation and modified land cover parameters, a region with the largest forest cover increase was selected (*figure 18*).

Here, the 95% afforestation leads to 96% larger leaf area, 13% lower albedo values and almost 1m increase of roughness length for the summer months, compared to the present land cover (*table 4*). Mostly grass crops have been replaced by forests, the changes of the land surface parameters in the selected region correspond to the difference between the characteristic parameters of these land cover types and forests (e.g. the small albedo-effect in this study is caused by the low albedo differences between forest and grass crops).

Table 4. Changes of the main land surface parameters on the region with the largest amount of afforestation (summer means)

Maximal afforestation vs. reference	Roughness length	Leaf area index	Albedo	Fractional vegetation cover
units	0.913	2.3	-0.023	-0.1
%		96	-13	-11.7

For the winter months, the very low values of LAI and albedo (figure 43) mean that additional forests are deciduous, assuming no photosynthetic active vegetation for this season. In this study the climatic feedbacks of forest cover change have been analysed for Mai, June, July and August.

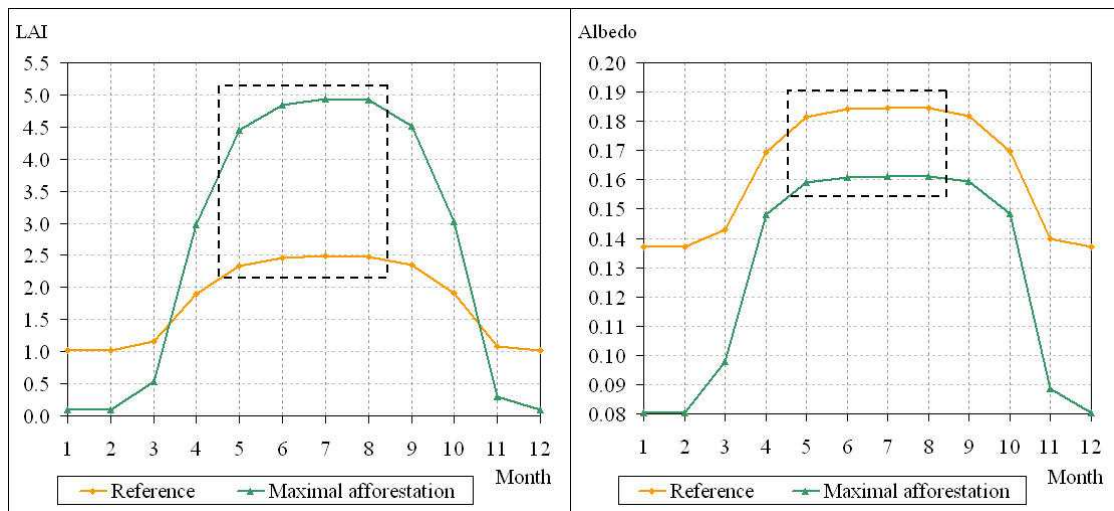


Figure 43. Annual cycles of leaf area index (left) and albedo (right) for the maximal afforestation and reference experiments

Evapotranspiration. Forests have larger leaf area and they are aerodynamically rough. These properties support the more intense vertical mixing compared to other vegetated surfaces, which leads to enhanced ability of evapotranspiration. For summer, total evapotranspiration is the sum of transpiration, interception and bare soil evaporation. Bare soil evaporation is negligible in the summer months, because vegetation is assumed to cover the whole region. Furthermore, in the model bare soil evaporation occur from the upper 10 cm water column, which is dry in summer.

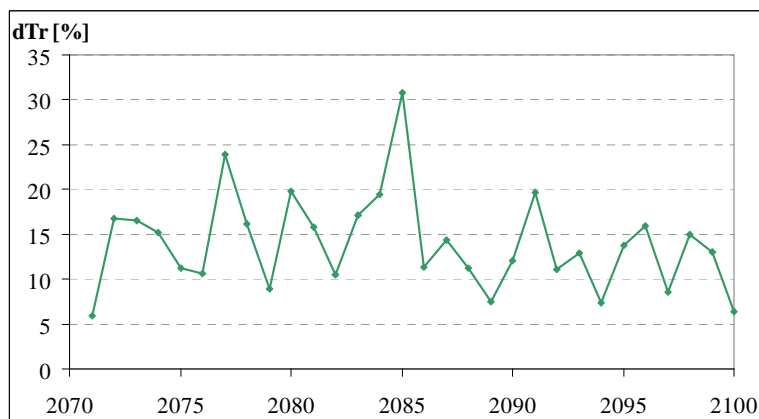


Figure 44. Effect of maximal afforestation on transpiration (dTr); maximal afforestation vs. reference (2071-2100)

For all summers in the investigated time period (2071-2100), maximal afforestation leads to 18 % higher transpiration rate in 30-year mean, compared to the reference forest cover (*figure 44*). If water uptake is not limited, deeper roots result in more available water for transpiration in the model. Stomatal resistance, dependent on photosynthetically active radiation, also influences the transpiration efficiency in the simulations.

Forests also influences climate via intercepting precipitation. The rate of precipitation can be stored on the vegetation surface increases with leaf area due to the larger skin reservoir, which leads to higher interception rate. In the selected area, increase of interception varies between 5% and 27% relative to the original land cover in the investigated 30-year time period (*figure 45*). Consequently, for the maximal afforestation scenario, total evapotranspiration is strengthened in the whole time period (not shown).

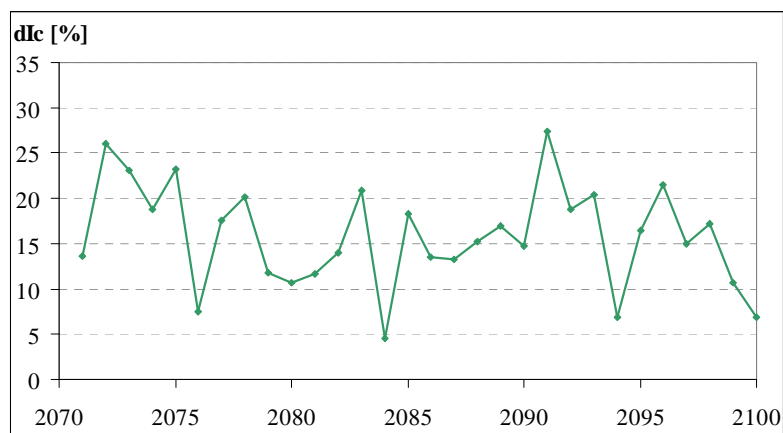


Figure 45. Effect of maximal afforestation on interception (*dlc*); maximal afforestation vs. reference (2071-2100)

Precipitation. Moist air, resulted by the local increase of evapotranspiration can be favourable for cloud and precipitation formation via convection. For the maximal afforestation experiment, precipitation increase is systematic, in larger part of the investigated time period exceeding 5% (*figure 46*). Variability of the precipitation difference between the maximal afforestation and the reference experiment is large among the 30 investigated summers (the increase due to maximal afforestation can reach the 25% in certain summers).

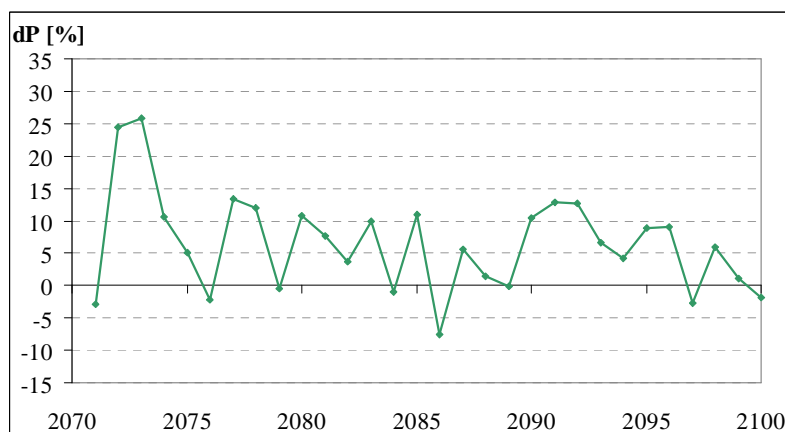


Figure 46. Effect of maximal afforestation on precipitation (*dP*); maximal afforestation vs. reference (2071-2100)

As discussed in Sect 5.2.1 this is not the area of the country with the largest increase of precipitation. It underlines that more complex processes are taking place, than the direct conversion of higher evapotranspiration from the surface into more precipitation.

Surface temperature. For the maximal afforestation scenario, surface temperature is up to 0.8°C lower compared to the reference land cover, which is the result of stronger evapotranspiration (figure 47). The simulated cooling trend corresponds to the reality, but in nature for summer, the forest soil surface is colder because of the shading effect of trees (interception of solar radiation) and the isolating effect of litter. In the model, vegetation has no height, therefore surface temperature is influenced by evapotranspiration and albedo. Forests are darker, have lower albedo, which leads to higher net solar radiation on the surface. Through the albedo-effect, surface could be warmer in the afforestation experiment. Despite of the 13% lower albedo in the selected region the cooling effect of evapotranspiration dominates, resulting in decrease of the surface temperature mean in summer.

2m-temperature. 2m-temperature difference between the maximal afforestation and reference experiment varies from -0.2 to +0.3°C (figure 47).

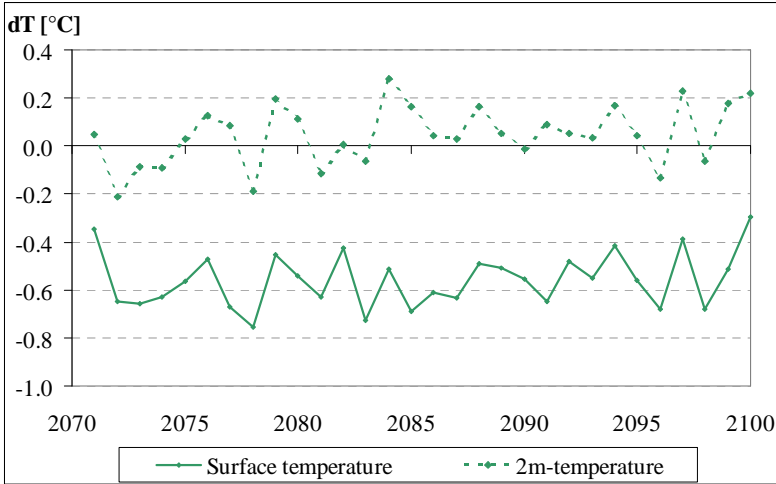


Figure 47. Effect of maximal afforestation on surface temperature and 2m-temperature; maximal afforestation vs. reference (2071-2100)

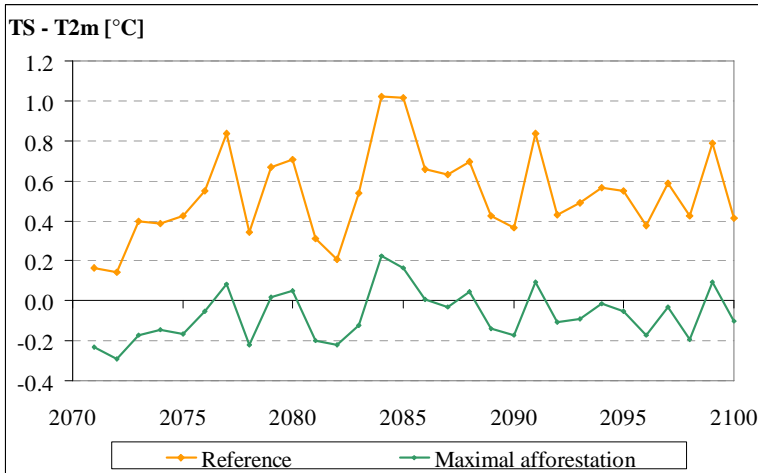


Figure 48. Difference between surface- and 2m-temperature (TS-T2m) for maximal afforestation and for reference (2071-2100)

Lower surface temperature seems to have only a slight influence on the 2m-temperature in the maximal afforestation simulation, which can be related to the weak albedo-effect and the small feedback of afforestation on the sensible heat flux. But due to the evaporative cooling of the surface, the difference between the surface- and 2m-temperature decreased significantly for the maximal afforestation scenario relative to the reference (*figure 48*). Further reason for it can be, that the larger roughness length of forests enhances the mechanical turbulence and the vertical mixing, which also reduce the temperature difference between the surface and the overlying air.

Heat fluxes. Forests are influencing not only the hydrologic cycle, they are also important determinant of the surface energy fluxes. The larger leaf area index and low aerodynamic resistance (through increased roughness length) have a positive effect on evapotranspiration, thus on latent heat flux.

Difference of the latent heat flux between the maximal afforestation and reference simulations varies between 7 and 29% (*figure 49*). Corresponding to the increase of latent heat, sensible heat flux decreased, but this signal is weaker. The decrease of the sensible heat flux can be observed in half of the investigated time period (*figure 49*). It is caused by the cooler surface temperature, leading to smaller difference between surface- and 2m-temperature. This temperature difference is directly proportional to the sensible heat flux.

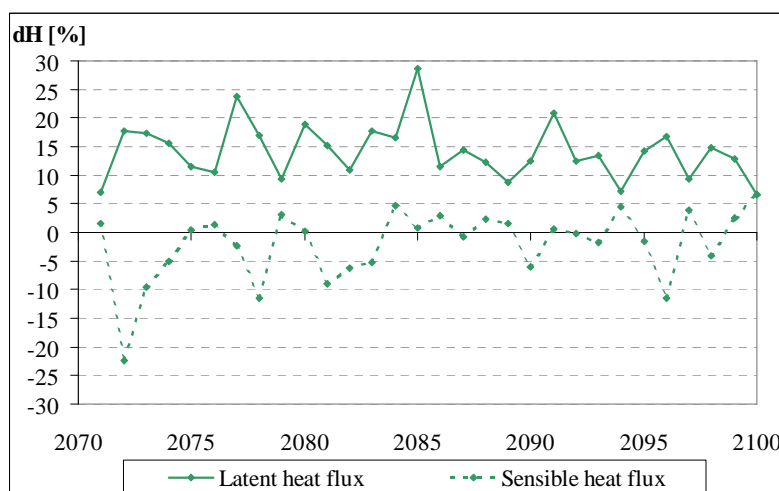


Figure 49. Effect of maximal afforestation on latent- and sensible heat flux; maximal afforestation vs. reference (2071-2100)

The feedback of maximal afforestation on sensible heat flux is weak in this study. Its decrease could be partly compensated by the opposite effect due to the lower albedo of forests, which leads to increased absorption of shortwave radiation, increased amount of net radiation and therefore higher sensible heat flux.

As theoretical basis, processes related to the forest cover increase in the model for summer are shown on *figure 50*. The simulated effects of maximal afforestation on surface water- and energy balance introduced in this section are summarized on *figure 51*. The columns visualise to the May-June-July-August means, the bars represent the variability of the results among the 30 investigated summers. The variability of the changes for all meteorological variables is quite large, the changes are not statistical significant. Whereas for most variables – except of 2m-temperature and sensible heat flux – the effect of maximal afforestation is systematic for the investigated time period.

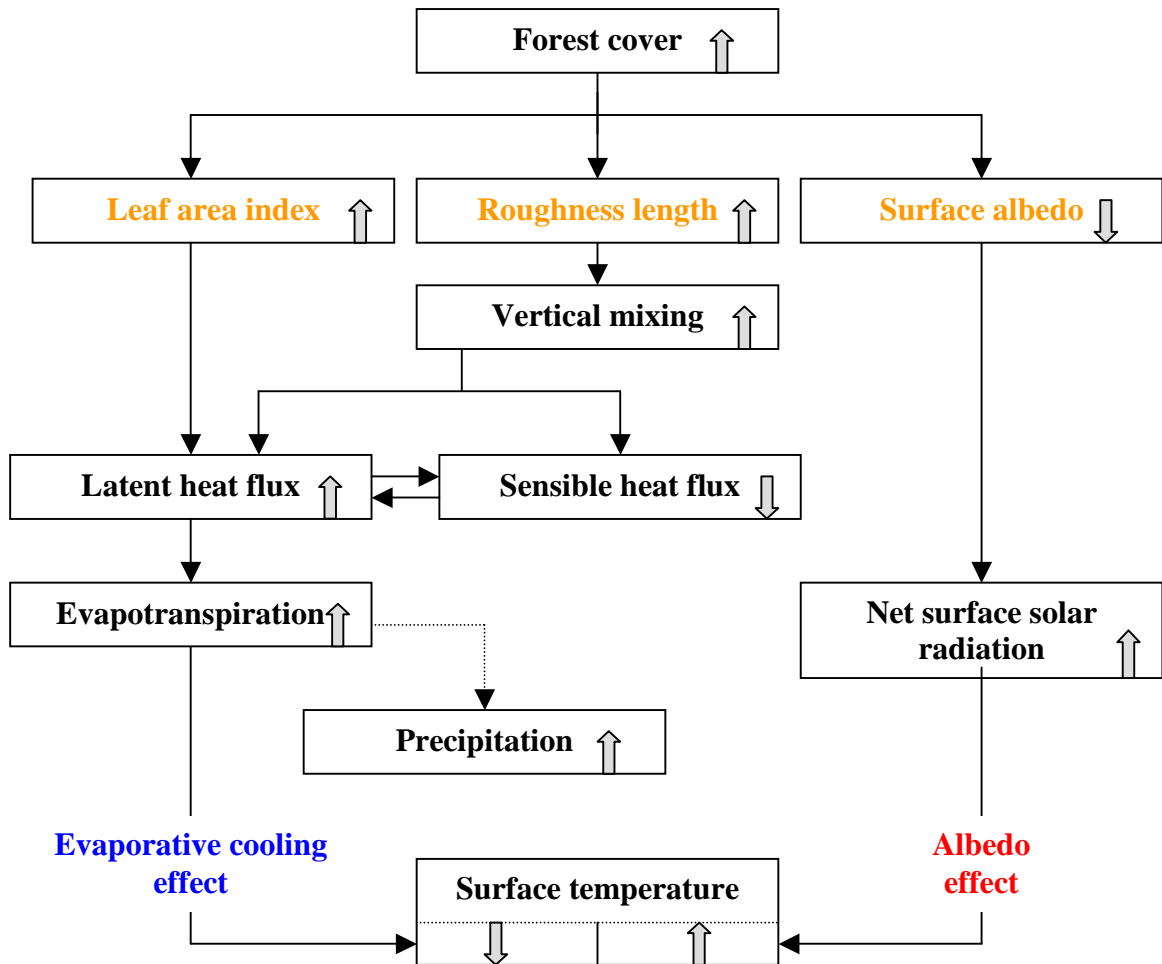


Figure 50. Processes related to the forest cover increase for summer

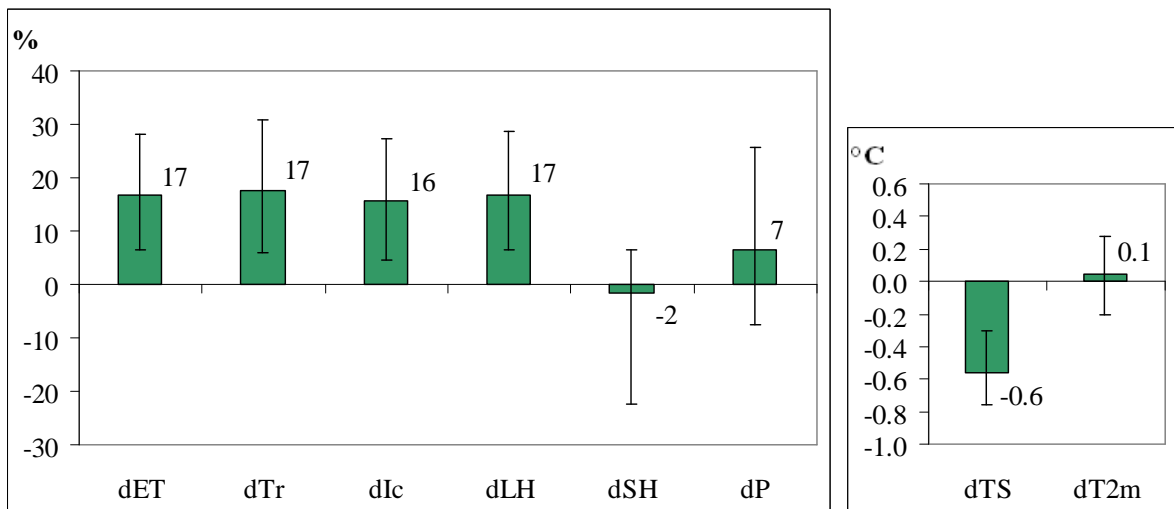


Figure 51. Effect of maximal afforestation on the main meteorological variables (maximal afforestation vs. reference 2071-2100). Error bars represent the minimum and maximum values. ET: evapotranspiration, Tr: transpiration, Ic: interception, LH: latent heat flux, SH: sensible heat flux, P: precipitation, TS: surface temperature, T2m: 2m-temperature

5.2.3 Interaction of the main climatic forcings of afforestation during the summer months

The investigated main climatic forcings of maximal afforestation are the evaporative cooling effect and the albedo-effect. They have opposed influence on the surface temperature (figure 50), the dominant of them decides whether the studied region cools or warms.

For 30-year summer mean, maximal afforestation resulted in decrease of the surface temperature relative to the reference land cover due to the evaporative cooling effect of the forest cover increase (figure 52). Interaction of the two forcings has been analysed on daily scale for a region with the largest amount of afforestation in Hungary (figure 18).

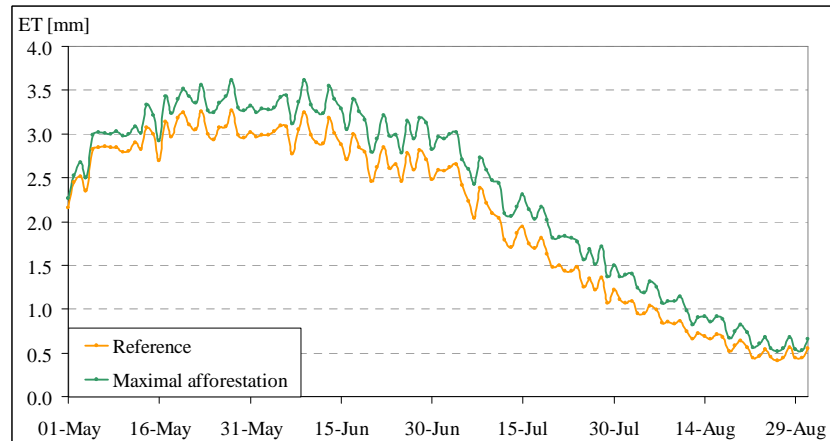


Figure 52. Daily evapotranspiration (ET) for the reference and the maximal afforestation experiment (2071-2100)

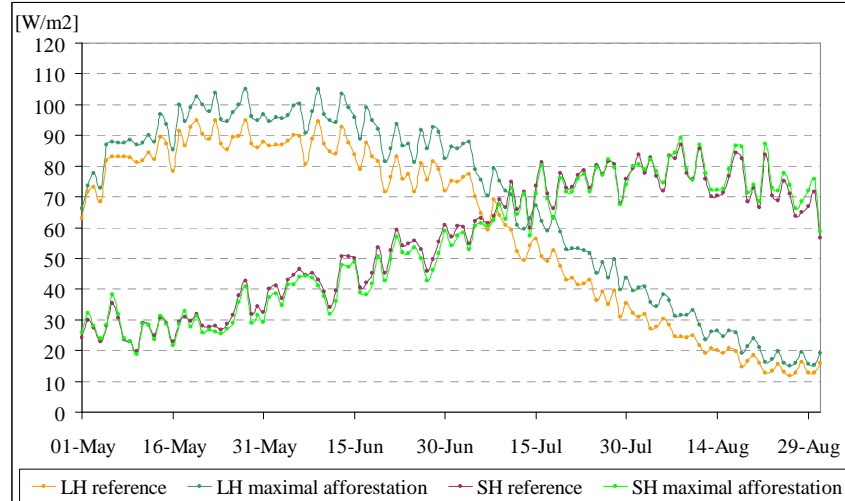


Figure 53. Latent- (LH) and sensible (SH) heat flux for the reference and the maximal afforestation simulations (2071-2100)

Until there was enough moisture in the soil, higher temperatures enhanced the intensity of evapotranspiration (figure 52). In the middle of July, soil moisture content reached its critical value, evapotranspiration and latent heat flux started to decrease for both the reference and the maximal afforestation experiments (figures 52-53). As sensible heat flux got larger than latent heat flux (figure 53), Bowen ratio exceeded 1 (figure 54), which corresponds to warmer and dryer boundary layer. (This occurs for the maximal afforestation experiment two days later than for the reference simulation.)

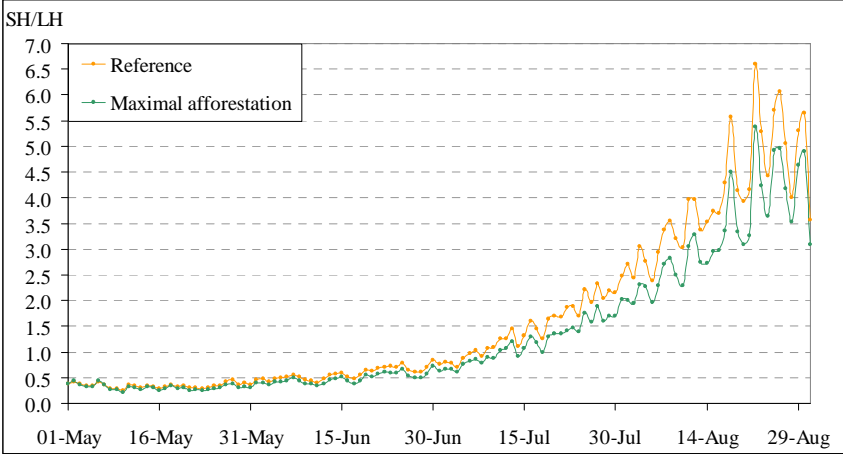


Figure 54. Bowen-ratio (SH/LH) for the reference and the maximal afforestation experiment (2071-2100)

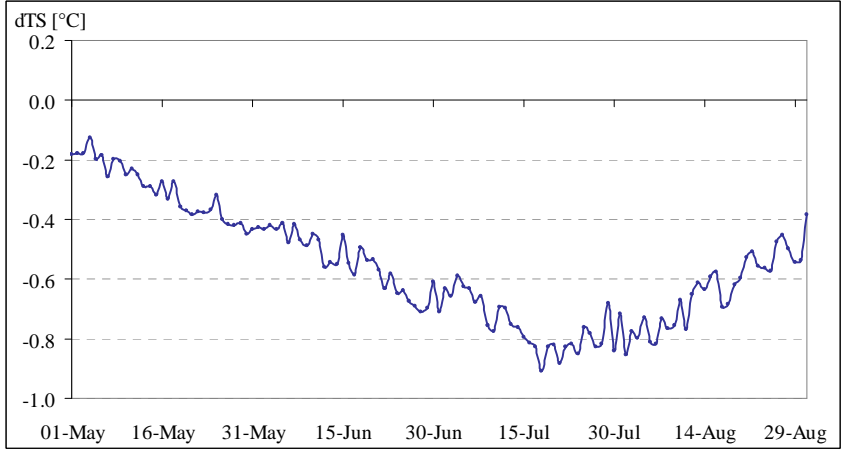


Figure 55. Change of daily surface temperature (dT_S); maximal afforestation vs. reference (2071-2100)

From May to August, the more intense evapotranspiration of forests resulted in cooler surface temperature for the maximal afforestation study than for the reference (figure 55). After the evaporative cooling effect decreased due to the limited transpiration, the albedo effect started to increase. This led to a smaller difference in the surface temperature between the two experiments (figure 55), corresponding to the smaller difference in evapotranspiration between the two simulations.

For maximal afforestation, the cooling and moistening effect of forests remained dominant in the whole summer period, causing higher evapotranspiration rate and latent heat flux than for the reference forest cover.

5.2.4 Climatic role of the potential afforestation survey

As a real practical example for the near future (2021-2025), it has been investigated, whether the 7% forest cover increase, which can be potential achieved under the Hungarian site conditions, can influence the regional climate (Gálos et al. 2009).

In this scenario a relative small fraction of the marginal agricultural croplands has been replaced by forests. Therefore only a small increase of *LAI* (mainly in the area, where more coniferous forests are proposed) and almost no changes in albedo, fractional vegetation cover and roughness length can be observed (figure 18) relative to the reference experiment. As comparison, for maximal afforestation, the magnitudes of the modification of these land surface parameters were quite large (figure 18-21). Considering the results of the maximal afforestation experiment, for the potential afforestation study, no significant feedback is expected.

In the investigated time period, changes of the summer evapotranspiration, transpiration and interception amount vary between -5 and 5% over the country, compared to the reference simulation (not shown). Neither changes of the summer precipitation sum show a clear signal. For surface- and 2m-temperature almost no changes occurred. For 2021-2025 effects of potential afforestation survey are significantly smaller for all investigated variables than the feedbacks of the maximal afforestation. A possible reason for it is that the potential afforestation is planned to be carried out in smaller fragments rather than in bigger continuous, homogenous forest blocks.

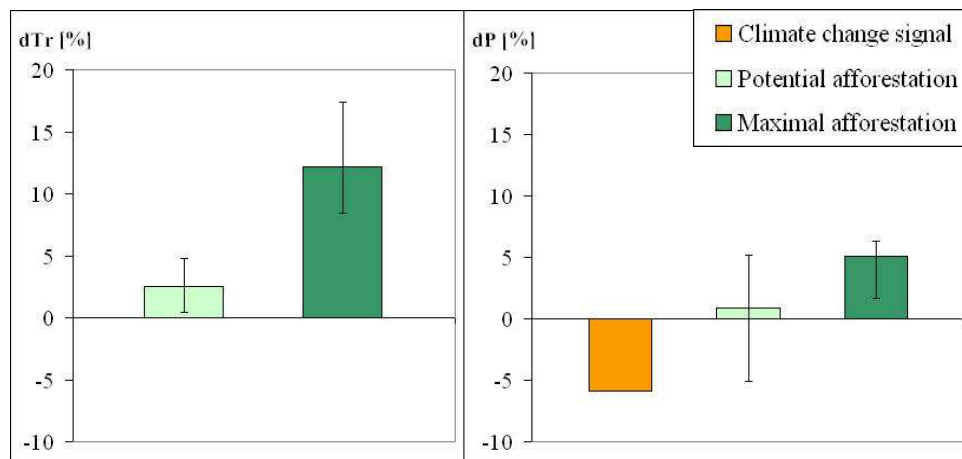


Figure 56. Effect of potential and maximal afforestation on transpiration (dTr ; left) and precipitation (dP ; right) for the period 2021-2025. Error bars represent the 5th and 95th percentiles.

The region with the largest increase (13%) of deciduous forests (and no changes of coniferous forests) is selected (figure 18) and analysed more in detail. Thus results from the maximal and potential afforestation experiments are comparable. Due to the higher leaf area index and roughness length of deciduous stands relative to crops, local increase of transpiration rate has been detected. Its amount is 2.5% higher for the potential afforestation, whereas 12% higher for maximal afforestation relative to the reference simulation (figure 56). (If grasslands would have been replaced by forests, larger local signal could be expected through the larger differences in the land cover parameters; Annex IV.) For 2021-2025, summer precipitation would not change significantly due to the proposed afforestation, whereas its amount would increase by 5% assuming maximal afforestation in the whole country. Thus, the latter could help to compensate the climate change signal for this period in the analysed region (figure 56).

5.2.5 Summary

Scientific questions related to these sensitivity experiments can be answered as follows:

What is the climatic effect of forest cover in Hungary on regional scale?

- In the period 2071-2100, maximal afforestation resulted in systematic increase of the simulated evapotranspiration and precipitation and decrease of surface temperature for summer.
- Climatic effects of deforestation are weaker and have the opposite sign than those of maximal afforestation.
- Changes of both evapotranspiration and surface temperature are localised in Hungary corresponding to the changes of the land surface parameters, whereas precipitation changes are spread out over larger areas.

How big are the climatic feedbacks of maximal afforestation in the region characterised by the largest possible increase of forest cover?

- For the 30-year summer means, transpiration (17%), interception (16%) and total evapotranspiration (17%) increased in the maximal afforestation simulation compared to the present land cover due to the larger leaf area index and roughness length of forests. This corresponds to 17% increase of latent heat flux and only a slight decrease (-2%) of sensible heat flux.
- Surface temperature decreased by -0.6°C , which means that cooling via enhanced transpiration was larger than the albedo-effect.
- Precipitation increased by 7% relative to the reference simulation.

How does the interaction of the main climatic forcings of afforestation change during the summer months?

- Until the middle of July, biogeophysical feedbacks of maximal afforestation were primarily determined by the evaporative forcing. Thereafter, available soil moisture limited transpiration, the evaporative cooling effect decreased and the role of the albedo-forcing started to increase.
- The cooling and moistening effect of forests remained dominant during the whole summer period.

Has the potential afforestation survey an effect on the regional climate?

- As expected, the 7% increase of forest cover only a slight effect on the regional climate in Hungary (the microclimatic processes within the stand are not represented in REMO)
- For 2021-2025 effect of maximal afforestation is significantly larger for all variables than the feedbacks of the potential afforestation survey in the investigated region.

The two extreme cases described by the complete afforestation and deforestation scenarios give information about the possible range of the model sensitivity to the forest cover change. For practical application, results of the potential forest cover experiment can be useful, which represents a real future survey for afforestation.

5.3 Climate change altering effect of afforestation

For 2071-2100, summer precipitation is projected to decrease significantly in Hungary, relative to 1961-1990 (*figure 57*; discussed in *Sect. 5.1.2*). As it has been concluded in *Sect. 5.2.5*, maximal afforestation resulted in increase of precipitation in the whole country (*figure 57*). Consequently, for summer, the effect of climate change can be reduced by the increase of forest cover. Magnitude of both climate change signal and feedback of maximal afforestation on precipitation differ among regions (*figure 57-58*). It was the motivation to study the spatial differences of the possible climate change weakening effect of afforestation in Hungary (*Gálos et al. 2010*).

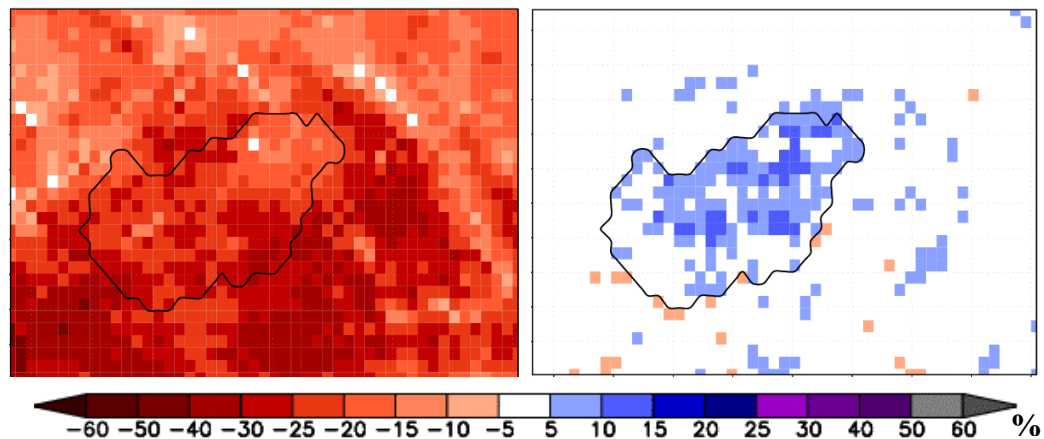


Figure 57. Change of summer precipitation due to climate change (2071-2100 vs. 1961-1990; left) and due to maximal afforestation (maximal afforestation vs. reference for 2071-2100; right).

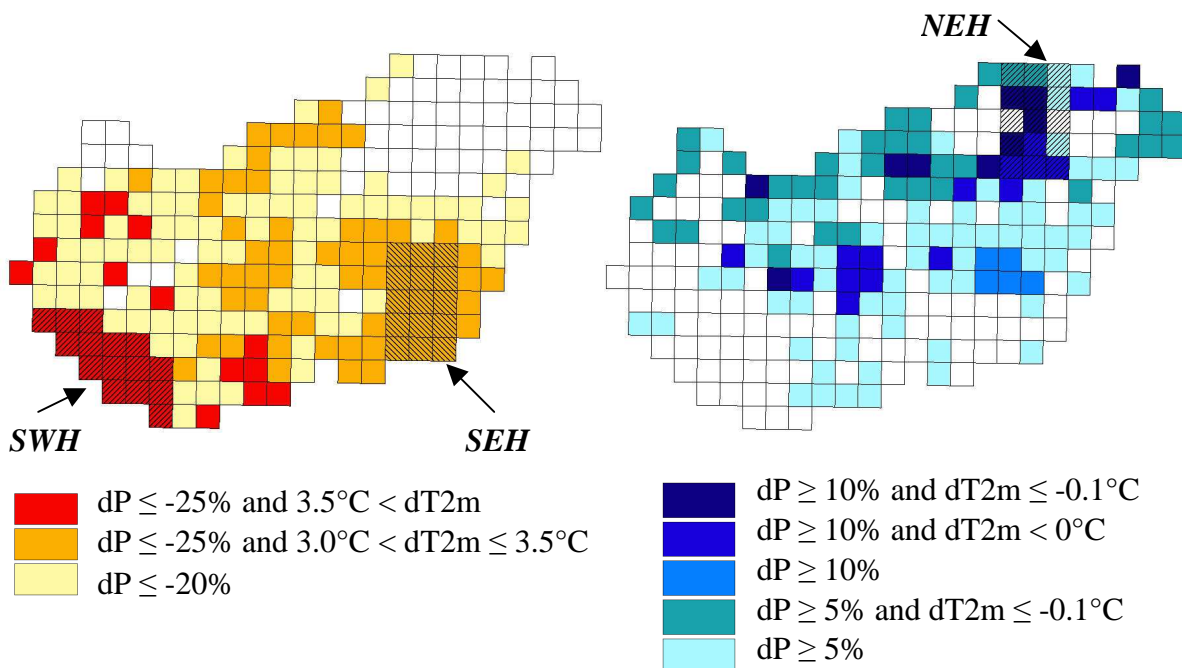


Figure 58. The most climate affected areas (left) and the spatial distribution of precipitation-increasing (dP) and temperature-decreasing ($dT2m$) effect of maximal afforestation relative to the reference (right). The three investigated regions are shaded: the most climate change affected area (SWH), the region with the largest amount of afforestation (SEH) and the area, where the effect of maximal afforestation on precipitation is the largest (NEH).

Based on the results of the previous chapters the following three regions have been selected for detailed analyses:

- *Southwest Hungary, SWH*: The most climate change affected region, where both positive temperature anomalies and negative precipitation anomalies are largest in the period 2071-2100 relative to 1961-1990 (*figure 57*, selection method is introduced in *Sect. 5.1.4*). For this area 62% afforestation is assumed in the sensitivity study.
- *Southeast Hungary, SEH*: The area characterised by largest forest cover increase (+95%) in the maximal afforestation experiment (*figure 57*).
- *Northeast Hungary, NEH*: Region, in which both precipitation-increasing and temperature-decreasing effect of maximal afforestation is the largest in the period 2071-2100 (*figure 58*, selection method is introduced in *Sect. 5.2.1*). Here, forested area is enhanced by 77%.

5.3.1 Magnitude of the feedback of maximal afforestation on precipitation compared to the climate change signal

For the three regions *figure 59* shows the climate change (2071-2100 vs. 1961-1990) and the effect of maximal afforestation on the summer precipitation (2071-2100). The columns represent the relative anomalies of the 30-year mean of precipitation sums.

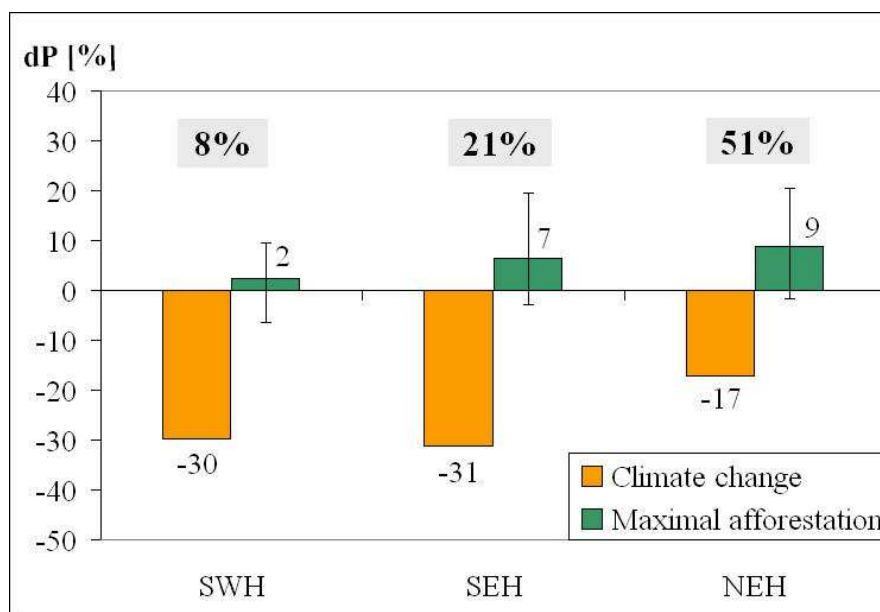


Figure 59. Effect of climate change (2071-2100 vs. 1961-1990) and maximal afforestation (maximal afforestation vs. reference 2071-2100) on precipitation (dP) in the three investigated regions.

Bars represent the 5th and 95th percentiles of the 30 summers.

The percent values are the ratios of maximal afforestation feedback and climate change signal.

In the case of the feedbacks of maximal afforestation, the bars visualise the variability of the simulation results among the 30 summers, which is quite large for all areas. The percent values are the ratios of the maximal afforestation feedback and climate change signal for precipitation. These values show the spatial differences of the climate change weakening effect of the increased forest cover on the example of the three selected regions. (Assumption: the whole country is completely afforested, not only the investigated areas.)

The region SWH can be characterised by 30% negative relative precipitation anomaly due to climate change, which could be hardly compensated by forest cover increase (*figure 59*). In

SEH, the significant decrease of summer precipitation has been weakened by 21% through the afforestation feedback, which is 7% in 30-year mean.

In the mountainous region NEH, the projected decrease of summer precipitation was the smallest (17%) from the three regions (figure 59). But also this is the area, in which both precipitation increasing (9%) and temperature-decreasing effect of maximal afforestation was the largest. Here, for precipitation, climate change signal has been halved by the increased forest cover.

Simulation results refer to large differences among the selected regions in the magnitude of forest feedback relative to the climate change signal. A possible reason for it can be that in the mountainous northeastern area, precipitation formation is easier due to orographic uplift. For summer, the moistured air resulted from the maximal afforestation of the country is transported to this region due to the characteristic circulation patterns.

Based on the results, feedback of afforestation on the 2m-temperature was very weak, therefore the projected tendency of warming due to climate change could not be diminished. In contrary to this, projected climate change signal for surface temperature has been reduced by 0.6°C in SEH, assuming maximal afforestation (not shown). It is caused by the higher evapotranspiration rate therewith larger evaporative cooling of the forests.

5.3.2 Effect of maximal afforestation on the probability and severity of droughts

It has been hypothesised that the probability and severity of droughts could be reduced by maximal afforestation for the period 2071-2100, because in the investigated regions maximal afforestation is associated with the increase of the simulated precipitation.

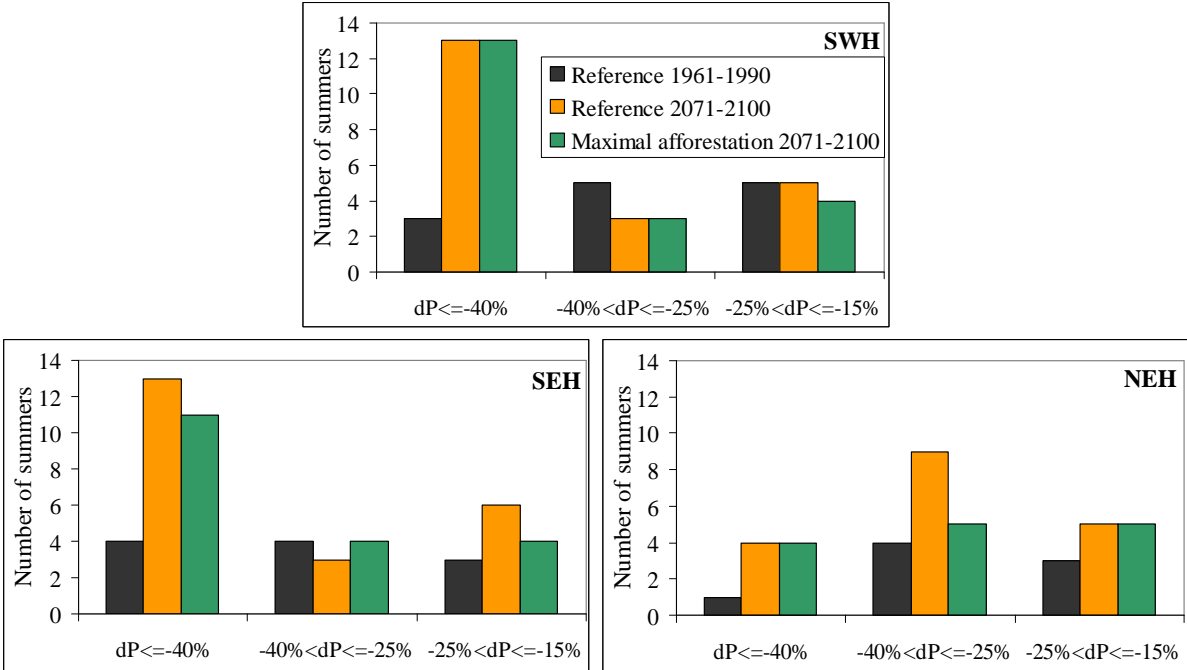


Figure 60. Changes of the number and severity of summer droughts in the three investigated regions SWH (southwest Hungary), SHE (southeast Hungary) and NEH (northeast Hungary) due to climate change and maximal afforestation

Based on the simulation results for the region SWH, number of moderate dry summers ($-25\% < dP \leq -15\%$) did not change, whereas probability of extreme dry summers ($dP \leq -25\%$) doubled by the end of the 21st century, compared to the reference period 1961-1990 (figure 60). Especially summers, characterised by larger than 40% negative precipitation anomaly are projected to be more frequent (discussed in Sect. 5.1.4). In this area the strong increase in probability and severity of droughts could not be reduced by maximal afforestation (figure 60).

For 2071-2100, tendency of drought probability is very similar on the SEH area (figure 60). But contrary to SWH, number of severe and moderate droughts could be slightly reduced assuming maximal afforestation.

In the NEH region, increase of the number of severe droughts is projected to be the lowest from the investigated areas. For summers with larger than 40% negative relative precipitation anomaly compared to 1961-1990, the severity could not be diminished by maximal afforestation. But number of dry summers characterised by 25-40% negative relative precipitation anomaly compared to 1961-1990 has been decreased (from 9 to 5) via enhanced forest cover.

5.3.3 Influence of the extent of the present forest cover on the projected climate change

Climate change signal between the two maximal afforestation experiments has been compared to the climate change signal between the two reference simulations for the period 2071-2100 relative to 2021-2050 (figure 24; C, H).

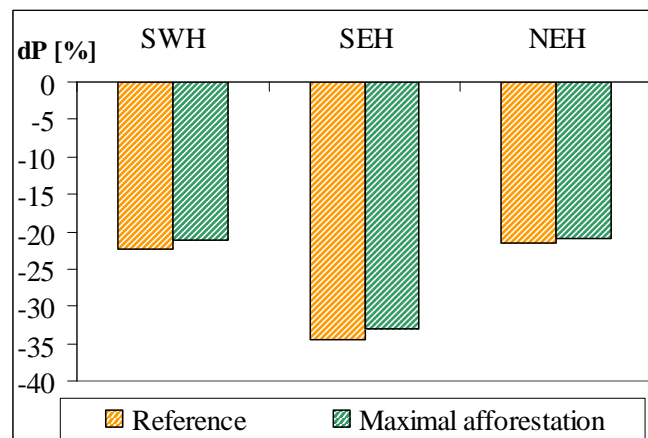


Figure 61. Climate change signal for precipitation (dP) between two reference and two maximal afforestation experiments (2071-2100 vs. 2021-2050)
SWH: southwest Hungary, SEH: southeast Hungary, NEH: northeast Hungary

The hypothesis was that in case of larger forest cover in the present, the climate change signal may be smaller, due to the moistening effect of the forests.

For Hungary, different extent of forested area (i.e. afforestation and present forest cover) resulted in slightly different future climates but produced similar climate change signal. For each of the three analysed regions, the 30-year mean of precipitation decrease was only 1% smaller with complete afforestation than with present forest cover (figure 61).

Consequently, the magnitude of the projected climate change for 2071-2100 relative to 2021-2050 is independent from the extent of the present forest cover.

5.3.4 Comparison of the feedbacks of maximal afforestation on precipitation under moderate and enhanced climate change

Feedback of maximal afforestation on the summer precipitation has been investigated for 2021-2050 and 2071-2100 (figure 24; D, F). It has been hypothesised that feedback of complete afforestation in these two periods can be different, because the warmer and dryer climatic conditions may have an influence on the water and energy exchange processes between forest and atmosphere.

Based on the results for the SWH area, maximal afforestation of the country has almost no effect on the 30-year mean of summer precipitation in the middle of the 21st century. This feedback remains low also at the end of the century (figure 62). In the SEH area, simulated increase of precipitation due to maximal afforestation was 5% for 2021-2050 and reached the 7% for the period 2071-2100. In the region NEH, the magnitude of the feedback of maximal afforestation on precipitation was the largest from the three selected regions, and had almost the same value (9%) under moderate and enhanced climate change (figure 62).

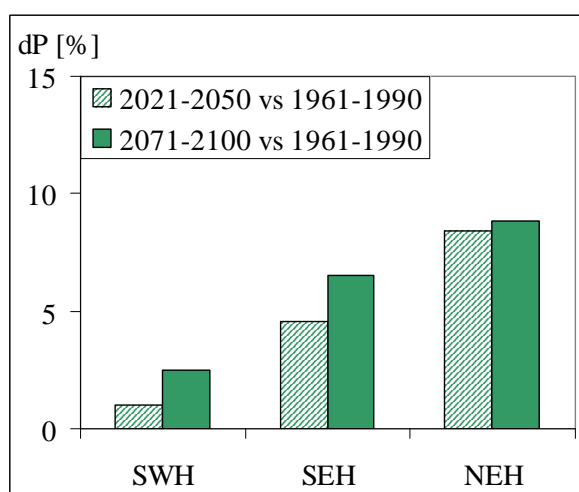


Figure 62. Effects of maximal afforestation on precipitation (dP) for 2021-2050 vs. 1961-1990 as well as for 2071-2100 vs. 1961-1990
SWH: southwest Hungary, SHE: southeast Hungary, NEH: northeast Hungary

Consequently, simulation results contradicted our hypothesis. The magnitude of climate change signal had almost no effect on the magnitude of the feedback of maximal afforestation on precipitation (with exception of the SEH region), though the difference in the climate change signal between the two investigated time periods is quite large (discussed in Sect. 5.1.2).

5.3.5 Magnitude of the effects of deforestation compared to the climate change signal

Regions have been also determined, where deforestation has a positive (enhancing) feedback on climate change at the end of the 21st century. *Figure 62* shows, that if the relative small forested area on the south part of the Hungarian lowland was replaced by grassland, the drying of the region enhanced.

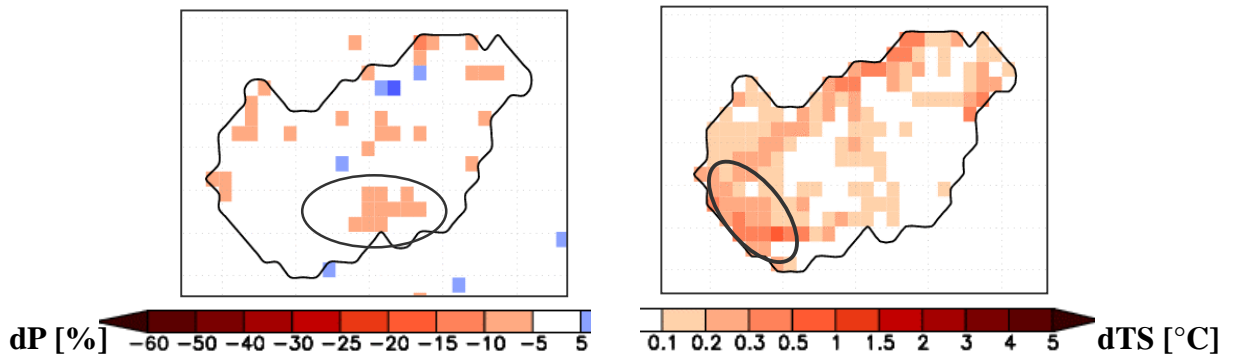


Figure 63. Changes of the summer precipitation (dP ; left) and surface temperature ($dTTS$ right); deforestation vs. reference (2071-2100). The most affected regions are marked with circles.

The other investigated area, SWH, was defined as the most affected by warming as well as by severe droughts. Here, assuming complete deforestation of the country, surface temperature increased by 0.3°C in 30-year mean additionally to the climate change signal. Consequently, if forests turn to grasslands due to climate change, the process – as a positive feedback – will induce the further warming of the area.

5.3.6 Summary

Based on the simulation results, our scientific questions can be answered as follows:

Are there any spatial differences in the forest-climate interactions in Hungary?

- Maximal afforestation is associated with precipitation increase in the whole country, which can weaken the climate change signal for the end of the 21st century.

How big is the effect of maximal afforestation on the summer precipitation compared to the climate change signal?

- The climate change weakening effect of the maximal afforestation differs among regions. For precipitation, climate change signal can be reduced by 51% via increased forest cover on the NEH area and by 21% on SEH, respectively. The region SWH can be characterised by large negative precipitation anomalies due to climate change, which could be hardly compensated by the increased forest cover.

Can probability and severity of droughts be reduced by maximal afforestation?

- The probability of droughts characterised by larger than 40% negative precipitation anomaly compared to the period 1961-1990, could not be reduced by maximal afforestation. But in the NEH region the probability and severity of extreme dry summers (25-40% negative precipitation anomaly compared to 1961-1990) was decreased significantly via enhanced forest cover.

Can projected climate change be influenced by the extent of the present forest cover?

- The projected climate change signal for precipitation is independent from the extent of the present forest cover.

Are the feedbacks of maximal afforestation different under moderate and enhanced climate change?

- The effect of forests on precipitation has almost the same magnitude under moderate and enhanced climate change.

Are there any regions, in which deforestation enhances climate change?

- Deforestation has a positive (enhancing) feedback on climate change at the end of the 21st century, especially on surface temperature in regions characterised by the largest decrease of forest cover.

5.4 Measuring and modelling of interception on local scale

5.4.1 Adaptation and validation of the hydrologic model BROOK90 for interception in the Hidegvíz-Valley

From the predefined interception parameters, simulated interception of BROOK90 has been calibrated with the maximal storage capacity for rain per unit LAI (*CINTRL*) and with the intercepted fraction of rain per unit LAI (*FRINTL*). Their representative values for the beech stand as well as the basic canopy-related parameters for interceptions are listed in *Annex IX*. After the calibration process, the interception output of the model has been validated against interception datasets calculated from measured precipitation (*figure 64*). For the validation, interception measurements were preferred, which corresponds to one single rainfall event. Furthermore the measurement errors have been filtered (e.g. overfilled containers), which explains the relative small number of the dots on *figure 64*.

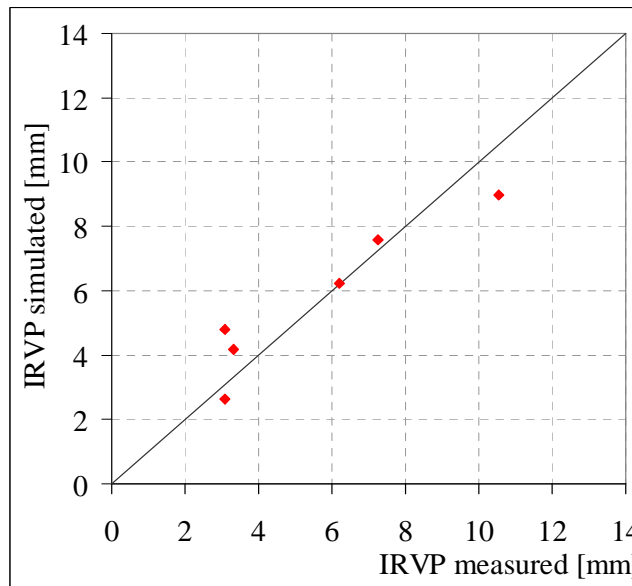


Figure 64. Validation of the interception output of the model (*IRVP simulated*) against interception calculated from the measured stand precipitation forms (*IRVP measured*)

On *figure 65*, the closer the dots to the least squares line (which represents the perfect model fit, when simulated interception equals to the measured ones), the closer are the simulated values to the measurements. The model bias (Φ [mm]) has been calculated as

$$\Phi = \sum_i (y_i - \hat{y}_i)^2 = \min \quad (27)$$

where y_i is the ordinate of the dots and \hat{y}_i is the ordinate of the corresponding dots on the least squares line. The smaller the Φ , the larger is the accuracy of the simulations. For the validation, $\Phi = 6.52$ mm.

The perfect fit is impossible because of the simplified model approach and the local characteristics of the process resulting in large spatial and temporal variability of the interception amount depending on the actual, local meteorological and canopy conditions.

5.4.2 Sensitivity of the simulated interception to the precipitation intensity

It has been tested whether the more accurate determination of the duration of the rainfall event have an influence on the simulated interception.

Rainfall duration is represented more realistically using hourly precipitation input than assuming the monthly mean duration for each rainfall event. Duration based on hourly precipitation measurements leads to a larger amount of interception (*figure 65*), because small rainfall events can be captured with higher frequency with hourly precipitation data. The determining role of the small precipitations in the total intercepted amount is also treated by *Kucsara (1996)*.

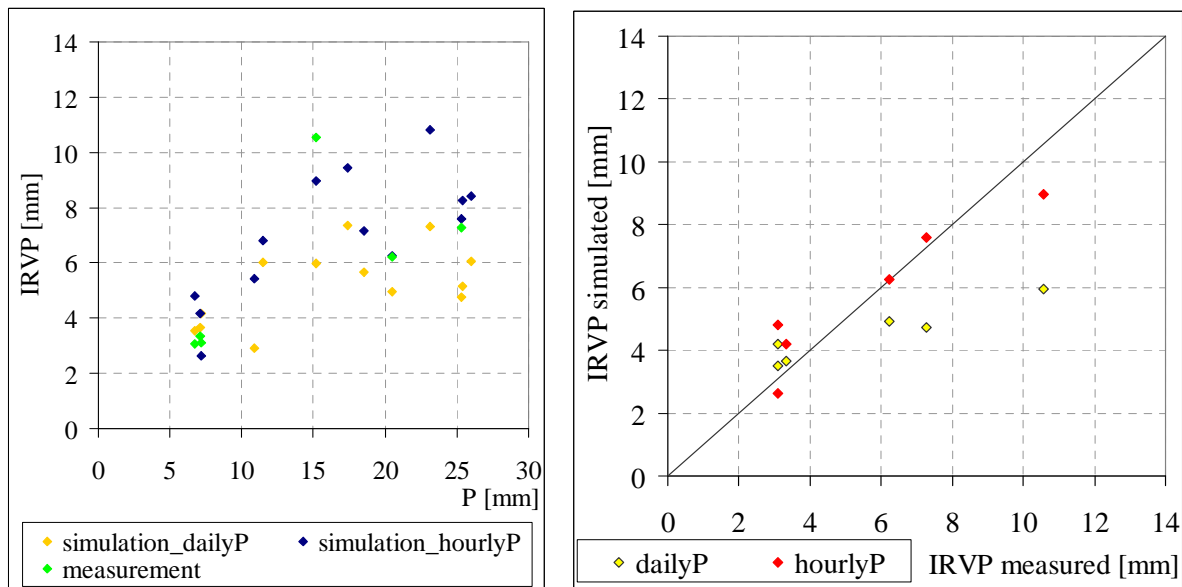


Figure 65. Sensitivity of the simulated interception to the duration of the rainfall event. IRVP: interception (left). Validation of the interception output of the model (IRVP simulated) against measurements (IRVP measured) for daily and hourly precipitation input (right).

Due to the more appropriate representation of rainfall duration results, simulation of interception from hourly precipitation data is in better agreement with the measurements, whereas daily precipitation input results larger model bias (*figure 65*). Based on *Eq. 27*, $\Phi_{hourlyP} = 6.52 \text{ mm}$ and $\Phi_{dailyP} = 30.51 \text{ mm}$.

5.4.3 Summary

For the beech site in the Hidegvízvölgy-Valley the model has been adapted and tested for interception. Based on the available measurements and simulation results the major findings of the analyses are the following:

How accurately can the one dimensional hydrologic model BROOK90 simulate the amount of interception in the Hidegvíz-Valley?

- The interception approach of the model is a simplification of the reality but it is sufficient for the simulation of process in a complex forest hydrology model.

Has the intensity of precipitation an influence on the simulated interception?

- Using hourly precipitation input data the duration and intensity of the rainfall event can be determined more accurate and the interception can be simulated more realistically.
- REMO and BROOK90 use a different approach for calculating interception. Both of them are a simplification of the reality. Parameters, which could be improved in the simulations, are mostly not available from measurements. Therefore answering this research question needs further investigations.

6. Discussion and Conclusions

The obtained simulation results indicate that for Hungary, in the 21st century, projected warming and drying of summers is quite strong. Not only the climatic means but also the extremes are affected by climate change, which are more important from ecological point of view. The significant tendency of drying during the last 100 years in Hungary (Szinell et al. 1998) seems to extend to the end of the 21st century. The expected increase in the number of droughts and the length of consecutive dry periods may have severe impact on agriculture and forestry. Forests are not able to adapt to the rapid changes of climatic conditions. Especially zonal tree species are affected at their lower (xeric) limit of distribution (Mátyás et al. 2009), which are determined primarily by climatic aridity.

At the end of the 20th century recurrent droughts caused health decline in beech forests at their lower limit of distribution in southwest Hungary (Berki et al. 2009, Molnár and Lakatos 2007). In this region was the reduction of the forest area the largest for 1975-2004 compared to 1901-1930 (Rasztovits and Móricz ex verb.). Based on orographical, meteorological and soil properties (Bella et al. 2005) this area is especially sensitive to droughts. It was the wettest part in Hungary and based on the results of in this work, here is the projected tendency of drying and warming the largest for the 21st century. Consequently, the simulated increase in probability and severity of droughts may cause drastic changes of zonal beech forests in this region.

Ecological models of forest distribution driven by results from global climate simulations have already shown the reduction of macroclimatically suitable areas for beech and the possible disappearance of this species from Hungary (Czúcz et al. 2010). Therefore, from practical point of view, the regional scale simulation of the distribution, occurrence, severity and duration of droughts under future climate conditions may provide cleaner insights for the review of adaptation and mitigation strategies and the maintenance of forest-related socio-economic and ecosystem services.

Based on the results of the land cover change experiments, reduction (e.g. due to droughts) or increase of the forested area affects the regional climate in Hungary through altering the surface energy fluxes and hydrological cycle. Whether temperate forests cool or warm the climate is determined by various contrasting vegetation feedbacks, which can diminish or counteract each other. In contrast to the Mediterranean region (Heck et al. 2001), for Hungary, the evaporative cooling effect of maximal afforestation dominates during the whole summer, which is reduced by the albedo-effect in August, under limited soil moisture conditions. These sensitivity studies confirm that albedo- and evaporating forcing of forests in the temperate zone are moderate compared to those of boreal and tropical forests (Bonan 2008a). The magnitude of the effects cannot be directly compared with other studies for temperate forests because of the differences in the applied models and experimental set-ups (e.g. domain, resolution, time period, parameterisation of the land surface processes).

Assuming maximal afforestation in Hungary, the projected climate change can be weakened but cannot be fully compensated. But regarding to the regional scale of the analyses, the length of the investigated time period (30-year), and the relative small afforested part of the simulation domain, the magnitude of the feedback of afforestation on the precipitation is quite large compared to the climate change signal. In certain regions, precipitation decrease due to climate change can be halved by the maximal afforestation of the country.

In these experiments forest cover has been modified only in Hungary (approx. 10000 km²), on the other parts of simulation domain (approx. 3.15 million km²) no land use change has been

implemented. Assuming afforestation over the whole domain, larger impacts can be expected, but the aim of the present study was the investigation of the country-scale effects of the country-scale changes.

Climatic benefit of the investigated potential afforestation is negligible. Although the effects of forests on the local climate are favourable (this microclimatic effects in the forest stand are not represented in the model), nevertheless, the survey shows that climatic conditions cannot be influenced by potential afforestation on regional scale.

Probability and severity of droughts projected for the 21st century can only be reduced by large, continuous forest areas. For evapotranspiration and surface temperature, the larger the change of forest cover in the region, the stronger its feedbacks on these variables. For precipitation, effects of maximal afforestation are spread out in space, which shows that land cover change affects climate not only on local scale.

Analyses of the spatial differences in the weakening effects of afforestations can help to identify the areas, where forest cover increase is the most beneficial and should be supported to reduce the projected tendency of drying. Areas, where forest cover increase has less or no effect on the climate can also be delineated. Based on the deforestation scenario, some regions can be identified, where decrease of forested area enhances the climate change signal. Here, the existing forests should be maintained to avoid the additional warming and drying of the region.

Though climate change cannot be relieved by the investigated potential afforestation, results of the dissertation concerning the climatic feedbacks of forest cover change and its spatial distribution for the 21st century could be an important basis of the future forest policy. They may improve also the public awareness of ecological services of forest cover and its role in adapting to climate change.

Results also provide useful information and experiences for the better understanding of the forest-related processes and vegetation-atmosphere interactions in the climate model simulations on regional scale. They can contribute to the further model development.

In this study the regional climate model REMO has been applied with the current state of land cover parameterisation. For studying climatic influence of land cover change on finer scale, subgrid variability of land cover parameters within a climate model grid box has to be taken into account more in detail. Field measurements and local scale models can help to a better understanding of the basic forest-related processes, thus could provide datasets to the validation and contribute to the improvement of the parameterisation of the climate model.

Own experiences regarding to the comparison of modelled and the available measured data confirm, that differences of the theoretical approaches between model and observations as well as the difference of the climatic role of forests in regional and micro-scale make validation difficult.

- It must be taken into account, that in the climate model, forests have no height. Therefore the simulated 2m-temperatures should be compared to observation 2 m above the canopy rather than 2 m above the forest soil surface. Unfortunately, such measurements are mainly not available.
- It is incorrect to validate the large-scale mean of the selected land cover type (e.g. annual cycle of the albedo of deciduous forests) with the land surface parameters of one single station and one single forest ecosystem for a short time slice (e.g. annual cycle of the albedo in a selected Hungarian beech forest).

For validation of the results of land use change studies, reliable long-term measurements over different land cover types, on large spatial distribution would be required, according to the special needs of the applied model.

For interception, approach of interception in REMO and BROOK90 are different. Through the different scale of the analyses, the comparison of their results is difficult and the possibility of improvement of the interception approach in the climate model based on the one-dimensional hydrologic model needs further investigations.

Both simulation results of BROOK90 and field measurements underline that the amount of water stored on the canopy is depending on the intensity of precipitation, which is affected by climate change. In nature, if the precipitation intensity increases (and the number of wet days decreases), less water can be stored the skin reservoir, which is available for evaporation. The more intense precipitation goes to runoff, less water infiltrates in the soil, which is available for transpiration. Consequently, the amount of interception and transpiration decreases. The other important process is that under dryer conditions, leaves are smaller and defoliation starts earlier in the autumn. Therefore effect of afforestation on evapotranspiration can be reduced, leading to smaller evaporative cooling under enhanced climate change. In contrast to these, leaves also get yellow and dry due to the absence of available water and the increase of surface albedo supports cooling. If these processes were taken into account in REMO by calculating interception, transpiration and surface temperature, changes of the climatic role of the forests due to climate change could be simulated.

Results of these analyses underline the importance of the forest-climate interactions, also from practical point of view. They contribute to a better understanding of land-atmosphere feedbacks on regional scale and represent the first assessment of the possible climate change weakening effect of forest cover increase in the region, for long future time periods.

7. Outlook

Based on the results of the dissertation, further research is needed in the following directions:

- Analysis climate change and drought trends based on the results of an ensemble of simulations to get information about the internal model variability.
- Investigation of the heat fluxes from the surface and the soil: why only surface temperatures gets cooler due to enhanced evapotranspiration whereas 2m-temperature are only slightly influenced.
- Study, how the experiences from the site-specific measurements could be help in the more detailed description of the energy fluxes and hydrologic processes in REMO.
- Test, on which spatial scale which forest-related processes have the largest influence on the climate.
- Investigation of the sensitivity of the simulated regional climate to the height of vegetation. Consideration of the height of vegetation could allow more vertical levels in the forest (with separated energy and water balance from the underlying soil), the more realistic description of vegetation density and fractional vegetation cover as well as the representation of temperature and wind profiles within the forest stand. The effects of these local-scale processes are microclimatically important, but the magnitude of their feedback on the regional climate is highly uncertain, therefore it should be further investigated.
- Extension of land use change studies to investigation of the climatic effect of further land cover types on different spatial and temporal scales, which is also essential for the complex analyse of the land-atmosphere interactions, also from practical point of view.
- Adaptation of the BROOK90 model for the whole hydrologic cycle of the investigated beech stand and for interception of oak and alder stands in the Hidegvíz-Valley. Thus the dependence of the hydrologic processes from age of the stand as well as the difference of the hydrologic role between the forest stands can be simulated.

In smaller areas with heterogeneous land cover, the more realistic description of land surface characteristics and processes in climate simulations become even more important. The higher the resolution, the more details of land surface and influencing factors should be taken into account. If more region-specific land cover categories were introduced (e.g. deciduous forest-types were distinguished) and the characteristic annual cycles of the land surface parameters needed for climate modelling were allocated to them, regional differences within the individual forest types and their climatic effects could be shown.

Reliable long-term field measurements over the individual land cover types according to the special needs of the models could support this aim. The largest challenge remains the upscaling of observed information from process-level to regional climate models, the coupling between the different scales. Depending on the abiotic and biotic environmental conditions, spatial and temporal variability of the land surface factors are very large. Inclusion of all these site-specific details in climate models would limit their adaptation for different areas. A possible solution would be to run the climate model with a region-depending land surface parameter-set.

Practical importance of the understanding the role of land surface in the climate system is increasing with the expected land use change due to climate change and human influences, that differ among regions. These regional differences in the climatic effects of forests and the

differences of the climatic effects among land cover types are also substantial to adapt to climate change. For long-term investigation of forest-climate interactions in the future, regional climate modelling is essential, with more detailed description of the forest cover related processes, combining the biogeophysical and biogeochemical effects. Complex understanding of the forest-climate interactions and exchange processes as well as continued improvement of land surface representation in regional climate models requires more multidisciplinary efforts and international cooperation by scientists with a wide range of skills.

8. Theses of the dissertation

1. Under enhanced climate change (2051-2100) for the B1, A1B and A2 emission scenarios, probability and severity of summer droughts are projected to be significantly higher, droughts may occur in every second summer. The consecutive dry periods will last longer than in the second half of the 20th century.
 - The tendency of warming and drying and the expected increase of the probability of extreme dry summers are largest in the southwest part of Hungary.
2. Based on the simulation results of the regional climate model REMO, changes of larger continuous and homogenous forest blocks influence the regional climate in Hungary.
 - In the period 2071-2100, maximal afforestation resulted in increase of the simulated evapotranspiration (10-15%) and precipitation (up to 10-15%) and decrease of surface temperature (up to 1°C) for summer, in the whole country.
 - During the whole summer the cooling and moistening effect of maximal afforestation dominates. After the available soil moisture limits transpiration, the evaporative cooling effect decreases and the role of the albedo effect starts to increase.
 - Climatic effects of deforestation are weaker and have the opposite sign than those of maximal afforestation.
3. Forest cover change according to the potential afforestation survey (7% increase of the forest cover in country mean) has a very slight feedback on the regional climate compared to the maximal afforestation scenario (microclimate in the forest stand is not represented in the model).
4. For the 21st century, maximal afforestation weakens the projected climate change signal in Hungary.
 - For summer, the simulated tendency of drying can be reduced in the whole country, due to the precipitation increasing effect of maximal afforestation.
 - The projected climate change signal for precipitation is independent from the extent of the present forest cover.
 - The effect of forests on precipitation has almost the same magnitude under moderate and enhanced climate change.
5. The climate change weakening effect of maximal afforestation differs among regions. It is simulated to be the largest in the northeastern area (here, 50% of the projected precipitation decrease can be relieved), whereas the smallest in the southwestern region.
 - In the investigated northeastern area, simulated number of extreme dry summers can be reduced (from 9 to 5) and severity can be decreased through maximal afforestation.
6. Applying the one-dimensional hydrologic model BROOK90 with hourly precipitation inputs, duration and intensity of the rainfall event can be determined more accurately than from the daily precipitation sums. Thus, the simulated interception is in better agreement with the measurements.

Acknowledgements

I would like to express my thanks to my supervisor Prof. Dr. Csaba Mátyás for the scientific guidance and exact comments during the period of my PhD and for the motivation to work on this interdisciplinary topic. Thanks for Your high level requirements in scientific working and for supporting my participation in international conferences.

I would like to thank my supervisor Prof. Dr. Daniela Jacob for accepting and supporting me in her working group in the Max Planck Institute for Meteorology in Hamburg. Thank You for offering me the opportunity to use the regional climate model REMO and for the kindly motivation, scientific inspiration and many interesting research questions during my work.

Spending one and a half year in Hamburg and working in the regional climate modelling group was a great pleasure for me. Thanks to all of the group members for the friendly working atmosphere, the fruitful scientific discussions, meetings and for the nice time together.

Special thanks to Holger Göttel for teaching me how to run REMO and for his patient guidance during my first steps in regional climate modelling. I am also very grateful to Philip Lorenz for giving me a lot of tips and tricks in the analyses of the model results. I would like to thank Stefan Hagemann and Diana Rechid for their experiences and suggestions during my work with land cover. Many thanks to Swantje Preuschmann, who was always prepared to long discussions and speculations about land surface processes and parameters. I would also like to thank Sven Kotlarski, Claas Teichmann, Kevin Sieck and Christopher Moseley for answering my ‘greenhorn-questions’ related to programming and for helping me to solve the technical problems.

Thanks to all of my colleagues in Sopron – Dr. Imre Berki, Áron Drüszler, Norbert Móricz and Ervin Rasztoivits – who never let me forget the practical site of my scientific topic. Many thanks to Dr. Mihály Kucsara, Dr. Zoltán Gribovszki and Dr. Péter Kalicz for the introduction in the forest hydrology and the many practical advises during the fieldwork. I thank Dr. Peter Vig for allowing to use his meteorological dataset for 1997 and Dr. Kornél Czimber for helping me at the beginning of my work with GIS.

I would like to thank the reviewers of the manuscript – Prof. Dr. János Mika, Dr. Sándor Szalai and Dr. Zoltán Gribovszki – for their useful comments and also the other colleagues for reading parts of my dissertation and giving helpful suggestions.

I am very grateful to Prof. Dr. Levente Albert for the encouragement and mentoring in working in environmental sciences.

I would like to thank my parents, who always support me in every possible way.

Staying in Hamburg during my PhD work was financially supported by the scholarships of the DBU (Deutsche Bundesstiftung Umwelt) and the DAAD (Deutscher Akademischer Austausch Dienst) as well as by the TÁMOP 4.2.2 project.

References

- Allen, C.D. 2009. Climate-induced forest dieback: an escalating global phenomenon? *Unasylva* 231/232: 43–49
- Aston, A.R. 1979. Rainfall interception by eight small trees. *Journal of Hydrology* 42: 383–396
- Avissar, R. and R.A. Pielke 1989. A parametrization of heterogeneous land surfaces for atmospheric numerical models and its impact on regional meteorology. *Mon. Wea. Rev.* 117: 2113–2136
- Balázs, Á. and E.Gy. Führer 1990–91. Methode und Ergebnisse der Inerzeptionsforschung in Waldbeständen. *Erdészeti Kutatások* 82–83: 5–21
- Bartholy J. and Pongrácz R. 2007. Regional analysis of extreme temperature and precipitation indices. *Global and Planetary Change* 57: 83–95 doi: 10.1016/j.gloplacha.2006.11.002
- Bartholy J., R. Pongrácz, Gy. Gelybó 2007. Regional climate change expected in Hungary for 2071–2100. *Applied Ecology and Environmental Research* 5: 1–17
- Bella Sz., Á. Németh, S. Szalai 2005. Examination of drought vulnerability with GIS tools: Somogy county case study. In: Erasmi, S., B. Cyffka, M. Kappas (eds.) *Remote sensing & GIS for environmental studies*. Göttinger Geographischer Abhandlungen, Vol. 113.
- Beniston, M., D.B. Stephenson, O.B. Christensen, C.A.T. Ferro, C. Frei, S. Goyette, K. Halsnaes, T. Holt, K. Jylhä, B. Koffi, J. Palutikof, R. Schöll, T. Semmler, K. Woth 2007. Future extreme events in European climate: an exploration of regional climate model projections. *Climatic Change* 81: 71–95 doi: 10.1007/s10584-006-9226-z
- Berki I., Móricz N., Rasztoivits E., Vig P. 2007. A bükk szárazság tolerancia határának meghatározása. In: Mátyás Cs., Vig P. (szerk.) *Erdő és klíma V*. Sopron, 213–228
- Berki, I., E. Rasztoivits, N. Móricz, Cs. Mátyás 2009. Determination of the drought tolerance limit of beech forests and forecasting their future distribution in Hungary. *Cereal Research Communations* 37
- Betts, R.A., P.M. Cox, S.E. Lee, F.I. Woodward 1997. Contrasting physiological and structural vegetation feedbacks in climate change simulations. *Nature* 387: 796–799
- Betts, R.A. 2001. Biogeophysical impacts of land use on present-day climate: near-surface temperature change and radiative forcing. *Atmospheric Science Letters* 1 (23pp) doi: 10.1006/asle.2001.0023
- Betts, R. 2007. Implications of land ecosystem-atmosphere interactions for strategies for climate change adaptation and mitigation. *Tellus* 59B: 602–615 doi: 10.1111/j.1600-0889.2007.00284.x
- Bisselink, B. and Dolman, A. J. 2009. Recycling of moisture in Europe: contribution of evaporation to variability in very wet and dry years. *Hydrol. Earth Syst. Sci.* 13: 1685–1697 doi: 10.5194/hess-13-1685-2009
- Bonan, G.B., D. Pollard, S.L. Thompson 1992. Effects of boreal forests on global climate. *Nature* 359: 716–718 doi: 10.1038/359716a0
- Bonan, G.B. 1995. Land-atmosphere CO₂ exchange simulated by a land surface process model coupled to an atmospheric general circulation model. *Journal of Geophysical Research* 100D: 2817–2831
- Bonan, G.B. 1997. Effects of land use on the climate of the United States. *Climatic Change* 37: 449–486
- Bonan, G.B., S. Levis, L. Kergoat, K.W. Oleson 2002. Landscapes as patches of plant functional types: an integrating concept for climate and ecosystem models. *Global Biogeochemical Cycles* 16 (30pp) 10.1029/2000GB001360

- Bonan, G.B. 2004. Biogeophysical feedbacks between land cover and climate. In: R.S. DeFries, G.P. Asner, and R.A. Houghton (eds) *Ecosystems and Land Use Change*. Geophysical Monograph 153: 61-72, American Geophysical Union, Washington, D.C.
- Bonan, G.B. 2008a. Forests and climate change: forcings, feedbacks, and the climate benefits of forests. *Science* 320: 1444–1449 doi: 10.1126/science.1155121
- Bonan, G.B. 2008b. *Ecological climatology*. Cambridge Univ. Press, Cambridge, ed. 2., 568p
- Bosch, J.M. and J.D. Hewlett, 1982. A review of catchment experiments to determine the effect of vegetation changes on water yield and evapotranspiration. *J. Hydrol.*, 55: 3-23
- Bounoua, L., R. Defries, G.J. Collatz, P. Sellers, H. Khan 2002. Effects of land cover conversion on surface climate. *Climatic Change* 52: 29-64
- Bréda, N., R. Huc, A. Granier, E. Dreyer 2006. Temperate forest trees and stands under severe drought: a review of ecophysiological responses, adaptation processes and long-term consequences. *Ann. For. Sci.* 63: 625–644 doi: 10.1051/forest:2006042
- Brovkin, V., A. Ganopolski, M. Claussen, C. Kubatzki, V. Petoukhov 1999. Modelling climate response to historical land cover change. *Global Ecology and Biogeography* 8: 509–517
- Brovkin, V. 2002. Climate-vegetation interaction. *J. Phys. IV France* 12: 57-82 doi: 10.1051/jp4:20020452
- Brutsaert, W. 2005. *Hydrology*. Cambridge University Press, 618p
- Bussay A., Szinell Cs., Szentimrey T. 1999. Az aszály magyarországi előfordulásának vizsgálata és mérhetősége. *Éghajlati és agrometeorológiai tanulmányok* 7, OMSZ, Budapest, 91p
- Bülow, K.G. 2010. *Zeitreihenanalyse von regionalen Temperatur- und Niederschlagssimulationen in Deutschland*. MPI-M Report 75
- Chang, M. 2006. *Forest Hydrology. An Introduction to Water and Forests*. Taylor & Francis Group, USA
- Chase, T.N., R.A. Pielke Sr, T.G.F. Kittel, R.R. Nemani, S.W. Running, 2000. Simulated impacts of historical land cover changes on global climate in northern winter. *Climate Dynam.* 16: 93-105.
- Christensen, J.H., 2005. Prediction of Regional scenarios and Uncertainties for Defining European Climate change risks and Effects – Final Report. DMI. 269p.
- Christensen .H., Christensen O.B., Lopez P., Van Meijgaard E., Botzet M. 1996. The HIRHAM4 Regional Atmospheric Climate Model, Scientific Report DMI, Copenhagen 96–4, 51
- Christensen, J.H., Christensen, O.B., 2003. Severe summertime flooding in Europe. *Nature* 421: 805–806 doi:10.1038/421805a
- Christensen, J.H., O.B. Christensen 2007. A summary of the PRUDENCE model projections of changes in European climate by the end of this century. *Climatic Change* 81: 7-30 doi: 10.1007/s10584-006-9210-7
- Copeland, J.H., R.A. Pielke, T.G.F. Kittel 1996. Potential climatic impacts of vegetation change: A regional modelig study. *Journal of Geophysical Research*, 101: 7409-7418 doi: 10.1029/95JD02676
- Crockford, R., D. Richardson 2000. Partitioning of rainfall into throughfall, stemflow and interception: effect of forest type, ground cover and climate. *Hydrological Processes* 14: 2903–2920 doi: 10.1002/1099-1085(200011/12)
- Czúcz B., L. Gálhidy, Cs. Mátyás 2010. Limiting climating factors and potential future distribution of beech (*Fagus sylvatica* L.) and sessile oak (*Quercus petraea* (Mattuscha) Liebl.) forests near their low altitude - xeric limit in Central Europe. *Ann. For. Sci* (in press)
- Csóka Gy., Koltay A., Hirka A., Janik G. 2007. Az aszályosság hatása kocsánytalan tölgyeseink egészségi állapotára. In: Mátyás Cs., Vig P. (szerk.) *Erdő és klíma V*. Sopron, 229-239

- Danszky I. (szerk.) 1963. Magyarország erőgazdasági tájainak erdőfelújítási, erdőtelepítési irányelvei és elvárásai. Országos Erdészeti Főigazgatóság, Budapest.
- Dearndorff, J.W. 1978. Efficient prediction of ground surface temperature and moisture, with inclusion of a layer of vegetation. *Journal of Geophysical Research* 83C: 1889-1903
- Déqué, M., R.G. Jones, M. Wild, F. Giorgi, J.H. Christensen, D.C. Hassell, P.L. Vidale, B. Rockel, D. Jacob, E. Kjellström, M. de Castro, F. Kucharski, B. van den Hurk 2005. Global high resolution versus Limited Area Model scenarios over Europe: results from the PRUDENCE project, *Climate Dynamics* 25: 653-670 doi: 10.1007/s0038200500521
- Dickinson, R.E. and A. Henderson-Sellers 1988. Modelling tropical deforestation: a study of GCM land-surface parameterizations. *Quarterly Journal of the Royal Meteorological Society* 114: 439-462
- DigiTerra Map Referencia kézikönyv 2004. DigiTerra GEOinformatikai Rendszerház Kft. Budapest, 164p
- Dingman, S., 2002. *Physical Hydrology*. Prentice Hall, Upper Saddle River. 646p
- DKRZ 1993. Deutsches Klimarechenzentrum: The ECHAM-3 general circulation model. DKRZ Technical Report, No. 6, Hamburg
- Drüsler Á., Csirmaz K., Vig P., Miska J. 2009. A földhasználat változásainak hatása az éghajlatra és az időjárásra. *Természet Világa* 140: 521-523
- Dunkel Z. 2009. Brief surveying and discussing of drought indices used in agricultural meteorology. *Időjárás* 113: 23-37
- Dunne, K.A. and C.J. Willmott 1996. Global distribution of plant-extractable water capacity of soil. *Int. J. Climatol.* 16: 841-859
- Dümenil Gates, L., S. Ließ 1999. Impacts of deforestation and afforestation in the Mediterranean region as simulated by the MPI atmospheric GCM. MPI Report No. 301 Hamburg
- Eidenshink, J.C. and J.L. Faundeen 1994. The 1 km AVHRR global land dataset: First stages in implementation. *Int J Remote Sens* 15: 3443-3462
- Ellenberg, H. 1988. *Vegetation ecology of Central Europe*. 4th ed. Cambridge Univ. Press, Cambridge, UK, 731p
- ESRI 1996. *ArcView 3.1 User Guide*. Environmental System Research Institute, Inc. Redlands, USA
- Feddema, J.J., K. W. Oleson, G. B. Bonan, L. O. Mearns, L. E. Buja, G. A. Meehl, W. M. Washington 2005. The Importance of Land-Cover Change in Simulating Future Climates. *Science* 310: 1674-1678 doi: 10.1126/science.1118160
- Feddes, R.A., P. Kabat, A.J. Dolman, R.W.A. Hutjes, M.J. Waterloo 1998. Large-scale field experiments to improve land surface parameterisations. In: R. Lemmelä and N. Helenius (eds) *Proceedings of 'The Second International Conference on Climate and Water'*, Espoo, Finland, 17-20 August, 1998: 619-646
- Federer, C.A., C. Vörösmarty, B. Fekete 2003. Sensitivity of annual evaporation to soil and root properties in two models of contrasting complexity. *Journal of Hydrometeorology* 4: 1276-1290
- Foken, T. 2008. *Micrometeorology*. Springer-Verlag Berlin Heidelberg, 306p.
- Foley, J.A., S. Levis, I.C. Prentice, D. Pollard, S.L. Thompson 1998. Coupling dynamic models of climate and vegetation. *Global Change Biology* 4: 561-579
- Franke, J., B. Köstner 2007. Effects of recent climate trends on the distribution of potential natural vegetation in Central Germany. *Int J Biometeorol* 52: 139-147 doi: 10.1007/s00484-007-0096-5
- Frenger, I. 2008. *Untersuchung der Auswirkungen der Landoberflächenänderungen in Westafrika auf das regionale Klima. Simulationen mit dem regionalen Klimamodell REMO*. Diplomarbeit, Universität Hamburg

- Führer E. 1984. A csapadék megoszlása és az interceptió különböző hazai erdőtársulásokban. Doktori értekezés. Sopron
- Führer E. 1994. Csapadékmérések bükkös-, kocsánytalantölgyes és lucfenyves ökoszisztémában. Erdészeti Kutatások 84: 11-35
- Führer E., Járó Z. 2000. Az aszály és a belvíz érvényesülése a Nagyalföld erdőművelésében Erdészeti Tudományos Intézet kiadványai, 12, 144p
- Führer E. 2005. Az erdővagyon bővítése a mezőgazdaságilag gazdaságtalan nem hasznosított földterületek beerdősítésével. In: Molnár S. (szerk.): Erdő – fa hasznosítás Magyarországon. Sopron, 132-136
- Gácsi Zs. 2000. A talajvízszint észlelés, mint hagyományos, s a vízforgalmi modellezés, mint új módszer alföldi erdeink vízháztartásának vizsgálatában. Doktori (PhD) értekezés, Kecskemét
- Gálos, B., Ph. Lorenz, D. Jacob 2007. Will dry events occur more often in Hungary in the future? Environ. Res. Lett. 2 034006 (9pp) doi: 10.1088/1748-9326/2/3/034006
- Gálos B., Mátyás Cs., Jacob D. 2009. Az erdő szerepe a klímarendszerben a 21. században – hatásviselő, vagy hatótényező? In: Lakatos F., Kui B. (szerk.). Nyugat-magyarországi Egyetem Erdőmérnöki Kar: Kari Tudományos Konferencia Kiadvány. NymE Kiadó Sopron, 127-130
- Gálos B., Mátyás Cs., Jacob D. 2010. A klímaváltozás hatáskorlátozásának esélyei erdőtelepítéssel. „Klíma-21” Füzetek (submitted)
- Gaertner, M.A., D. Jacob, V. Gil, M. Dominguez, E. Padorno, E. Sanchez, M. Castro 2007. Tropical cyclones over the Mediterranean Sea in climate change simulations. Geophysical Research Letter, 34, L14711, (5 PP) doi: 10.1029/2007GL029977
- Gash, J.H.C., A.J. Morton 1978. An application of the Rutter model to the estimation of the interception loss from Thetford Forest, Journal of Hydrology, 38: 49-58
- Giorgi F. and L.O. Mearns 1999. Introduction to special section: regional climate modeling revisited. J Geophys Res 104: 6335–6352
- Giorgi, F., X. Bi, J.S. Pal 2004. Mean, interannual variability and trends in a regional climate change experiment over Europe. II: climate change scenarios (2071–2100). Climate Dynamics 23: 839–858 doi: 10.1007/s00382-004-0467-0
- Göttel, H., J. Alexander, E. Keup-Thiel, D. Rechid, S. Hagemann, T. Blome, A. Wolf, D. Jacob 2008. Influence of changed vegetation fields on regional climate simulations in the Barents Sea Region. Climatic Change (BALANCE Special Issues) 87: 35-50
- Graßl, H. 2003. Natürliche Klimaschwankungen – eine Einführung. Promet 29: 1-2
- Gribovszki Z., P. Kalicz, M. Kucsara 2006. Streamflow characteristics of thwo forested catchments in Sopron Hills. Acta Sylv. Lign. Hung. 2: 81-92
- Gribovszki Z., P. Kalicz, J. Szilágyi, M. Kucsara 2008. Riparian zone evapotranspiration estimation from diurnal groundwater level fluctuations. Journal of Hydrology 349: 6–17
- Hagemann, S., D. Jacob, E. Roeckner, H. Göttel, P. Lorenz 2008. Improved regional scale processes reflected in projected hydrological changes over large European catchments Climate Dynamics. Climate Dynamics 32: 767-781 doi: 10.1007/s0038200804039
- Hagemann, S. and D. Jacob 2007. Gradient in the climate change signal of European discharge predicted by a multi-model ensemble. Climatic Change 81: 309–327 doi: 10.1007/s10584-006-9225-0
- Hagemann, S., B. Machenhauer, R. Jones, O.B. Christensen, M. Déqué, D. Jacob, P.L. Vidale 2004. Evaluation of water and energy budgets in regional climate models applied over Europe. Climate Dynamics 23: 547–567 doi: 10.1007/s00382-004-0444-7

- Hagemann, S. and L.D. Gates 2003. Improving a subgrid runoff parameterization scheme for climate models by the use of high resolution data derived from satellite observations. *Climate Dynamics* 21: 349–359 doi: 10.1007/s00382-003-0349-x
- Hagemann, S. 2002. An improved land surface parameter dataset for global and regional climate models. Report 336, Max-Planck-Institute for Meteorology, Hamburg
- Hagemann, S., M. Botzet, B. Machenhauer 2001. The summer drying problem over south-eastern Europe: Sensitivity of the limited area model HIRHAM4 to improvements in physical parameterization and resolution. *Physics and Chemistry of the Earth, Part B*, 26/5-6: 391-396
- Hagemann, S., M. Botzet, L. Dümenil, M. Machenhauer 2000. Impact of new global surface parameter fields on ECHAM T42 climate simulations. In: H. Ritchie (ed) *Research activities in atmospheric and oceanic modelling*. Report 30 WMO/TD 987, WMO, Geneva
- Hagemann, S., M. Botzet, L. Dümenil, M. Machenhauer 1999. Derivation of global GCM boundary conditions from 1 km land use satellite data. Report 289, Max-Planck-Institute for Meteorology, Hamburg
- Heck, P., D. Lüthi, H. Wernli, Ch., Schär 2001. Climate impacts of European-scale anthropogenic vegetation changes: A sensitivity study using a regional climate model. *Journal of Geophysical Research*, 106: 7817-7835 doi: 10.1029/2000JD900673
- Hewlett, J. D. 1982. *Principles of forest hydrology*, The University of Georgia Press, Athens, GA 183p
- Hogg E.H., D.T. Price, T.A. Black 2000. Postulated feedbacks of deciduous forest phenology on seasonal climate patterns in the Western Canadian interior. *Journal of Climate* 13: 4229-4243
- Horton, R.E. 1919. Rainfall interception. *Monthly Weather Rev.* 47: 603-623
- Hörmann, G., A. Branding, T. Clemen, M. Herbst, A. Hinrichs, F. Thamm, 1996. Calculation and simulation of wind controlled canopy interception of a beech forest in Northern Germany. *Agricultural and Forest Meteorology* 79: 131–148
- Hungate, B.A., G.W. Koch 2002. *Global Environmental Change: Biospheric Impacts and Feedbacks*. In J Holton, J Pyle, J Currie (eds.) *Encyclopedia of Atmospheric Science* Academic Press, Ltd. 876-885
- Imbery, F. 2004. *Langjährige Variabilität der aerodynamischen Oberflächenrauigkeit und Energieflüsse eines Kiefernwaldes in der südlicher Oberrheinebene*. PhD thesis. Albert-Ludwigs-Universität, Freiburg im Breisgau
- IPCC 2001. *Climate Change 2001: The Scientific Basis*. of working group I to the third assessment report of the Intergovernmental Panel on Climate Change <http://www.ipcc.ch>
- IPCC 2007. *Climate change 2007: Synthesis Report*. Contribution of Working Groups I, II and III to the Fourth Assessment Report of the Intergovernmental Panel on Climate Change <http://www.ipcc.ch>
- Jackson, R.B., J.T. Randerson, J.G. Canadell, R.G. Anderson, R. Avissar, D.D. Baldocchi, G.B Bonan, K. Caldeira, N.S. Diffenbaugh, C.B. Field, B.A. Hungate, E.G. Jobbágy, L.M. Kueppers, M.D. Noretto, D.E. Pataki 2008. Protecting climate with forests. *Environ. Res. Lett.* 3 044006 (5pp) doi: 10.1088/1748-9326/3/4/044006
- Jacob, D., L. Kotova, P. Lorenz, C. Moseley, S. Pfeifer 2008. Regional climate modeling activities in relation to the CLAVIER project. *Időjárás* 112: 141-153
- Jacob, D., L. Bärring, O.B. Christensen, J.H. Christensen, M. de Castro, M. Déqué, F. Giorgi, S. Hagemann, M. Hirschi, R. Jones, E. Kjellström, G. Lenderink, B. Rockel, E. Sánchez, C. Schär, S.I. Seneviratne, S. Sommot, A. van Ulden, B. van den Hurk 2007. An inter-comparison of regional climate models for Europe: model performance in present-day climate. *Climatic Change* 81:31-52 doi: 10.1007/s10584-006-9213-4
- Jacob, D., U. Andrae, G. Elgered, C. Fortelius, L. P. Graham, S. D. Jackson, U. Karstens, Chr. Koepken, R. Lindau, R. Podzun, B. Rockel, F. Rubel, H.B. Sass, R.N.D. Smith, B.J.J.M. Van

- den Hurk, X. Yang 2001. A Comprehensive Model Intercomparison Study Investigating the Water Budget during the BALTEX-PIDCAP Period. *Meteorology and Atmospheric Physics*, Vol.77, Issue 1-4, 19-43
- Jacob, D., 2001. A note to the simulation of the annual and inter-annual variability of the water budget over the Baltic Sea drainage basin. *Meteorology and Atmospheric Physics* 77: 61-73
- Jacob, D., R. Podzun 1997. Sensitivity Studies with the Regional Climate Model REMO. *Meteorol. Atmos. Phys.* 63: 119-129
- Jankó Szép I., J. Mika, Z. Dunkel 2005. Palmer severity index as soil moisture indicator: physical interpretation, statistical behaviour and relation to global climate change. *Phys. Chem. Earth* 30: 231–243
- Járó Z. 1959. A levélfelület nagysága néhány erdőtípusban. *Erdészeti Kutatások* 6: 103-108
- Járó Z. 1980. Intercepció a gödöllői kultúrterei ökoszisztémában, *Erdészeti kutatások*, 73: 7-17
- Jensen, L.U., J.E. Lawesson, H. Balslev, M.C. Forchhammer 2004. Predicting the distribution of *Carpinus betulus* in Denmark with Ellenberg's Climate Quotient. *Nordic Journal of Botany* 23: 57-67 doi: 10.1111/j.1756-1051.2003.tb00368.x
- Jump, A.S., C. Mátyás, J. Penuelas 2009. The altitude-for-latitude disparity in the range retractions of woody species. *Tree* 1147 (8pp)
- Jungclaus, J.H., N. Keenlyside, M. Botzet, H. Haak, J-J. Luo, M. Latif, J. Marotzke, U. Mikolajewicz E. Roeckner 2006. Ocean circulation and tropical variability in the coupled model ECHAM5/MPI-OM. *J. Climate* 19: 3952–3972
- Kalicz P. 2006. Hidrológiai folyamatok modellezése a Sopron melletti Hidegvíz-völgyben. Doktori (PhD) értekezés. NymE, Sopron
- Kalicz P., Gribovszki Z., Kucsara M., Vig P. 2007. A patak-menti vegetáció hatása az alapvízhozamra. In: Mátyás Cs., Vig P. (szerk.) *Erdő és klíma V*. Sopron, 357-384
- Kjellström E., Bärring L., Jacob D., Jones R., Lenderink G and Schär C. 2007. Modelling daily temperature extremes: Recent climate and future changes over Europe. *Climatic Change* 81: 249-265 doi: 10.1007/s105800692205.
- Kleidon, A., K. Fraedrich, C. Low 2007. Multiple steady-states in the terrestrial atmosphere-biosphere system: a result of a discrete vegetation classification? *Biogeosciences*, 4: 707-714 doi: 10.5194/bg-4-707-2007
- Kleidon, A. 2004. Optimized stomatal conductance of vegetated land surfaces and its effects on simulated productivity and climate. *Geophysical Research Letters* 31: L21203, doi: 10.1029/2004GL020769
- Kleidon, A., K. Fraedrich, M. Heimann 2000. A green planet versus a desert world: Estimating the maximum effect of vegetation on the land surface climate. *Clim Chang* 44: 471-493
- Kleidon, A. and M. Heimann 1998. Optimised rooting depth and its impacts on the simulated climate of an Atmospheric General Circulation Model. *Geophysical Research Letters* 25: 345-348
- Klein Tank, A.M.G. and G.P., Können 2003. Trends in indices of daily temperature and precipitation extremes in Europe, 1946–99. *J. Climate* 16: 3665–3680
- Knorr, W. 1998. Constraining a global mechanistic vegetation model with satellite data. In: 'IEEE International Geosciences and Remote Sensing Symposium' Proceedings, Seattle, WA, 6-10 July 1998
- Kolozsár J. 1981. Természetes erdei ökoszisztémák és a csapadék, *Erdő és víz*. VEAB kiadvány: 75-88
- Kotlarski, S. 2007. A Subgrid Glacier Parameterisation for Use in Regional Climate Modelling. MPI-M Report 47
- Kucsara M. 1996. Csapadék és lefolyás erdészeti kisvízgyűjtőn. Doktori (PhD) értekezés. Sopron

- Láng F. (szerk.) 2002. Növényélettan. ELTE Eötvös Kiadó, Budapest 296p
- Legates, D.R. and C.J. Wilmott 1990. Mean seasonal and spatial variability in global surface air temperature. *Theor. Appl. Climatol.* 41: 11-21
- Lenderink, G., B. van den Hurk, E. van Meijgaard, A. van Ulden, H. Cuijpers 2003. Simulation of present-day climate in RACMO2: first results and model developments. KNMI technical report 252:24
- Levis, S., and G.B. Bonan, 2004. Simulating springtime temperature patterns in the Community Atmosphere Model coupled to the Community Land Model using prognostic leaf area. *J. Climate* 17: 4531-4540
- Lloyd-Hughes, B., M.A. Saunders 2002. A drought climatology for Europe. *Int. J. Climatol.* 22: 1571–1592 doi: 10.1002/joc.846
- Lorenz, Ph. 1999. Simulation von Starkniederschlägen während des Oderhochwassers 1997 mit REMO. Diplomarbeit, Universität Hamburg
- Lorenz, Ph. and D. Jacob 2005. Influence of regional scale information on the global circulation: A twoway nesting climate simulation, *Geophysical Research Letters*, Vol. 32, L18706, doi: 10.1029/2005GL023351
- Machenhauer, B., M. Windelband, M. Botzet, J.H. Christensen, M. Déqué, R.G. Jones, P.M. Ruti, G. Visconti 1998. Validation and analysis of regional present-day climate and climate change simulations over Europe. Report No. 275, Max Planck Institute for Meteorology Hamburg, Germany.
- Majewski, D., 1991. The Europa-Modell of the Deutscher Wetterdienst. ECMWF Seminar on numerical methods in atmospheric models 2: 147-191
- Makra, L., Sz. Horváth, R. Pongrácz, J. Míka 2002. Long term climate deviations: an alternative approach and application on the Palmer drought severity index in Hungary. *Physics and Chemistry of the Earth* 27: 1063–1071 doi: 10.1016/S1474-7065(02)00142-0
- Manabe, S., J. Smagorinsky, R.F. Strickler 1965. Simulated climatology of a general circulation model with a hydrologic cycle. *Monthly Weather Review* 97: 739-774
- Maracchi, G. 2000. Agricultural drought- a particular approach to definition, assessment and mitigation strategies. In: Vogt, J.V., F. Somma (eds.) 2000. *Drought and Drought Mitigation in Europe* Netherland, Kluwer Academic Publishers, 63-78
- Mason, P.J. 1988. The formation of areally-averaged roughness lengths. *Q. J. R. Meteor. Soc.* 114: 399-420
- Mátyás Cs. and Czimmer K. 2004. Climatic sensibility of the zonal closed forest limit in Hungary: preliminary results. [A zonális alsó erdőhatár klímaérzékenysége Magyarországon – előzetes eredmények] In: Mátyás Cs., Vig P. (eds) *Erdő és klíma IV*. Sopron, 35-44
- Mátyás Cs. 2010. Forecasts needed for retreating forests. *Nature* 464: 1271 doi: 10.1038/4641271a
- Mátyás, Cs, B. Fady G.G. Vendramin 2009. Forests at the limit: evolutionary – genetic consequences of environmental changes at the receding (xeric) edge of distribution. Report from a researcher workshop. *Acta Silv. Lign. Hung.* 5: 201-204
- Mátyás Cs. 2009. Ecological perspectives of climate change in Europe's continental, drought-threatened Southeast. In: P. Y. Groisman, S. V. Ivanov (eds.): *Regional aspects of climate-terrestrial-hydrologic interactions in non-boreal Eastern Europe*. NATO Science Series, Springer Verl., 31-42
- Mátyás, Cs., L. Nagy, É. Ujvári Jármay 2008. Genetic background of response of trees to aridification at the xeric forest limit and consequences for bioclimatic modelling. In: Strelcova, K., Cs. Mátyás, A. Kleidon, et al. (eds.) *Bioclimatology and natural hazards*. Springer Verl., Berlin, 179-196

- Mátyás Cs., Nagy L., Ujváriné J. É. 2007. Klimatikus stressz és a fafajok genetikai válaszreakciója az elterjedés szárazsági határán: elemzés és előrejelzés. In: Mátyás Cs., Vig P. (szerk.) Erdő és klíma V. Sopron, 241-255
- McGregor, J.L. 1997. Regional climate modelling. *Meteorol. Atmos. Phys.* 63: 105-117 doi: 10.1016/j.jcp.2006.10.024
- McKee, T. B., N. J. Doesken, J. Kleist 1993. The relationship of drought frequency and duration to timescales *Proc. 8th Conf. On Applied Climatology (Anaheim, CA)*, 179–184
- Mika J. 1988. A globális felmelegedés regionális sajátosságai a Kárpát-medencében. *Időjárás*, 95: 265-278
- Mika J., Sz. Horváth, L. Makra 2006. Effects of documented land use changes on the albedo of Eastern Hungary (1951-2000). *Időjárás* 110: 49-62
- Mika J. 2007. Új eredmények és összevetések a klímaváltozás hazai sajátosságairól. In: Mátyás Cs., Vig P. (szerk.) Erdő és klíma V. Sopron, 13-29
- Mitchell, T.D., T.R. Carter, P.D. Jones, M. Hulme, M. New 2004. A comprehensive set of high-resolution grids of monthly climate for Europe and the globe: the observed record (1901–2000) and 16 scenarios (2001–2100) Tyndall Centre Working Paper 55
- Molnár M., Lakatos F. 2007. A bükkpusztulás Zala megyében – klímaváltozás? In: Mátyás Cs., Vig P. (szerk.) Erdő és klíma V. Sopron, 257-267
- Móricz N., Gálos B., Gribovszki Z. 2009. Az erdők intercepciójának mérési és modellezési lehetőségei. *Hidrológiai Közlöny* 39: 35-46
- Oleson, K.W., G.B. Bonan, S. Levis, M. Vertenstein 2004. Effects of land use change on North American climate: impact of surface datasets and model Biogeophysics. *Climate Dynamics* 23: 117–132 doi: 10.1007/s00382-004-0426-9
- Olson, J.S. 1994a. Global ecosystem framework: definitions. USGS EROS Data Center Internal Report, Sioux Falls, SD, 37pp.
- Olson, J.S. 1994b. Global ecosystem framework: translation strategy. USGS EROS Data Center Internal Report, Sioux Falls, SD, 39pp.
- Paeth, H., K. Born, R. Girmes, R. Podzun, D. Jacob 2009. Regional Climate change in Tropical and Northern Africa due to Greenhouse Forcing and Land Use Change, *Journal of Climate* 22: 114-132
- Pal, J.S., F. Giorgi, X. Bi 2004. Consistency of recent European summer precipitation trends and extremes with future regional climate projections *Geophys. Res. Lett.* 31 L13202 (4pp) doi: 10.1029/2004GL019836
- Pálfai I. 1994. Aszályos évek. *Víztükör* 6: 12-13
- Pálfai I., Boga T.L., Sebesvári J. 1999. Adatok a magyarországi aszályokról 1931-1998. *Éghajlati és agrometeorológiai tanulmányok* 7, OMSZ, Budapest, 67-91
- Pálfai I. 2004. Belvizek és aszályok Magyarországon. *Közlekedési Dokumentációs Kft.* p. 492
- Palmer, W.C. 1965. Meteorological drought. US Weather Bur., Res. Paper No. 45., Washington D.C. 1-58
- Patterson, K.A. 1990. Global distribution of total and total-available soil water-holding capacities. Master's thesis, University of Delaware, Newark, DE
- Pielke R.A., S r, R. Avissar, M. Raupach, A . J. Dolman, X. Zeng, A .S. Denning 1998. Interactions between the atmosphere and terrestrial ecosystems: influence on weather and climate. *Global Change Biology* 4: 461–475
- Pitman 2003. The evolution off, and revolution in, land surface schemes designed for climate models. *Int. J. of Climatol.* 23: 479-510 doi: 10.1002/joc.893

- Pitman, A.J. and G. T. Narisma 2005. The role of land surface processes in regional climate change: a case study of future land cover change over south western Australia. *Meteorol Atmos Phys* 89: 235–249 doi: 10.1007/s00703-005-0131-1
- Pitman, A.J., N. de Noblet-Ducoudre, F. T. Cruz, E. L. Davin, G. B. Bonan, V. Brovkin, M. Claussen, C. Delire, L. Ganzeveld, V. Gayler, B.J.J.M. van den Hurk, P.J. Lawrence, M.K. van der Molen, C. Müller, C.H. Reick, S.I. Seneviratne, B.J. Strengers, A. Voldoire 2009. Uncertainties in climate responses to past land cover change: First results from the LUCID intercomparison study. *Geophysical Research Letters* 36: L14814, doi:10.1029/2009GL039076
- Pongratz, J., T. Raddatz, C.H. Reick, M. Esch, and M. Claussen 2009. Radiative forcing from anthropogenic land cover change since A.D. 800, *Geophys. Res. Lett.*, 36, L02709, doi: 10.1029/2008GL036394.
- Potter, C.S. and S.A. Klooster 1999. Dynamic global vegetation modelling for prediction of plant functional types and biogenic trace gas fluxes. *Global Ecology and Biogeography* 8: 473–488
- Radvánszky B. and D. Jacob 2009. The Changing Annual Distribution of Rainfall in the Drainage Area of the River Tisza during the Second Half of the 21st Century. *Zeitschrift für Geomorphologie*, 53, 171195(25)
- Radvánszky B. and D. Jacob 2008. A Tisza vízgyűjtőterületének várható klímaváltozása és annak hatása a Tisza vízhozamára regionális klímamodell (REMO) és a lefolyási model (HD) alkalmazásával, *Hidrológiai Közlöny*, Journal of the Hungarian Hydrological Society 88: 33-42
- Rechid, D., D. Jacob 2006. Influence of monthly varying vegetation on the simulated climate in Europe. *Meteorol Z.* 15: 99-116
- Rechid, D., T.J. Raddatz, D. Jacob 2008a. Parameterization of snow-free land surface albedo as a function of vegetation phenology based on MODIS data and applied in climate modelling. *Theor. Appl. Climatol.*, doi: 10.1007/s00704-008-0003-y
- Rechid, D., S. Hagemann, D. Jacob 2008b. Sensitivity of climate models to seasonal variability of snow-free land surface albedo. *Theor. Appl. Climatol.* doi: 10.1007/s00704-007-0371-8
- Roeckner, E., K. Arpe, L. Bengtsson, M. Christoph, M. Claussen, L. Dümenil, M. Esch, M. Giorgetta, U. Schlese, U. Schulzweida 1996. The atmospheric general circulation model ECHAM-4: Model description and simulation of the present day climate. Max-Planck-Institut für Meteorologie Report No. 218.
- Roeckner, E., R. Brokopf, M. Esch, M. Giorgetta, S. Hagemann, L. Kornblueh, E. Manzini, U. Schlese, U. Schulzweida 2006. Sensitivity of simulated climate to horizontal and vertical resolution in the ECHAM5 atmosphere model. *J. Clim.* 19: 3771–3791
- Rutter, A.J., A. Kershaw, P.C. Robins, and A.J. Morton. 1972. A predictive model of rainfall interception in forests, 1. Derivation of the model from observations in a plantation of Corsican pine. *Agric Meteorol* 9: 367-384
- Sánchez, E., M.A. Gaertner, C. Gallardo, E. Padorno, A. Arribas, M. Castro 2007. Impacts of a change in vegetation description on simulated European summer present-day and future climates. *Clim Dyn* 29: 319–332 doi: 10.1007/s00382-007-0240-2
- Schär, C., P. L. Vidale, D. Lüthi, C. Frei, C. Häberli, M.A. Liniger, C. Appenzeller 2004. The role of increasing temperature variability in European summer heatwaves. *Nature* 427: 332–336 doi: 10.1038/nature02300
- Schrum, C., U. Hübner, D. Jacob, R. Podzun 2001. A coupled atmosphere/ice/ocean model for the North Sea and the Baltic Sea. MPI Report Nr. 41.
- Schwärzel, K., J. Häntzschel, A. Menzer, K.-H. Feger, U. Spank, B. Köstner, C. Bernhofer 2006. Klassifikation des Wasserhaushaltes von Waldstandorten der Mittelgebirge. *AFZ-Der Wald* 21: 1168-1169
- Sellers, P.J., Y. Mintz, Y.C. Sud, A. Dalcher 1986. A simple biosphere model (SiB) for use within general circulation models. *Journal of the Atmospheric Sciences* 43: 505-531

- Sellers, P.J., D.A. Randall, G.J. Collatz, J.A. Berry, C.B. Field, D.A. Dazlich, C. Zhang, L. Bounoua 1996. A revised land surface parameterization (SiB2) for atmospheric GCMs. *J. of Clim.* 9: 676-705
- Semmler, T. and D. Jacob 2004. Modeling extreme precipitation events – a climate change simulation for Europe. *Special Issue in Planetary and Global Change* 44: 119-127
- Semmler, T. 2002. *Der Wasser- und Energiehaushalt der arktischen Atmosphäre.* PhD thesis, University of Hamburg.
- Seneviratne, S.I., D. Lüthi, M. Litschi, C. Schär 2006. Land-atmosphere coupling and climate change in Europe. *Nature* 443: 205–209 doi: 10.1038/nature05095
- Shukla, J., C. Nobre, P. Sellers 1990. Amazon deforestation and climate change. *Science* 247: 1322-1325 doi: 10.1126/science.247.4948.1322
- Shuttleworth, W.J. and R.J. Gurney. 1990. The theoretical relationship between foliage temperature and canopy resistance in sparse crops. *Quart J Royal Meteorol Soc* 116: 497-519
- Shuttleworth, W.J. and J.S. Wallace. 1985. Evaporation from sparse crops - an energy combination theory. *Quart J Royal Meteorol Soc* 111: 839-855
- Simmons, A. J. and D. M. Burridge (1981). An energy and angular-momentum conserving vertical finite-difference scheme and hybrid vertical coordinate. *Monthly Weather Review* 109: 758-766
- Simonffy Z. 1978-79. *Intercepció vizgálatok (Helyzetfelmérő tanulmány) VITUKI No. 7631(1)21*
- Sitkey J. 1996. *Erdős vízgyűjtő élővízminősége a csapadék és a faállomány összefüggésében.* Doktori értekezés. Sopron
- Standovár T., K. Kenderes 2003. A review on natural stand dynamics in beechwoods of East-Central Europe. *Applied Ecology and Environmental Research* 1: 19-46
- Stich, S., B. Smith, I.C. Prentice, et al. 2003. Evaluation of ecosystem dynamics, plant geography and terrestrial carbon cycling in the LPJ dynamic global vegetation model. *Global Change Biology*, 9: 161-185
- Szász G. 1988. *Agrometeorológia.* Mezőgazdasági Kiadó, Budapest, 462p
- Szalai S., Konkolyiné B. Z., Lakatos M., Szentimrey T. 2005. *Magyarország éghajlatának néhány jellemzője 1901-től napjainkig.* OMSZ, 12p
- Szalai S. and Cs. Szinell 2000. Comparison of two drought indices for drought monitoring in Hungary - a case study. In: Vogt, J.V., F. Somma (eds). *Drought and Drought Mitigation in Europe*, Kluwer: Dordrech, 161–166
- Szépszó G., and A. Horányi 2008. Transient simulation of the REMO regional climate model and its evaluation in Hungary. *Időjárás* 112: 203-231
- Szépszó G. 2008. Regional change of climate extremes in Hungary based on different regional climate models of the PRUDENCE project. *Időjárás* 112: 265-283
- Szinell, Cs., A., Bussay, T. Szentimrey 1998. Drought tendencies in Hungary. *Int. J. Climatol.* 18: 1479-1491
- Teichmann, C. 2010. *Climate and Air Pollution Modelling in South America with Focus on Megacities.* MPI-M Report 76, Hamburg
- Tibaldi, S. and J.-F. Geleyn 1981. The production of a new orography, land-sea mask and associated climatological surface fields for operational purposes. *ECMWF Technical Memorandum* 40
- Tomassini, L. and D. Jacob 2009. Spatial analysis of trends in extreme precipitation events in highresolution climate model results and observations for Germany, *J. Geophys. Res.* 114: D12113 doi: 10.1029/2008JD010652.
- Tuhkanen, S. 1980. Climatic parameters and indices in plant geography. *Acta Phytogeographica Suecica* 67: 1-105

- Uppala, S.M., P.W. Kallberg, A.J. Simmons, U. Andrae, V.D. Bechtold, M. Fiorino, J.K. Gibson, J. Haseler, A. Hernandez, G.A. Kelly, X. Li, K. Onogi, S. Saarinen, N. Sokka, R.P. Allan, E. Andersson, K. Arpe, M.A. Balmaseda, A.C.M. Beljaars, L. Van De Berg, J. Bidlot, N. Bormann, S. Caires, F. Chevallier, A. Dethof, M. Dragosavac, M. Fisher, M. Fuentes, S. Hagemann, E. Holm, B.J. Hoskins, L. Isaksen, P.A.E.M. Janssen, R. Jenne, A.P. McNally, J.F. Mahfouf, J.J. Morcrette, N.A. Rayner, R.W. Saunders, P. Simon, A. Sterl, K.E. Trenberth, A. Untch, D. Vasiljevic, P. Viterbo, J. Woollen 2005. The ERA-40 Re-analysis. *Q. J. R. Meteorol. Soc.* 131: 2961-3012
- US Geological Survey 2002. Global land cover characteristics database version 2.0. http://edcdaac.usgs.gov/glcc/globedoc2_0.html
- US Geological Survey 1997. Global land cover characteristics database. http://edcwww.cr.usgs.gov/landdaac/glcc/globe_int.html
- Valente, F., J.S. David, J.H.C. Gash 1997. Modelling interception loss for two sparse eucalypt and pine forests in central Portugal using reformulated Rutter and Gash analytical models. *J. Hydrol.* 190: 141-162
- Varga-Haszonits Z. 1987. Agrometeorológiai információk és hasznosításuk. Mezőgazda Kiadó, Budapest, 248p
- Vidale, P.L., D. Lüthi, C. Frei, S.I. Seneviratne, C. Schär 2003. Predictability and uncertainty in a regional climate model. *J. Geophys. Res.* 108 (D18): 4586 doi: 10.1029/2002JD002810
- Vidale, P.L., D. Lüthi, R. Wegmann, C. Schär 2007. European summer climate variability in a heterogeneous multi-model ensemble. *Climatic Change* 81: 209–232 doi: 10.1007/s10584-006-9218-z
- Vig P. 2002. A klimatikus változások hatásai egy középkorú bükkös vízháztartására. Doktori (PhD) értekezés. Debreceni Egyetem, Debrecen
- Vig P. 2004. Egy bükkös vízháztartása. In: Mátyás Cs., Vig P. (szerk.) Erdő és klíma IV. Sopron, 197-208
- Vig P. 2007. Az inszoláció változásainak hatása erdeink vízháztartására. In: Mátyás Cs., Vig P. (szerk.) Erdő és klíma V. Sopron, 351-360
- Vygodskaya, N.N, P.Ya Groisman, N.M. Tchebakova, J.A Kurbatova, O. Panfyorov, E.I. Parfenova, A.F. Sogachev 2007. Ecosystems and climate interactions in the boreal zone of northern Eurasia. *Environ. Res. Lett.* 2 045033 (7pp) doi: 10.1088/1748-9326/2/4/045033
- Wilhite, D.A., M.H. Glantz 1985. Understanding the drought phenomenon: the role of definitions. *Water Int.* 10: 111-120
- Zeng, N., J.W. Shuttleworth, J.H.C. Gash 2000. Influence of temporal variability of rainfall on interception loss. Part I. Point analysis, *J. Hydrol.*, 228: 228–241 doi: 10.1016/S0022-1694(00)00140-2
- Zhao, M., A.J. Pitman, T. Chase 2001. The impact of land cover change on the atmospheric circulation. *Climate Dynamics* 17: 467-477
- Zierl, B. 2001. A water balance model to simulate drought in forested ecosystems and its application to the entire forested area in Switzerland. *J. Hydrol.* 242: 115–136 doi: 10.1016/S0022-1694(00)00387-5

<http://www.cecilia-eu.org>

<http://www.clavier-eu.org>

http://www.cru.uea.ac.uk/projects/stardex/reports/STARDEX_FINAL_REPORT.pdf

<http://www.drought.unl.edu/>

<http://dataservice.eea.eu.int/>

<http://ensembles-eu.metoffice.com/>

http://www.fomi.hu/corine/clc2000_hun.html

<http://www.ileaps.org>

<http://www.pa.op.dlr.de/climate/mercure.html>

<http://prudence.dmi.dk/>

Annex

Annex I. The Emissions Scenarios of the Special Report on Emissions Scenarios (SRES) (IPCC 2001)

A1. The A1 storyline and scenario family describes a future world of very rapid economic growth, global population that peaks in mid-century and declines thereafter, and the rapid introduction of new and more efficient technologies. Major underlying themes are convergence among regions, capacity building and increased cultural and social interactions, with a substantial reduction in regional differences in per capita income. The A1 scenario family develops into three groups that describe alternative directions of technological change in the energy system. The three A1 groups are distinguished by their technological emphasis: fossil intensive (A1FI), non-fossil energy sources (A1T), or a balance across all sources (**A1B**) (where balanced is defined as not relying too heavily on one particular energy source, on the assumption that similar improvement rates apply to all energy supply and end use technologies).

A2. The A2 storyline and scenario family describes a very heterogeneous world. The underlying theme is self-reliance and preservation of local identities. Fertility patterns across regions converge very slowly, which results in continuously increasing population. Economic development is primarily regionally oriented and per capita economic growth and technological change more fragmented and slower than other storylines.

B1. The B1 storyline and scenario family describes a convergent world with the same global population, that peaks in mid-century and declines thereafter, as in the A1 storyline, but with rapid change in economic structures toward a service and information economy, with reductions in material intensity and the introduction of clean and resource-efficient technologies. The emphasis is on global solutions to economic, social and environmental sustainability, including improved equity, but without additional climate initiatives.

B2. The B2 storyline and scenario family describes a world in which the emphasis is on local solutions to economic, social and environmental sustainability. It is a world with continuously increasing global population, at a rate lower than A2, intermediate levels of economic development, and less rapid and more diverse technological change than in the B1 and A1 storylines. While the scenario is also oriented towards environmental protection and social equity, it focuses on local and regional levels.

An illustrative scenario was chosen for each of the six scenario groups A1B, A1FI, A1T, A2, B1 and B2. All should be considered equally sound.

Annex II. Logarithmic aggregation of roughness length $z_{0,veg}$

Instead of roughness values $z_{0,veg}$, drag coefficients

$$c_d = (\kappa / \ln(z_b / z_{0,veg}))^2 \quad (1)$$

are averaged, where c_d are taken at the so-called blending height z_b .

This leads to

$$\frac{1}{\ln^2\left(\frac{z_b}{z_{0,veg}}\right)} = \sum_j \left(\frac{f_j}{\ln^2\left(\frac{z_b}{z_{0,veg,j}}\right)} \right) \quad (2)$$

f_j - proportion of a gridbox covered with land cover type j

$z_{0,veg,j}$ - roughness length allocated to the land cover type j

according to *Claussen et al. (1994)* $z_b = 100$ m.

Annex III. Evapotranspiration efficiency in REMO

Based on *Sellers et al. (1986)*, the evaporation efficiency e is expressed as a function of the stomatal resistance of the canopy R

$$e = (1 + c_h * |v_h| * R)^{-1} \quad (1)$$

with

$$R = \frac{R_0}{F(W_s)} \quad (2)$$

where C_h is the transfer coefficient for heat and v_h [m s^{-1}] the horizontal velocity R_0 [s m^{-1}] is the minimum value of R [s m^{-1}] dependent on the photosynthetically active radiation (PAR) and the water stress factor $F(W_s)$, which is an empirical function of the available water in the root zone (*Roeckner et al. 1996*):

$$\frac{1}{R_0} = \frac{1}{k * c} * \left[\frac{b}{d * PAR} * \ln\left(\frac{d * e^{k * LAI} + 1}{d + 1}\right) - \ln\left(\frac{d + e^{-k * LAI}}{d + 1}\right) \right] \quad (3)$$

The photosynthetically active radiation (PAR) is taken as 55% of the net surface short wave radiation and the standard parameter values are: $k = 0.9$, $a = 5000 \text{ J m}^{-3}$, $b = 10 \text{ W m}^{-2}$, $c = 100 \text{ s m}^{-1}$, $d = \frac{a + b * c}{c * PAR}$

Annex IV. Classification of the CLC2000 types into the global ecosystem type defined by Olson (1994a, 1994b), and the corresponding land surface parameters (Hagemann et al. 1999, Hagemann 2002) for the representative categories in Hungary

CORINE2000 categories	CLC Code	Olson-types	Olson Code	albedo	z0veg	cv_g	cv_d	LAI_g	LAI_d	cf	Wava	fwp	Wcap
Continuous urban fabric	111	Urban	1	0.2	2.5	0	0	0	0	0	0	0.48	0.00
Discontinuous urban fabric	112												
Industrial or commercial units	121												
Road and rail networks and associated land	122												
Port areas	123												
Airports	124												
Mineral extraction sites	131												
Dump sites	132												
Construction sites	133												
Sport and leisure facilities	142	Low Sparse Grassland	2	0.19	0.1	0.91	0.2	2.5	1.1	0	240	0.47	452.83
Pastures	231												
Natural grasslands	321												
Sparsely vegetated areas	333												
Coniferous forest	312	Coniferous Forest	3	0.13	1	0.96	0.95	9.2	9	0.9	130	0.41	220.34
Broad-leaved forest	311	Deciduous Broadleaf Forests	5	0.16	1	0.8	0	5.1	0.1	0.8	300	0.53	638.30
Water courses	511	Inland Water	14	0.07	0.0002	0	0	0	0	0	0	0	0.00
Water bodies	512												
Transitional woodland-shrub	324	Shrub Deciduous	17	0.16	0.26	0.53	0.1	4.6	0.5	0.26	350	0.32	514.71
Mixed forest	313	Mixed Forest	24	0.16	0.68	0.97	0.3	7	1	0.83	220	0.51	448.98
Peat bogs	412	Mire, Bog, Fen	44	0.12	0.03	0.67	0	2.6	0.1	0	160	0.39	262.30
Inland marshes	411	Marsh Wetland	45	0.12	0.03	0.85	0	3.1	0.1	0	300	0.55	666.67
Rice fields	213	Rice Paddy and Field	36	0.15	0.06	0.95	0.19	4.6	0.26	0	350	0.49	686.27
Green urban areas	141	Forest and Field	56	0.16	0.25	0.8	0.21	5.9	2.5	0.45	310	0.5	620.00
Vineyards	221	Broadleaf Crops	92	0.17	0.175	0.95	0.12	5	2	0.3	240	0.42	413.79
Fruit trees and berry plantations	222												
Non-irrigated arable land	211	Grass Crops	93	0.185	0.1	0.91	0.2	2.5	1.1	0.2	240	0.47	452.83
Complex cultivation patterns	242	Crops, Grass, Shrubs	94	0.19	0.1	0.65	0.33	2.7	0.4	0	530	0.46	981.48
Land principally occupied by agriculture, with significant areas of natural vegetation	243												

albedo: surface albedo, *z0veg*: surface roughness length due to vegetation, *cv_g*: fractional vegetation cover (growing season), *cv_d*: fractional vegetation cover (dormancy season), *LAI_g*: leaf area index (growing season), *LAI_d*: leaf area index (dormancy season), *cf*: forest ratio, *Wava*: plant available water holding capacity, *fwp*: volumetric wilting point, *Wcap*: soil water holding capacity

Annex V. Calculation of potential evapotranspiration in BROOK90

The Penman-Monteith equation is (the symbols are the same as applied in the model)

$$L_v \rho_w E = \frac{\Delta(R_n - S) + c_p \rho D_a / r_a}{\Delta + \gamma + \gamma(r_c / r_a)} \quad (1)$$

where E [mm] is the evaporation rate, L_v [W m⁻²] is the latent heat of vaporization for water, ρ_w [kg m⁻³] is the density of water, Δ [kPa K⁻¹] is the rate of change of vapor pressure with temperature, R_n [W m⁻²] is the net radiation above the surface, S [W m⁻²] is the subsurface heat flux, c_p is the heat capacity of air, ρ [kg m⁻³] is the density of air, D_a [kPa] is the vapor pressure deficit in the air, r_c [s m⁻¹] is the canopy resistance, r_a [s m⁻¹] is the aerodynamic resistance between the canopy and a reference height at which D_a is measured, γ [Pa K⁻¹] is the psychrometer constant.

Transpiration (E_c [mm]) using the *Shuttleworth and Wallace* modification of the Penman-Monteith equation is

$$L_v \rho_w E_c = \frac{\Delta(A - A_s) + c_p \rho D_0 / r_{ac}}{\Delta + \gamma + \gamma(r_{sc} / r_{ac})} \quad (2)$$

where D_0 [kPa] is the vapor pressure deficit at the effective source height, A [W m⁻²] is $R_n - S$ or the available energy above the canopy, A_s [W m⁻²] is the available energy at the ground, r_{sc} is the canopy surface resistance, r_{ac} restricts vapor movement from the leaf surfaces to the effective source height for water vapor in the canopy.

Soil evaporation (E_s [mm/d]) using the *Shuttleworth and Wallace* modification of the Penman-Monteith equation is

$$L_v \rho_w E_s = \frac{\Delta^* A_s + c_p \rho D_0 / r_{as}}{\Delta + \gamma + \gamma(r_{ss} / r_{as})} \quad (3)$$

where r_{ss} [s m⁻¹] is the resistance to movement of water vapor from inside the soil to the soil surface and r_{as} [s m⁻¹] is the resistance to vapor movement from the soil surface to the source height.

Potential interception rate (*PINT* [mm]) is calculated from *Eq. 2* with a canopy resistance of zero.

Annex VI. Subroutines for calculation of interception in BROOK90

```

Attribute VB_Name = "EVP"
Option Explicit
DefSng A-Z

'*****
Sub INTER(RFAL, PINT, LAI, SAI, FRINTL, FRINTS, CINTRL, CINTRS, DTP, INTR, RINT,
IRVP)
'rain interception, used when NPINT% > 1
'same routine is used for snow interception, with different calling variables
'input
' RFAL      rainfall rate, mm/d
' PINT      potential interception rate, mm/d
' LAI       projected leaf area index, m2/m2
' SAI       projected stem area index, m2/m2
' FRINTL    intercepted fraction of RFAL per unit LAI
' FRINTS    intercepted fraction of RFAL per unit SAI
' CINTRL    maximum interception storage of rain per unit LAI, mm
' CINTRS    maximum interception storage of rain per unit SAI, mm
' DTP       precipitation interval time step, d
' INTR      intercepted rain, mm
'output
' RINT      rain catch rate, mm/d
' IRVP      evaporation rate of intercepted rain, mm/d
'local
Dim INTRMX  'maximum canopy storage for rain, mm
Dim CATCH   'maximum RINT, mm/d
Dim NEWINT  'first approximation to new canopy storage (INTR)
'
CATCH = (FRINTL * LAI + FRINTS * SAI) * RFAL
INTRMX = CINTRL * LAI + CINTRS * SAI
NEWINT = INTR + (CATCH - PINT) * DTP
If (NEWINT > 0!) Then
' canopy is wet throughout DTP
  IRVP = PINT
  If (NEWINT > INTRMX) Then
' canopy capacity is reached
  RINT = PINT + (INTRMX - INTR) / DTP
' RINT can be negative if INTR exists and LAI or SAI is decreasing over time
  Else
' canopy capacity is not reached
  RINT = CATCH
  End If
Else
' canopy dries during interval or stays dry
  RINT = CATCH
  IRVP = (INTR / DTP) + CATCH
' IRVP is < PINT
End If
End Sub

'*****
Sub INTER24(RFAL, PINT, LAI, SAI, FRINTL, FRINTS, CINTRL, CINTRS, DURATN, INTR,
RINT, IRVP)
'rain interception with duration in hours, used when NPINT% = 1
'same routine is used for snow interception, with different calling variables
'input
' RFAL      24-hour average rainfall rate, mm/d
' PINT      potential interception rate, mm/d
' LAI       projected leaf area index, m2/m2
' SAI       projected stem area index, m2/m2
' FRINTL    intercepted fraction of RFAL per unit LAI
' FRINTS    intercepted fraction of RFAL per unit SAI
' CINTRL    maximum interception storage of rain per unit LAI, mm
' CINTRS    maximum interception storage of rain per unit SAI, mm

```

```

'   DURATN    average storm duration, hr
'   INTR      intercepted rain storage, mm,
'output
'   RINT      rain catch rate, mm/d
'   IRVP      evaporation rate of intercepted rain, mm/d
'local
Dim INTRMX    'maximum canopy storage for rain, mm
Dim INTRNU    'canopy storage at end of hour, mm
Dim NEWINT    'first approximation to INTRNU, mm
Dim RINTHR    'rain catch rate for hour, mm/hr
Dim CATCH     'maximum RINTHR, mm/hr
Dim IRVPHR    'evaporation rate for hour, mm/hr
Dim SMINT     'daily accumulated actual catch, mm
Dim SMVP      'daily accumulated actual evaporation, mm
Dim IHD%      'half DURATN in truncated integer hours
Dim I%        'hour, 0 to 23
Dim DTH       'time step, = 1 hr
'intrinsic
'   CSNG, INT
'
IHD% = Int((DURATN + 0.1) / 2)
INTRMX = CINTRL * LAI + CINTRS * SAI
INTRNU = INTR
SMINT = 0!
SMVP = 0!
DTH = 1!
For I% = 0 To 23
  If (I% < (12 - IHD%) Or I% >= (12 + IHD%)) Then
    '   before or after rain
    CATCH = 0!
  Else
    '   during rain, mm/hr is rate in mm/d divided by hr of rain/d
    CATCH = (FRINTL * LAI + FRINTS * SAI) * RFAL / CSng(2 * IHD%)
  End If
  NEWINT = INTRNU + (CATCH - PINT / 24!) * DTH
  If (NEWINT > 0.0001) Then
    '   canopy is wet throughout hour, evap rate is PINT
    IRVPHR = PINT / 24!
    If (NEWINT > INTRMX) Then
      '   canopy capacity is reached
      RINTHR = IRVPHR + (INTRMX - INTRNU) / DTH
      '   INTRMX - INTRNU can be negative if LAI or SAI is decreasing over time
    Else
      '   canopy capacity is not reached
      RINTHR = CATCH
    End If
  Else
    '   canopy dries during hour or stays dry
    RINTHR = CATCH
    IRVPHR = INTRNU / DTH + CATCH
    '   IRVPHR for hour is < PI/24
  End If
  INTRNU = INTRNU + (RINTHR - IRVPHR) * DTH
  SMVP = SMVP + IRVPHR * DTH
  SMINT = SMINT + RINTHR * DTH
Next I%
IRVP = SMVP
'   / 1 d
RINT = SMINT
'   / 1 d
End Sub

```

Annex VII. Climate change signals for summer temperatures and precipitations

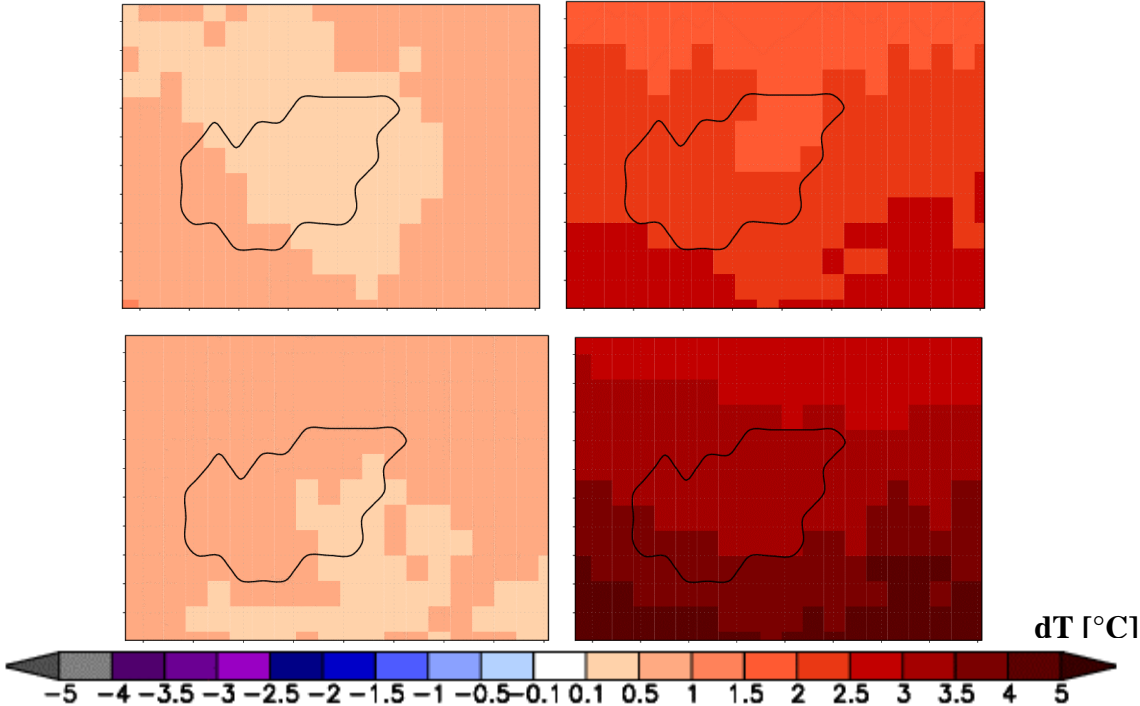


Figure 1. Climate change signal for summer temperatures (0.44° horizontal resolution): for emission scenario B1, 2021-2050 vs. 1961-1990 (top left) and 2071-2100 vs. 1961-1990 (top right), for emission scenario A2, 2021-2050 vs. 1961-1990 (bottom left) and 2071-2100 vs. 1961-1990 (bottom right)

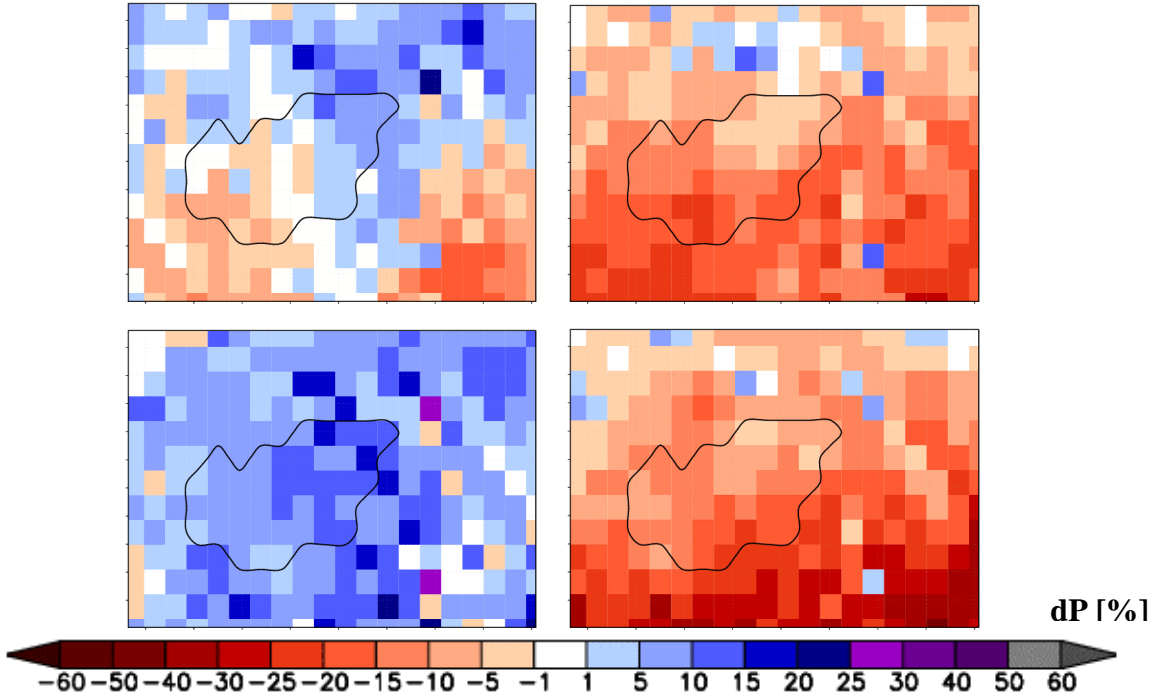


Figure 2. The same as figure 1 but for precipitation

Annex VIII. Climatic effects of deforestation

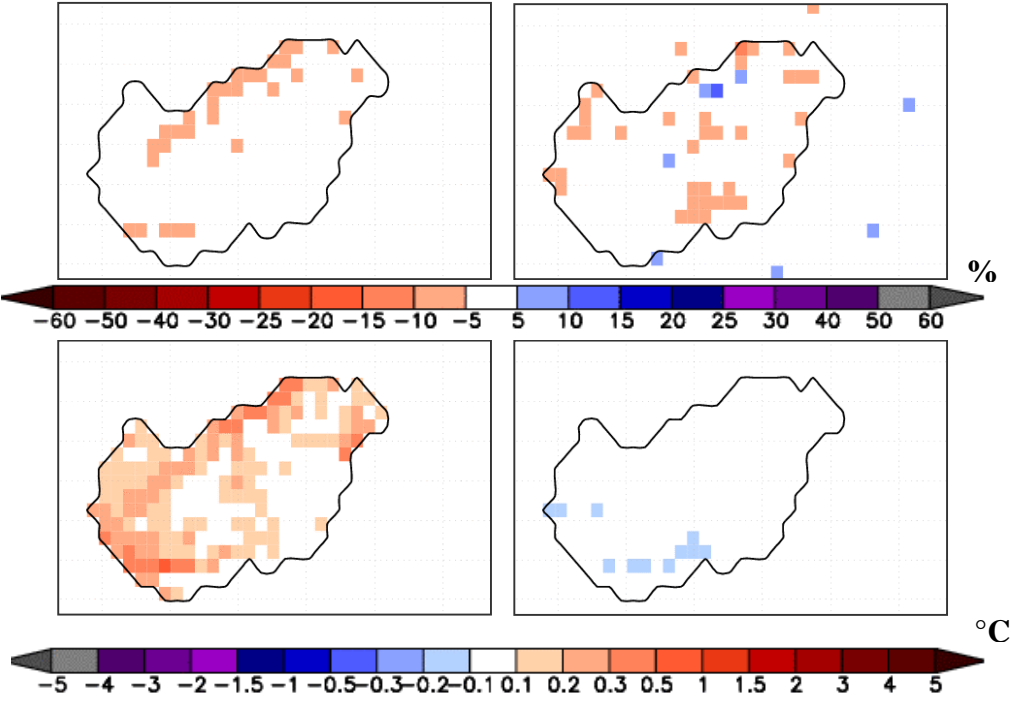


Figure 1. Changes of evapotranspiration (top left), precipitation (top right), surface temperature (bottom left) and 2m-temperature (bottom right); deforestation vs. reference (2071-2100)

Annex IX. Most important canopy-related parameters for interception used in the simulations in BROOK90

Canopy-related parameters	Abbreviation in BROOK90	Value
Maximum canopy height	MAXHT	14 m
Canopy density	DENSEF	1
Maximum projected LAI	MAXLAI	7
Intercepted fractions per unit LAI	FRINTL	0.08
Intercepted fractions per unit SAI	FRINTS	0.06
Maximum interception storages of rain per unit LAI	CINTRL	0.3
Maximum interception storages of rain per unit SAI	CINTRS	0.15